A kinetic study of the emulsion polymerization of vinyl acetate

Forskningscenter Risø, Roskilde

Publication date:
1973

Document Version
Publisher's PDF, also known as Version of record

Risø Report No. 282

Risø Report No. 282

Danish Atomic Energy Commission

Research Establishment Risø

A Kinetic Study of the Emulsion Polymerization of Vinyl Acetate

by Nils Friis

June 1973

Sales distributors: Jul. Gjellerup, 87, Sølvgade, DK-1307 Copenhagen K, Denmark

Available on exchange from: Library, Danish Atomic Energy Commission, Risø, DK-4000 Roskilde, Denmark

June 1973 Risø Report No. 282

A Kinetic Study of the Emulsion Polymerization of Vinyl Acetate[x)]

by

Nils Friis

Danish Atomic Energy Commission
Research Establishment Risø
Chemistry Department

and

Instituttet for Kemiindustri
Technical University of Denmark
Lyngby

Abstract

This report deals with the chemically and the radiation-initiated emulsion polymerization of vinyl acetate.

In experiments with potassium persulphate as initiator and sodium lauryl sulphate (SLS) as emulsifier the rate of polymerization is approximately proportional to the square root of initiator concentration and to the 0.25 power of the number of particles. The number of particles is proportional to the 0.5 power of the emulsifier concentration. The rate of polymerization is constant in the interval 15 to 70-85% conversion.

x) This report is submitted to the Technical University of Denmark in partial fulfilment of the requirements for obtaining the lic. techn. (Ph.D.) degree. Part of the report has been submitted for publication in Journal of Applied Polymer Science.

UDC 678.744: 66.095.26

The limiting viscosity number of the polymers produced is independent of initiator concentration and number of particles. In experiments with the emulsifier sodium dodecylbenzene sulphonate (SDBS) it is observed that the shape of the polymerization curve is entirely changed when the concentration of SDBS is increased from 2.9 to 11.5 g/l H_2O. At the high concentration the rate of polymerization declines already from 35-45% conversion.

On the basis of the experiments with SLS as emulsifier it is suggested that the mechanism of vinyl acetate emulsion polymerization is similar to that of vinyl chloride. The linearity of the conversion versus time curve is explained as being due partly to a decrease in the desorption rate of radicals from the particles and partly to a decrease in the termination rate constant with the progress of the polymerization. The peculiar effect observed in experiments with the emulsifier SDBS is explained as being due to retardation caused by this compound. However, the data are insufficient to prove this hypothesis unequivocally.

In experiments with radiation initiation, performed at dose rates of 62 and 301 krads/h in a recycle flow reactor system, the rate of polymerization is proportional to the square root of the dose rate. The effect of the number of particles and concentration of SLS is similar to that observed with chemical initiation. The rate of polymerization increases when the flow rate is increased from the beginning of the polymerization. At conversions beyond 40% there is no effect of flow rate. The rate of polymerization per unit volume of in-source reactor increases as the reactor volume is decreased, although the overall rate of polymerization increases with increasing reactor volume.

ISBN 87 550 0195 5

CONTENTS

1. INTRODUCTION

The primary purpose of the present work was to accomplish the radiation-induced emulsion polymerization of vinyl acetate in a recycle flow reactor system and to elucidate by means of a stimulus-response technique the mechanism of this particular process.

The direct antecedent of this study was the work of Stannett and Stahel[1] and Omi and Stahel[2] who investigated the emulsion polymerization of styrene in a similar system. By means of the classic hypothesis for emulsion polymerization, proposed by Smith and Ewart[3] and generally accepted for chemically initiated emulsion polymerization of styrene, these investigators explained the specific behaviour of the radiation-induced emulsion polymerization of styrene in such a system.

It is generally accepted that the mechanism of vinyl acetate emulsion polymerization does not fall within the classic hypothesis of emulsion polymerization. Indeed, when the present study was commenced, the mechanism of vinyl acetate emulsion polymerization was obscure. Several investigations were reported in the literature, but with conflicting results and conclusions.

To make the basis better for the interpretation of the radiation-induced experiments and to make the investigation more comprehensive I decided to extent the experimental work also to comprise chemically initiated emulsion polymerization of vinyl acetate, the primary purpose being the deduction of a rate expression for this process.

2. FUNDAMENTAL PRINCIPLES IN EMULSION POLYMERIZATION

2.1. Introduction

Emulsion polymerization is essentially a process in which an aqueous dispersion of a sparingly soluble monomer or a mixture of monomers is converted into a stable dispersion of polymer particles. The product of an emulsion polymerization is called a latex.

Harkins[4] was the first to propose a mechanism for emulsion polymerization which could successfully account for the experimental observations. The qualitative picture presented by Harkins was later treated quantitatively by Smith and Ewart[3] who expressed the steady-state kinetics of emulsion polymerization with a recursion formula. At the time when it was deduced, this formula could only be solved for three limiting cases. The general

solution was later given by Stockmayer[5] and extended by O'Toole[6].

Since the formulation of the quantitative theory numerous investigations on emulsion polymerization of various monomers have been performed, and it has appeared that the theory of Smith and Ewart is outstandingly successful in explaining the experimental behaviour of several monomers. However, for some monomers, among which are vinyl chloride and vinyl acetate, it is necessary to modify the theory to make it reconcile with experimental observation.

2.2. Qualitative Theory of Harkins

A conventional emulsion polymerization recipe comprises at least four ingredients, namely water, monomer, initiator, and emulsifier.

Free radicals are produced by the spontaneous decomposition of the initiator. Since the initiator is usually insoluble in the monomer, the primary free radicals are produced solely in the aqueous phase. Typical initiators used in emulsion polymerization are inorganic persulphates such as ammonium and potassium persulphate.

The emulsifier consists of molecules that are hydrophobic at one end and hydrophilic at the other. Owing to the attractive forces between the hydrophobic ends of the emulsifier molecules, these molecules form molecular aggregates, so-called micelles, when their concentration exceeds a certain value, the critical micelle concentration. A micelle can be visualized as a cluster of emulsifier molecules with their hydrophilic ends directed towards the aqueous phase. However, the exact structure of micelles is not known. Since the interior of micelles is hydrophobic, they are able to dissolve a certain amount of monomer. This phenomenon is termed solubilization.

Thus, initially the monomer is to be found in three different loci. The major part is present as 1 to 10 μm large monomer droplets. A considerably smaller amount is present in the micelles, being 50 to 100 Å in diameter. Finally a small amount is present as an actual solution in the aqueous phase. The distribution of monomer on these three loci is dependent on the nature of the monomer and the concentration of the emulsifier.

For the nucleation of polymer particles and the progression of polymerization in such a system Harkins[4] adduced the following essential postulates:

I Free radicals are produced in the aqueous phase and are captured by the micelles. The monomer in the micelle is polymerized, whereby the micelle is transformed into a polymer particle. Thus, the micelles are the principal locus for the nucleation of polymer particles.

II The principal locus of polymer formation is the polymer particles being swollen with monomer.

III The monomer droplets serve as reservoirs from which by diffusion through the aqueous phase monomer molecules are transferred to the growing polymer particles. Since the total surface area of the monomer droplets is approximately two orders of magnitude smaller than that of the micelles and the polymer particles, few radicals enter the monomer droplets. Therefore, little or no polymer is formed in the monomer droplets.

In consequence of the qualitative scheme proposed by Harkins, emulsion polymerization may be considered as a three-stage process. During stage 1 polymer particles are generated. Part of the micelles are used for nucleation of new particles and part of them desorb to deliver the emulsifier necessary for stabilization of the growing polymer particles. At the end of stage 1 all micelles are consumed, and the generation of polymer particles ceases. During stage I the overall rate of polymerization increases with time.

During stage 2 the polymer particles grow. Owing to a rapid diffusion of monomer into the particles from the aqueous phase, the particles will contain a considerable amount of monomer. The monomer-polymer ratio in the particles is constant until the separate monomer phase (i. e. the monomer droplets) is exhausted. Since the number of polymer particles is also constant, the overall rate of polymerization remains constant during stage 2. At the end of stage 2 the separate monomer phase vanishes.

In stage 3 the dispersion consists of only two phases, namely the water phase, which is the continuous phase, and the dispersed phase, which is made up of the monomer-swollen polymer particles. Since no new monomer is supplied to the particles, the concentration of monomer in the particles decreases during this stage, and so does the overall rate of polymerization.

In fig. 1 is shown a schematical representation of the different stages in emulsion polymerization.

The point of transition from one stage to another is determined by the nature of the monomer and the emulsifier type and concentration. In a typical styrene emulsion polymerization the number of particles becomes

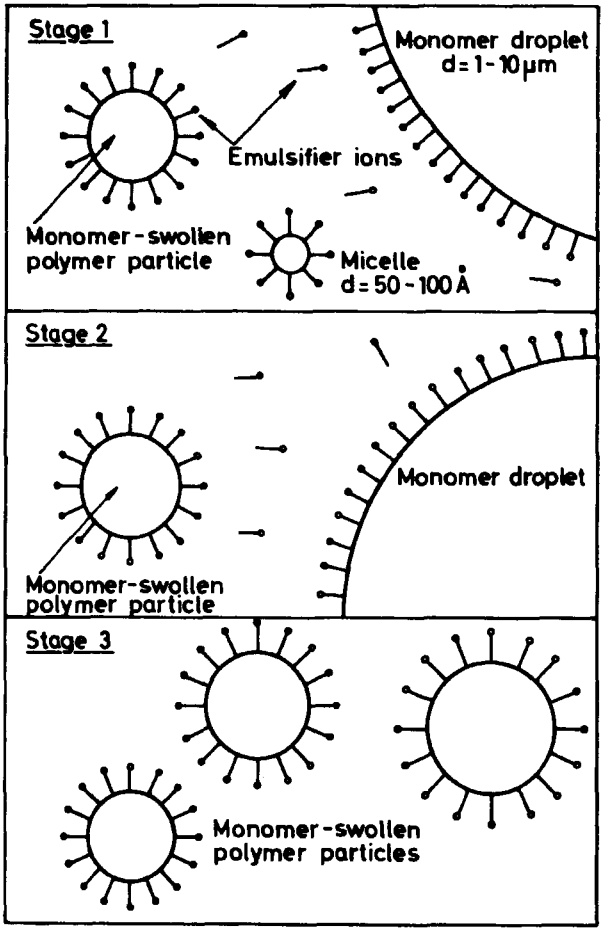

Fig. 1. Schematic representation of emulsion polymerization.

constant at 15% conversion and the monomer phase disappears at 40-50% conversion.

From the preceding it follows that the conversion versus time curve in emulsion polymerization is s-shaped. A typical plot from a styrene polymerization is shown in fig. 2.

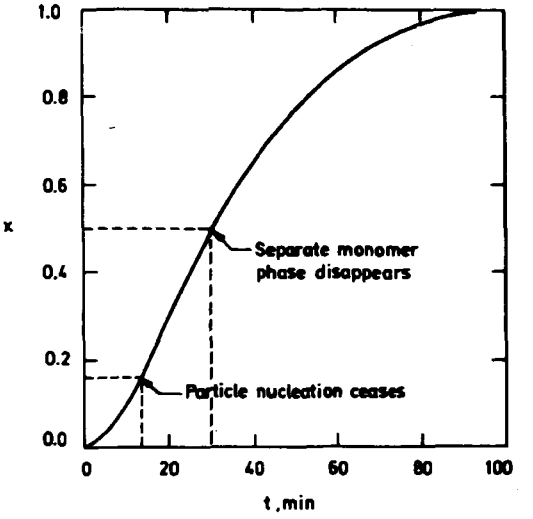

Fig. 2. Typical styrene emulsion polymerization curve.

It appears that the emulsifier plays a triple role during the polymerization. Firstly, it serves to stabilize the monomer droplets. Secondly, it generates micelles, the major locus for the particle nucleation. Thirdly, it is adsorbed on the surface of the polymer particles, thus preventing them from coalescing.

2.3. Quantitative Theory of Smith and Ewart

Smith and Ewart[3] considered the problem of the kinetics of emulsion polymerization as twofold. Firstly, there is the problem of establishing the major factors governing the polymerization in a single polymer particle. Secondly, there is the problem of determining the principal factors governing the number of particles being formed.

Smith and Ewart solved the first problem by presuming that the kinetics were governed by three variables.

1. The rate of radical entry into a single particle, given as

$$dn/dt = \rho'/N,$$

where ρ' is the overall rate of entrance into all N particles, and n is the number of free radicals.

2. The rate of radical transfer out of the particles, given as

$$dn/dt = -k_o a_p (n/v),$$

where k_o is a specific rate constant for the event, a_p the interfacial area through which the transfer takes place, and v is the volume of a single polymer particle. n/v is thus the concentration of free radicals in a particle.

3. The rate of mutual termination within a particle, given as

$$dn/dt = -2k_{tp} n((n-1)/v),$$

where k_{tp} is the termination rate constant, and (n-1)/v is the concentration of free radicals with which any of the n free radicals can react.

By assuming that the rate at which particles containing n free radicals are formed equals the rate of their disappearance, the following steady-state equation is obtained:

$$N_{n-1}(\rho'/N) + N_{n+1} k_o a_p ((n+1)/v) + N_{n+2} k_{tp} [(n+2)(n+1)/v] = N_n [(\rho'/N) + k_o a_p (n/v) + k_{tp} n(n-1)/v], \quad (1)$$

where N_n denotes the number of particles containing *n* radicals. Smith and Ewart solved this equation for three limiting cases.

Case 1. Number of free radicals per particle is small compared with unity

In this case only particles containing zero or one radical need be considered, and the recursion formula (eq. 1) reduces to

$$N_1 k_o a_p / v = N_o \rho'/N. \quad (2)$$

Since $N_o \cong N$, the following approximate expression is obtained for N_1:

$$N_1 \cong \rho' v / k_o \cdot a_p . \quad (3)$$

If termination is largely in the polymer phase and occurs instantly upon the entry of a radical into a particle already containing one radical, then

$$\rho = 2(\rho'/N) N_1 , \quad (4)$$

where ρ is the rate of formation of radicals in the water phase. This is a steady-state equation expressing that the rate at which radicals are generated equals the rate of their disappearance.

By combination of eqs. 3 and 4 and elimination of ρ' the rate of polymerization is obtained as

$$R_p = k_p [M_p] N_1 = k_p [M_p] (Nv\rho/2k_o a_p)^{1/2} = k_p [M_p] (V_p \rho / 2k_o a_p)^{1/2} \quad (5)$$

where k_p is the propagation rate constant, $[M_p]$ the concentration of monomer within the polymer particles, and V_p the total volume of polymer particles. From eq. 5 it appears that the rate of polymerization depends on the surface area of the polymer particles. An expression giving the dependence of polymerization rate on number of particles can be obtained by using the relationship between a_p, N, and V_p

$$a_p = 4\pi \left(\frac{3 \cdot V_p}{4\pi N} \right)^{2/3} .$$

Substitution of this expression into eq. 5 gives

$$R_p = k_p [M_p] N^{1/3} \left(\frac{V_p}{36\pi} \right)^{1/6} \left(\frac{\rho}{2k_o} \right)^{1/2} . \quad (6)$$

If termination is largely in the water phase, then

$$\rho = 2k_{tw} (C_w)^2 , \quad (7)$$

where C_w is the concentration of free radicals in the water phase, and k_{tw} is the termination rate constant for the event. Assuming a rapid equilibrium of free radicals between water phase and polymer particles, C_w can be related to the concentration of free radicals in the polymer phase, C_p:

$$\delta = C_p/C_w , \tag{8}$$

where δ is a partition coefficient.

Since only a very small proportion of the particles contain more than one radical, N_1 can approximately be equalled to $V_p \cdot C_p$, and from eqs. 7 and 8 the rate of polymerization is obtained as

$$R_p = k_p[M_p]N_1 = k_p[M_p]V_p\delta(\rho/2k_{tw})^{1/2} . \tag{9}$$

It appears that in this case the rate of polymerization is independent of the number of polymer particles.

Case 1 kinetics, as here presented, have, as far as is known, not been shown to apply to emulsion polymerization of any of the monomers previously investigated. Nevertheless, this case is of primary importance for the present investigation, since in vinyl acetate emulsion polymerization the average concentration of free radicals per particle is usually much less than unity.

Case II. Number of free radicals per particle is approximately equal to 0.5

If transfer of radicals out of the particles is negligible and termination within a particle rapid compared with the average time interval between successive entrances of free radicals into a particle, solution of the recursion formula leads to an average concentration of 0.5 free radicals per particle. In this case the rate of polymerization is given as

$$R_p = k_p[M_p]N/2. \tag{10}$$

Case II kinetics have been shown to apply to emulsion polymerization of various monomers including styrene, butadiene, and isoprene[7].

Case III. Number of free radicals per particle is large compared with unity

In this case the emulsion polymerization can be regarded as a bulk polymerization taking place in a large number of discrete loci, and the

steady-state condition for a single particle can be written as

$$\rho/N = 2k_{tp}(n^2/v), \tag{11}$$

assuming that termination takes place exclusively in the particles, and that every free radical generated in the aqueous phase is captured by the particles. The rate of polymerization is thus given as

$$R_p = k_p[M_p]Nn = k_p[M_p](V_p\rho/2k_{tp})^{1/2} \tag{12}$$

and is, as one might expect, independent of the number of particles.

Case III is particularly interesting, when the later stages of emulsion polymerization of certain monomers are considered. During the polymerization the particles become richer in polymer and therefore the termination rate constant decreases rapidly[8]. This means that during the polymerization there is an increasing probability that a single particle may simultaneously contain several radicals. Thus, it has been shown that the emulsion polymerization of methyl methacrylate can adequately be described by case II kinetics[9,10], but only to a limited conversion. Between 30 and 50% there is a transition from case II to case III. The complete description of methyl methacrylate emulsion polymerization requires a complete solution of the recursion formula together with a suitable expression for k_{tp} as function of conversion[11].

The second problem in emulsion polymerization concerns the formation of particles. On the basis of the micellar initiation hypothesis proposed by Harkins[4], Smith and Ewart[3] have considered two idealized situations. In the first of these it is supposed that free radicals, generated in the aqueous phase, are all captured by the micelles. No radicals enter the polymer particles as long as micelles are present. In this case the total number of particles is found to be

$$N = 0.53(\rho/\mu)^{2/5}(Sa_s)^{3/5} . \tag{13a}$$

In this equation a_s is the area occupied by one emulsifier molecule, S is the number of emulsifier molecules per unit volume of aqueous phase, and μ is the rate of volume increase of a polymer particle. Eq. 13a is derived on the assumption that μ is constant during stage 1, and it is therefore applicable only to systems for which case II kinetics hold. The number of particles predicted by eq. 13a is too large owing to the neglecting of radicals

being captured by polymer particles.

In the second idealized situation it is supposed that free radicals diffuse into both the latex particles and the micelles, and, to avoid complications arising from strict application of diffusion laws, it is assumed that a given interfacial area on polymer particles and micelles has the same effectiveness in capturing radicals. This leads to a number of particles which is too small, since the flux of radicals per unit area is inversely proportional to the radius of the particle involved. The second idealized situation leads to the following expression for N:

$$N = 0.37(\rho/\mu)^{2/5}(Sa_s)^{3/5} . \qquad (13b)$$

Thus, both formulations lead to expressions in which N has the same functional dependence on the various parameters and the only deviation appears in the value of the numerical constants.

Recently, Roe[61] has discussed the theory of particle population and pointed out that the micellar initiation hypothesis is not an essential feature of the theory. Roe[61] has suggested an alternative mechanism for particle nucleation, in which the particles arise from radicals polymerizing in the aqueous phase. These radicals are initially dissolved in the aqueous phase where they react with dissolved (not solubilized) monomer. As the growing radicals attain a certain magnitude they assume the aspect of a polymer particle stabilized by adsorbed emulsifier. Thus, the major role of the emulsifier is to stabilize the particles being formed.

By assuming that the emulsifier is quantitatively adsorbed on the surface of the polymer particles Roe[61] has expressed the rate at which the emulsifier is consumed. By integration of this expression and by assuming that no new particles are being generated after all emulsifier is consumed, Roe has obtained two expressions for N, which are identical to eqs. 13a and b. Thus the functional relationship between N and S, and N and ρ, which is expressed in eqs. 13a and b, and which is supported by data from styrene polymerization, can be deduced without reference to the micellar initiation hypothesis invoked by Harkins.

It has been generally supported by most investigators that the polymerization takes place within the polymer particles. This is the basic point in the analysis of Harkins[4] and Smith and Ewart[3]. However, it should be mentioned that some investigators have considered the polymerization to take place on the surface of the particles, and a quantitative theory based on this point of view has been presented by Medvedev[12]. However, this

theory has not been verified to the same extent as the theory of Smith and Ewart and will therefore not be further considered in this treatment.

2.4. General Solution of the Recursion Formula

By simple rearrangement eq. 1 can be written as

$$(n+2)(n+1)N_{n+2} + m(n+1)N_{n+1} + \epsilon N_{n-1} = N_n(n(n-1)+m\cdot n+\epsilon), \qquad (14)$$

where

$$\epsilon = v\cdot\rho'/k_{tp}N$$

and

$$m = k_o a_p/k_{tp} .$$

Stockmayer[5] was the first to obtain a general solution for the recursion formula given in eq. 14. Later Stockmayer's treatment was corrected and extended by O'Toole who obtained the explicit solution

$$\tilde{n} = \frac{\zeta}{4}\frac{I_m(\zeta)}{I_{m-1}(\zeta)} , \qquad (15)$$

where

$$\zeta^2 = 8\epsilon$$

and $\tilde{n}$ is the average concentration of free radicals per particle, while I denotes the Bessel functions of the first kind. From $\tilde{n}$ the rate of polymerization can be obtained as

$$R_p = k_p[M_p]N\tilde{n}.$$

In fig. 3 is shown a plot of $\tilde{n}$ as function of the parameter ζ for different values of m. The plot is obtained by means of eq. 15. For $m = 0$ and $\zeta \ll 1$ transfer of radicals out of the particles is negligible, and termination in the particles is rapid. In this case the plot gives a value of $\tilde{n}$ equal to 0.5 in agreement with Smith-Ewart case II. For $m/\zeta \gg 1$ the rate of transfer of radicals out of the particles is large compared with the rate of entry of radicals into particles already containing one radical. In this case the plot shows that n becomes much less than unity. This is in agreement with Smith-Ewart case I.

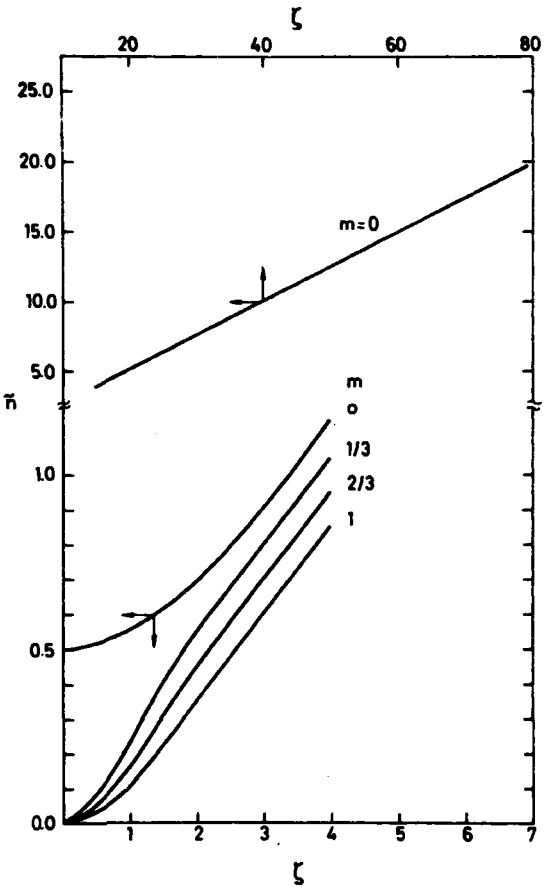

Fig. 3. Average number of radicals per particle, $\bar{n}$, as a function of the parameters ζ and m. The plots are obtained with the aid of eq. 15.

Finally, for large values of ζ, tantamount to slow termination within the particles, the value of $\bar{n}$ becomes large compared with unity. This is in agreement with Smith-Ewart case III.

3. CHEMICALLY INITIATED EMULSION POLYMERIZATION OF VINYL ACETATE

3.1. Literature Survey

In spite of rather extensive research during the past decade it has not been possible to establish in detail the kinetics of vinyl acetate emulsion polymerization. Data in the literature are widely different and contradictory. Unfortunately, most of the reports do not give detailed information about experimental techniques and purity of materials. Therefore, the numerous discrepancies are not easy to explain.

In the following will be given a brief review of the research cited in the literature and pertinent to the present work. References 13-34 comprise the majority of investigations on vinyl acetate emulsion polymerization conducted during the past twenty years.

It is tempting to compare vinyl acetate emulsion polymerization with that of styrene, which has been studied most extensively. Such a comparison reveals the following qualitative points of distinction:

I In styrene emulsion polymerization the polymerization rate decreases proportionally to the monomer concentration from the point of disappearance of the separate monomer phase. This is in agreement with Smith-Ewart's theory. In the vinyl acetate system the rate of polymerization remains constant until 85% conversion, although the separate monomer phase has vanished at or before 30%[15,16,25,28].

II In styrene emulsion polymerization the average concentration of free radicals per particle equals one half. In the vinyl acetate system this quantity is usually much less than unity[25,27,28].

III In the styrene system there is no effect on polymerization rate upon addition of an extra amount of initiator during stages 2 and 3[35]. In the vinyl acetate system the rate of polymerization increases when more initiator is added[27].

IV In the styrene system there is a precipitous fall in polymerization rate in going from a supercritical to a subcritical emulsifier concentration[18]. This is to be expected from Harkin's and Smith-Ewart's

theory of particle formation. This effect is not observed in the vinyl acetate system[18].

The above remarks concerning styrene emulsion polymerization apply only to systems with relatively low initiation rates and relatively small particles, i.e. to systems where gel effect does not occur. At sufficiently high rates of initiation or in systems with large particles the average concentration of free radicals per particle may exceed 0.5. In this case the rate of polymerization does not decrease proportionally to the monomer concentration. Furthermore, the rate of polymerization will be sensitive to initiator pertubations.

The low concentration of free radicals per particle suggests that vinyl acetate emulsion polymerization can be described in terms of Smith-Ewart's case I. However, the constant rate behaviour observed in the vinyl acetate system is incompatible with this theory unless it can be assumed that the specific rate constant k_o in eq. 5 decreases proportionally to the square of monomer concentration. This situation has not been considered by Smith and Ewart.

In order to establish the point at which the separate monomer phase disappears some investigators have followed the diffusion of monomer into the polymer particles during polymerization. This can be done either by vapour pressure measurements[15] or by centrifuging samples withdrawn at regular intervals during polymerization[13]. The results from such measurements reported in the literature are somewhat scattered. Thus French[13] has found that the separate monomer phase vanishes at 13.5% conversion, while Nomura et al.[28] have reported a value of 23% and Vanzo[15] 32%. The differences might be attributed to the application of different emulsifier types and different experimental techniques in these investigations. Thus French used a nonionic emulsifier, while Nomura used an anionic emulsifier.

The results can be compared with styrene emulsion polymerization where it has been found that the monomer droplets disappear in the interval 40-50% conversion. Thus, it can be concluded that the monomer-polymer ratio within the particles is somewhat higher in the vinyl acetate system than in the styrene system.

Only few investigators have studied the number of polymer particles as function of conversion. From the data of Napper and Parts[20] it appears that the number of particles remains constant in the interval 10 to 100% conversion. In contrast to this result Priest[19] has reported a decrease in number of particles from a certain critical conversion. Priest has

explained this as being due to an increased rate of particle coalescence as the particles become larger.

In the search for a mechanism of vinyl acetate emulsion polymerization many investigators have studied the effect of initiator and emulsifier concentration on rate of polymerization. Also the effect of these parameters on number of particles and the influence of number of particles on rate of polymerization has been studied. The effect of the different parameters is usually expressed in an equation of the form

$$Y = P^z,$$

where P is the quantity of the independent parameter, Y is the quantity of the dependent variable, and z is the wanted exponent characteristic of the relationship between Y and P.

As already mentioned nearly all reports on vinyl acetate emulsion polymerization are contradictory. Thus, Gershberg[25] has reported that the order of reaction with respect to initiator concentration is 0.6, while Litt et al.[27] have found an order of 1.0. Recently Nomura et al.[28] have reported a value of 0.5. In all investigations the same type of initiator and emulsifier was used. Also, the concentrations of these ingredients were similar to allow a comparison of the experimental results.

Litt et al.[27] and Breitenbach[30] have reported that there is no effect of emulsifier concentration on rate of polymerization. In contrast to this result Gershberg[25] has found that the rate of polymerization is proportional to the 0.25 power of emulsifier concentration. A slightly smaller effect has been reported by Okamura[18] and Nomura[28]. All investigators have used sodium lauryl sulphate as emulsifier.

From the data of Nomura et al.[28] it can be computed that the number of particles increases proportionally to the 0.5 power of emulsifier concentration. Gershberg[25] has reported a value of 0.2, while French[13] has found that the number of particles increases by the third power of emulsifier concentration.

Thus, it appears that a certain confusion prevails in the research of vinyl acetate emulsion polymerization, and apart from the above-mentioned points I-IV no certain conclusions can be drawn on the basis of the results reported in the literature. In table 1 is given a survey of some of the results published in the literature.

Table 1

Summary of data on vinyl acetate emulsion polymerization reported in the literature

$R_p \propto S^p$	$R_p \propto I^p$	$N \propto S^p$	$N \propto I^p$	$R_p \propto N^p$	Emulsifier	Initiator	Temperature	Reference
p	p	p	p	p			°C	
0.6	0.7	-	-	-	Evanol 52-22	$K_2S_2O_8$	70	17
0	1	-	1.2	0.2	SLS	$K_2S_2O_8$	60	27.14
-	0.5	0.5*	0	-	SLS	$K_2S_2O_8$	50	28
0.25	0.6	0.2	-	-	SLS	$K_2S_2O_8$	50	25
0	0.7	-	-	-	SLS	$K_2S_2O_8$	50	30
0.1	0.64	-	-	-	SLS	$K_2S_2O_8$	60	26

* Calculated from data in ref. 28.

In comparison with styrene, vinyl acetate has a relatively high solubility in water. The solubility of vinyl acetate in water is 2.1 wt% at 50°C[36], while that of styrene is only 0.037 wt% at the same temperature[37]. This fact compared with the constant rate behaviour observed in vinyl acetate emulsion polymerization has led some investigators[16, 24, 25] to propose a hypothesis according to which polymerization takes place in the water phase. In this hypothesis the monomer-swollen polymer particles are regarded as monomer reservoirs keeping the water phase saturated with vinyl acetate. The reaction medium will thus have a constant composition, and this will imply a constant rate of reaction.

However, this hypothesis is reprehensible, since it has been shown by Dunn and Taylor[26] that the concentration of monomer in the water phase will drop by at least a factor of 2 in going from 30 to 85% conversion. Furthermore, in the quantitative treatment of the water phase hypothesis Gershberg[25] had to assume a termination rate constant in the aqueous phase several orders of magnitude lower than that reported for vinyl acetate in bulk and solution polymerization[38]. There is no obvious reason why this should be the case.

In a study of the polymerization of vinyl acetate in aqueous media Napper and Parts[20] have observed a marked increase in the polymerization rate as soon as the initially formed polymer separated from the solution as polymer particles. This suggests that the principal locus of polymerization is not the water phase, but rather the monomer-swollen polymer particles.

Recently three different mathematical models have been proposed for vinyl acetate emulsion polymerization[27, 28, 34]. Common to these models is that they all assume that polymerization takes place in the polymer particles, and they all involve a mechanism allowing radicals to escape the polymer particles. As previously mentioned such a mechanism is necessary to explain the low concentration of free radicals per particle usually observed in vinyl acetate emulsion polymerization. However, the implications of the three models are vastly different, and the experimental results on which they are based are contradictory.

A detailed examination of the derivation of these models would make the present text too extensive. Only the conclusions and final expressions will be discussed. For convenience this discussion will be placed in subsection 3.4.4 to include a comparison with the model presented in this work.

3.2. Experimental

3.2.1. Materials and Polymerization Equipment

Vinyl acetate, obtained from Edison Société, was distilled 24 hours prior to use on a 2-ft column filled with glass helices. Before each experiment the distillate was analysed on a Perkin Elmer model 881 gas chromatograph at 80°C with a diisodecyl phthalate column. The analysis showed traces of acetone. However, in all cases the amount of acetone was less than 0.2%, and since acetone in such small quantities has no noticeable effect on vinyl acetate polymerization[39], further purification of the distillate was omitted.

The initiator used in the emulsion experiments was an analytical grade of potassium persulphate obtained from Merck, and in the bulk experiments an analytical grade of α, α'-azobisisobutyronitrile, obtained from Fluka AG.

The emulsifiers, sodium lauryl sulphate (Quolac ON WD) and sodium dodecylbenzene sulphonate (Quolac ATE-DS 10), were both of purified grade, obtained from the American Alcolac Corporation. These materials were used without further purification.

K_2SO_4 and Na_2HPO_4 were both of analytical grade and obtained from Merck. In all experiments was used redistilled water with a specific conductivity of less than 2×10^{-6} mho.

The polymerization was carried out in a standard experimental set-up consisting of a 2-litre pyrex vessel provided with stirrer, thermometer, N_2-inlet, and reflux condenser. The emulsion was purged with nitrogen 30 minutes prior to the addition of initiator. The nitrogen was obtained from a standard cylinder and deprived of oxygen by passing through a 5% solution of pyrogallol in 2N NaOH. The temperature was controlled within $\pm$ 0.2°C.

In all experiments the emulsion was composed of 550 ml vinyl acetate and 1150 ml redistilled water, and varying amounts of emulsifier and initiator.

The degree of conversion was determined from samples withdrawn at regular intervals. The emulsion was broken by freezing in liquid nitrogen. The precipitated polymer was washed thoroughly with distilled water at 50°C and dried to constant weight in a vacuum oven at 50°C.

Bulk polymerization of vinyl acetate was performed in 5-ml ampoules immersed in a thermostat bath. Before the polymerization the vinyl acetate was degassed by using the freezing-evacuation-thawing technique.

3.2.2. Particle Size Analysis

The number of polymer particles can be determined by electron microscopy and light scattering. Both methods involve a determination of the average particle volume, which by comparison with the total volume of polymer gives the number of particles per unit volume.

From a practical point of view light scattering is by far the most straightforward of the two. The procedure is rapid, particles are not deformed, and all particles are counted. However, light scattering only yields the weight-average particle volume and therefore also only the weight-average particle number. In a kinetic investigation of emulsion polymerization it is the number-average particle number that is of particular interest, and therefore it is necessary to convert the weight-average particle volume obtained from light scattering into a number-average volume. This can be obtained by means of electron microscopy which yields not only the number- and weight-average particle volumes, but also the particle size distribution.

Electron microscopy is a standard procedure for determining particle sizes and particle numbers in latices consisting of hard polymers, e.g. polystyrene, poly(vinyl chloride), and poly(methyl methacrylate). However, this method implies complications when applied to latices consisting of soft, so-called film-forming polymers, such as poly(vinyl acetate) and poly(ethyl acrylate). Latex particles made up of these polymers tend to flatten on the specimen membrane, and on the micrographs the particles appear blurred. Obviously, particle sizes obtained from such measurements without special precautions are in great error.

Particles of soft polymers can be hardened by high-energy radiation from an electron accelerator[40]. At sufficiently high doses (30 Mrads) the particles become rigid owing to crosslinking of the polymer making up the particles. Unfortunately, this treatment also changes the diameter of the particles, thus making the estimation of particle size inaccurate. A better method has been introduced by Vanzo[15] who has shown that particles of soft polymers can be hardened by γ-radiation after addition of a small amount of styrene to the latex. The total dose necessary for the hardening is only 1 Mrad, and it has been shown that the size of the particles is not altered substantially by this treatment. Furthermore, Vanzo has shown that styrene is absorbed quantitatively into the particles, and that no new generation of particles consisting of pure polystyrene is formed.

Addition of 5-10% styrene in proportion to the amount of poly(vinyl acetate) and subsequent irradiation cause a build-up of a polystyrene frame-

work within the particles, sufficient to make the particles hard and rigid.

The hardening technique developed by Vanzo[15] has been adopted in the present work and will be treated in further detail below.

3.2.2.1. Light Scattering. The light scattering instrument used in this investigation was a SOFICA model 42000 with a 546.1 nm mercury lamp. The instrument was calibrated against a glass standard with pure benzene as reference.

To obtain the Raleigh ratio, R_{90}, and the dissymmetry ratio, [Z], at infinite dilution the following procedure was used:

1. The latex was diluted to a concentration of 3×10^{-5} - 3×10^{-4} g polymer/cm^3. Redistilled water was used as diluent. The temperature of the sample was adjusted to 25.0°C.
2. The galvanometer deflection was measured at scattering angles 45, 90, and 135°. Each measurement was repeated twice.
3. The sample was diluted by a factor 2, and the above measurements were repeated at the new concentration. This procedure was repeated four times.

The use of the light scattering equation for particle size determination also involves evaluation of $d\bar{n}/dc$, the change in refractive index with concentration. $d\bar{n}/dc$ was determined at 25°C by means of a Shimadzu model DR 4 differential refractometer in the range of concentration 7.5×10^{-4} - 6×10^{-3} g polymer/cm^3.

The evaluation of number of particles from light scattering data will be considered in detail in Appendix I.

3.2.2.2. Electron Microscopy. The electron microscope used in this investigation was a Hitachi model HU-11A. Only samples of complete conversion were investigated by electron microscopy, since samples containing vinyl acetate monomer could not be hardened successfully.

The major problem in this investigation was to avoid deformation of the particles during the transfer of latex to the slide grid. On the basis of several experiments the following procedure proved very suitable for the preparation of high-quality electron micrographs:

1. The latex was diluted to a content of 5-10% poly(vinyl acetate).
2. Styrene monomer was added in a quantity of 5% of the poly(vinyl acetate) polymer.

3. The latex was flushed with nitrogen to remove oxygen.
4. The latex was irradiated from a ^{60}Co-source with a total dose of 1 Mrad and a dose rate of 60 krads/h.
5. The latex was diluted 50 times, and one drop of the latex was placed on a copper grid which had previously been covered with a carbon film. The slide was dried in a vacuum chamber, and then washed six times with droplets of cold water to remove emulsifiers.
6. After drying, the slide was shadowed with palladium in a vacuum evaporator. The best result was obtained with shadowing from a small angle (20°).
7. The slide was investigated in the electron microscope and the ratio particle diameter/shadow length was compared with the shadowing angle in order to estimate a possible flattening of the particles.

3.2.3. Viscometry

The specific viscosity of poly(vinyl acetate) solutions was measured with an Ubbelohde viscometer. Acetone was used as solvent, and the viscosity was measured at 30.0°C.

The specific viscosity was measured at four concentrations in the interval 0.03 - 0.5 g/dl, and each measurement was repeated three times.

3.3. Results

3.3.1. Particle Size Analysis

Figs. 4 and 5 show typical electron micrographs which were obtained by using the hardening technique described in subsection 3.2.2.2. For comparison fig. 6 shows a micrograph obtained without hardening of the latex particles. The effect of hardening on the quality of the micrographs speaks for itself.

The height of the particles can be calculated from the shadow length and the shadowing angle, as shown in fig. 7. The shadowing angle is obtained from the geometry of the evaporator. By comparing the height measured in this way with the diameter directly measurable from the micrographs it is found that their ratio equals approximately 1, indicating that the particles are spherical and undeformed.

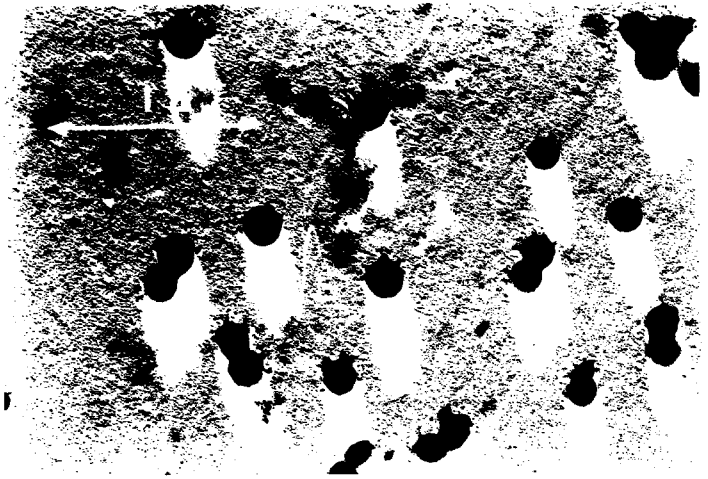

Fig. 4. Electron micrograph of a hardened poly (vinyl acetate) latex.

Fig. 5. Electronmicrograph of a hardened poly (vinyl acetate) latex.

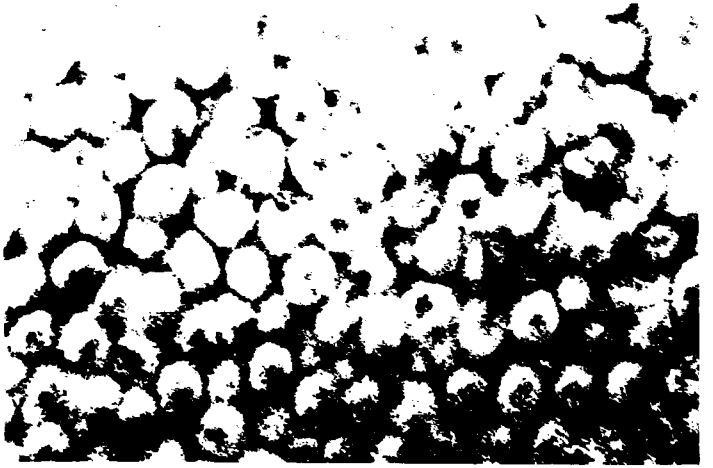

Fig. 6. Electronmicrograph of an untreated poly (vinyl acetate) latex. (x 35000).

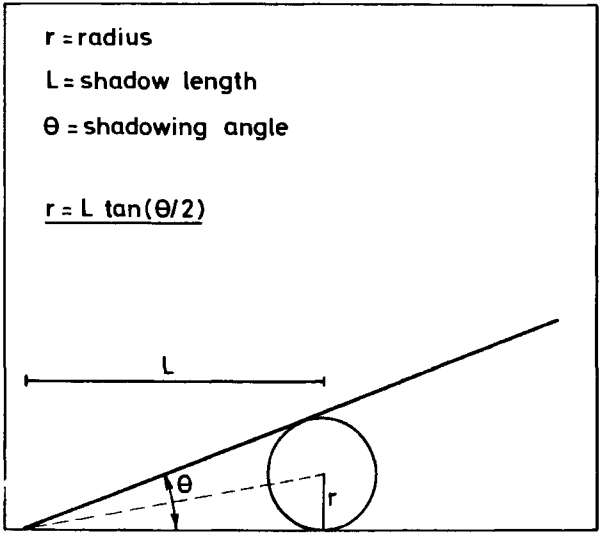

Fig. 7. Schematic representation of the procedure used to determine the particle height.

From the micrographs it is possible to compute the weight-average particle volume, $\bar{v}_W$, and the number-average particle volume, $\bar{v}_N$, defined as

$$\bar{v}_W = \frac{\pi}{6} \sum N_i d_i^6 / \sum N_i d_i^3 \qquad (16)$$

and

$$\bar{v}_N = \frac{\pi}{6} \sum N_i d_i^3 / \sum N_i, \qquad (17)$$

where N_i denotes number of particles with a diameter d_i.

During an investigation of solubility effects in emulsion polymerization Vanzo[15] has computed the ratio $\bar{v}_W/\bar{v}_N$ for several latices of different polymers. The magnitude of this ratio, which is a numerical measure of the particle size heterogeneity, was in all cases found to lie within 1.5 - 3.0. Thus, for poly(vinyl hexanoate) the ratio equalled 1.7, for polystyrene 2.3, and for poly(vinyl acetate) 2.6. Assuming the respective values being representative of the different systems, Vanzo[15] used the ratio $\bar{v}_W/\bar{v}_N$ to calculate the number-average particle volume from the weight-average particle volume.

In the present investigation the ratio $\bar{v}_W/\bar{v}_N$ was computed by measuring approximately 400 particles, and it is most interesting to notice that the ratio $\bar{v}_W/\bar{v}_N$ takes on exactly the same value, 2.6, as was found by Vanzo. Furthermore, the shape of the particle size distribution observed in this work is very similar to that reported by Vanzo[15]. Fig. 8 shows a particle size distribution. The curve is asymetric, tailing off at large particle sizes. There is a relatively sharp peak at 700 Å. Finally, as shown in Appendix I there is very good agreement between the weight-average particle volume determined by light scattering and electron microscopy. In this investigation it has therefore also been assumed that the ratio $\bar{v}_W/\bar{v}_N = 2.6$ is representative of the polymerizing systems investigated, and the number-average particle volume and number have been determined from light scattering data in conjunction with the weight-average to number-average ratio.

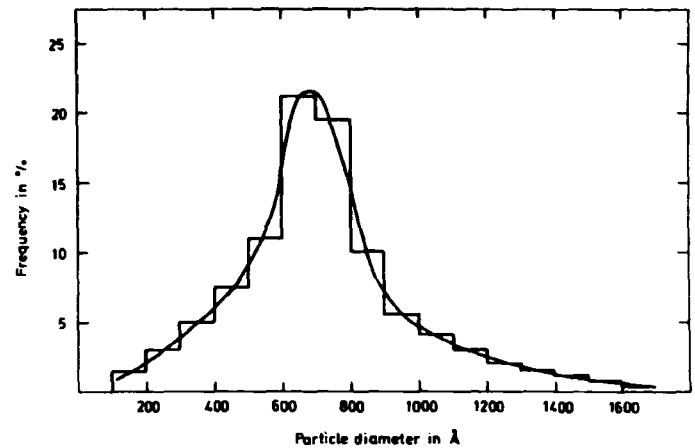

Fig. 8. Particle size distribution.

3.3.2. Reproducibility of the Conversion versus Time Curve

It will appear from the subsequent sections that the various parameters studied here only exert relatively small effects on the rate of polymerization and on the shape of the polymerization curve. This is particularly the case with the emulsifier concentration. It is therefore reasonable to consider the reproducibility of the conversion versus time curve in relation to the effect exerted by the various parameters studied here. Figs. 9 and 10 show polymerization curves from experiments with different emulsifier types. In both cases the curves are obtained by double determination, and it appears that the reproducibility is very good. Figs. 9 and 10 should be compared with fig. 12 which shows the effect of emulsifier concentration on the course of polymerization.

In polymerization of vinyl monomers it is generally observed that a certain time elapses between the addition of initiator and the commencement of polymerization. This was also observed in the present investigation. This induction period is generally attributed to the presence of oxygen. It has been shown by Dunn and Taylor[26] and Napper and Parts[20] that the duration of the induction period does not affect the subsequent course of the reaction, and therefore the induction period has been deducted in the plots shown in figs. 9 and 10 and also in the various plots shown in the following

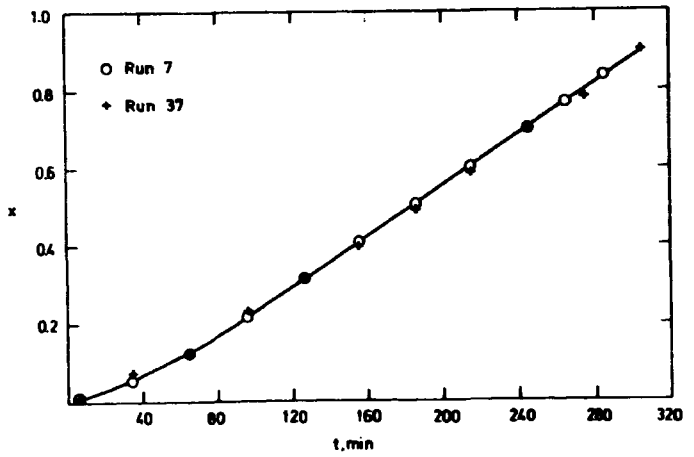

Fig. 9. Conversion versus time plots showing experimental reproducibility. 9.5 g SLS/1 H_2O. 5×10^{-4} moles $K_2S_2O_8$/1 H_2O. 50°C.

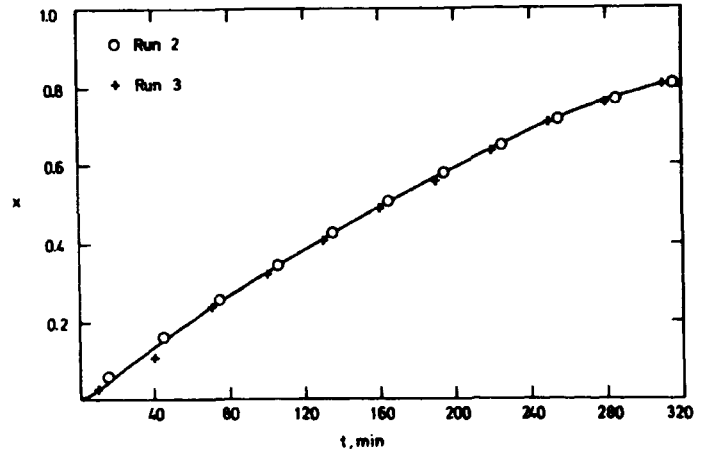

Fig. 10. Conversion versus time plots showing experimental reproducibility. 11.5 g SDBS/1 H_2O. 10^{-3} moles $K_2S_2O_8$/ H_2O. 50°C.

sections. In most of the experiments the induction period amounted to 20 - 40 minutes. However, it was not possible to reproduce the length of the induction period with great accuracy.

3.3.3. Shape of the Conversion versus Time Curve

For the deduction of emulsion polymerization kinetics it may be illuminating to study the shape of the polymerization curve and the change in shape upon variation of various parameters.

Fig. 11 shows typical conversion versus time plots obtained at different initiation rates. It appears that the rate of polymerization is constant over most of the conversion range. This is in agreement with the general conception of vinyl acetate emulsion polymerization. Furthermore, the shape of the curves is independent of the initiation rate.

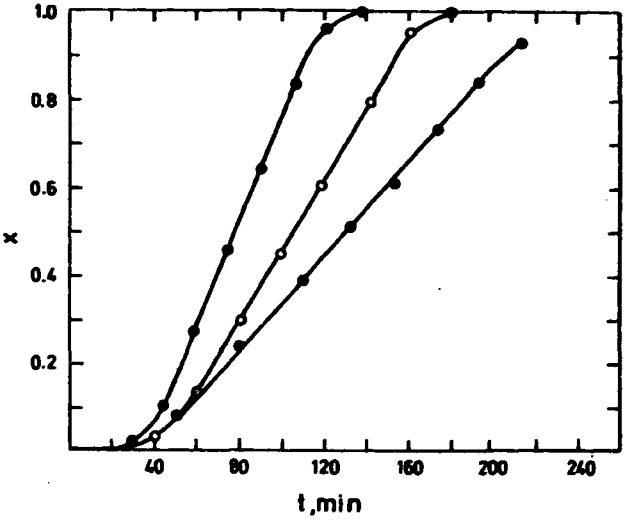

Fig. 11. Conversion versus time plots at different initiation rates. ● 4×10^{-3}, ○ 2×10^{-3}, ⊕ 10^{-3} moles $K_2S_2O_8$/1 H_2O. 9.5 g SLS/1 H_2O. 50°C.

During a study of the effect of emulsifier concentration on polymerization rate it was observed that the emulsifier concentration exerts a certain effect on the shape of the polymerization curve. At high emulsifier concentrations the rate of polymerization begins to decrease from 80% conversion. At low concentration, i. e. when the particles are relatively large, there is a slight acceleration in polymerization rate beginning at 70% conversion. This effect, which was reproduced several times, is shown in fig. 12.

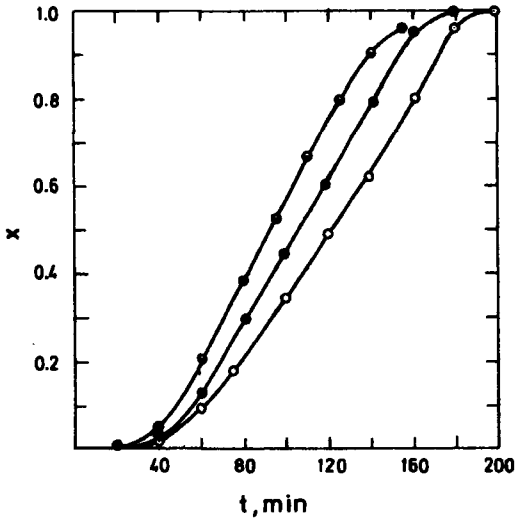

Fig. 12. Conversion versus time plots at different emulsifier concentrations. ⊖ 24.0, ● 9.5, ○ 2.4 g SLS/l H_2O. 2×10^{-3} moles $K_2S_2O_8$/l H_2O. 50°C.

The above results were all obtained from experiments with sodium lauryl sulphate (SLS) as emulsifier, which is the emulsifier generally used in research and for industrial application. However, a few experiments with sodium dodecylbenzene sulphonate (SDBS) were also performed, and in these experiments some very peculiar effects were observed. Thus, at low concentrations of SDBS the conversion versus time plot takes a form similar to that obtained with SLS. At higher concentrations of SDBS the shape of the curve is completely different, in that the rate of polymerization is declining already at 35 - 45% conversion as shown in fig. 13b. As far as

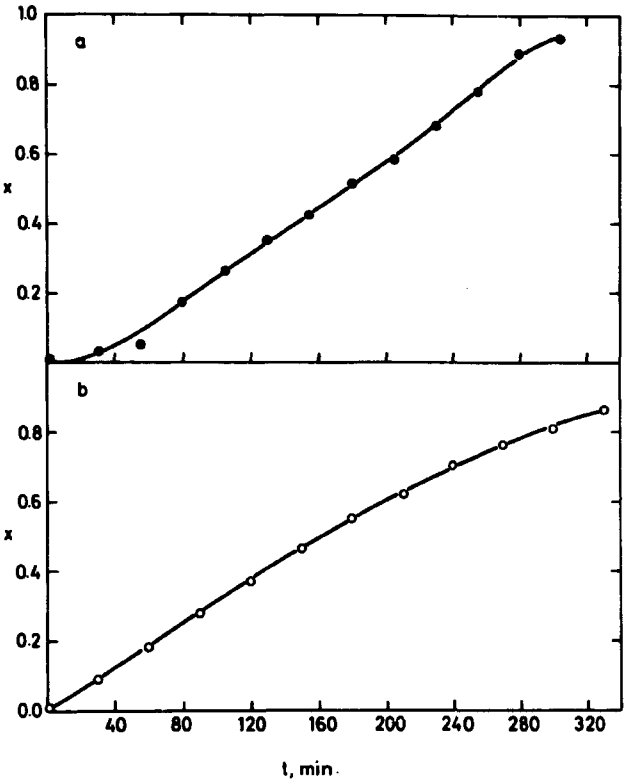

Fig. 13. Conversion versus time plots at different emulsifier concentrations. ● 2.9, ○ 11,5 g SDBS/l H_2O. 10^{-3} moles $K_2S_2O_8$/l H_2O. 50°C.

it is known such a behaviour has not been reported from any previous investigation of vinyl acetate emulsion polymerization. Although the cause of the change-over in polymerization kinetics is not clear, it is believed that it is due to a chemical rather than a physical effect, such as instability of the emulsion, resulting in particle coalescing. Thus, as will be shown in subsection 3. 3. 5, the particle number remains constant even though the rate of polymerization decreases. Furthermore, with the same molar concentration of emulsifier the rate of polymerization is approximately

twice as high with SLS as with SDBS as emulsifier although the number of particles is very nearly the same. Finally, if SDBS is added to a polymerizing system initially containing only a small amount of SDBS (2.9 g/l H_2O), the rate of polymerization begins to decrease if the new concentration of SDBS equals the concentration (11.5 g/l H_2O) at which the rate of polymerization would begin to decrease already at 35 - 45% conversion. This appears from fig. 14.

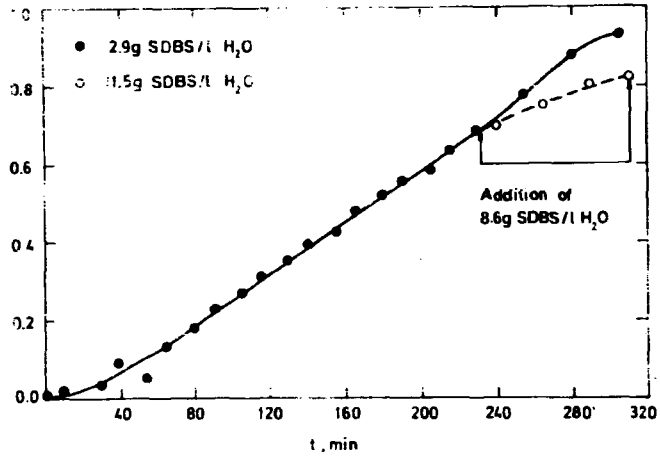

Fig. 14. Effect of addition of an extra amount of SDBS to a polymerising system initially containing 2.9 g SDBS. 10^{-3} moles $K_2S_2O_8$/l H_2O. 50°C.

It cannot be excluded that the emulsifier SDBS interferes chemically with the polymerization. SDBS contains a benzene group, and it has been reported[42] that benzene, ethylbenzene, isopropylbenzene, and several other compounds containing benzene are all strong retarders in vinyl acetate polymerization.

3.3.4. Disappearance of the Separate Monomer Phase

In order to establish the point at which the separate monomer phase disappears, latex samples were withdrawn at regular intervals early in the polymerization. The samples were centrifuged for 15 minutes at 2000 rpm. The amount of vinyl acetate separated in this way was measured with a graduated scale and taken to equal the amount of vinyl acetate present as monomer droplets in the emulsion. Fig. 15 shows a plot of this quantity in ml vinyl acetate/ml emulsion as a function of conversion. From this curve it appears that the separate monomer phase vanishes at 20% conversion, independently of the concentration of emulsifier. This result compares favourably with the value 23% reported by Nomura[28].

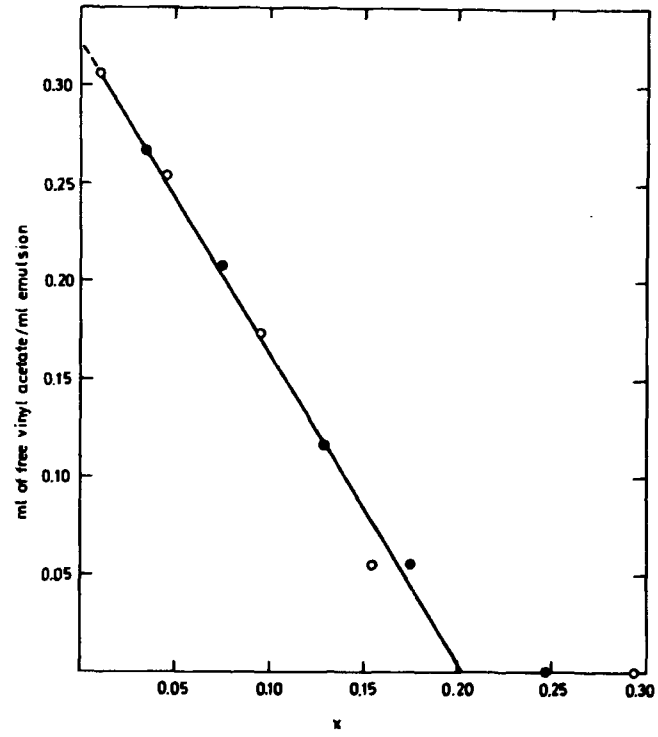

Fig. 15. Amount of vinyl acetate present as a separate monomer phase as a function of conversion. ○ 24.0, ● 2.4 g SLS/l H_2O. 10^{-3} moles $K_2S_2O_8$/l H_2O. 50°C.

Further evidence of the validity of the results obtained by this technique is the fact that extrapolation to zero conversion gives a value of 0.32 ml vinyl acetate/ml emulsion, which is the initial composition of the emulsion.

3.3.5. Number of Particles during Polymerization

For the elucidation of emulsion polymerization kinetics it is of fundamental importance to know the variation of the number of particles during the polymerization. In the present work the number of particles was determined as a function of conversion by light scattering measurements on samples withdrawn at regular intervals during the polymerization. In figs. 16 and 17 are shown plots of the number of particles, N, versus conversion and it appears that N remains constant in the interval 10 - 15 to 100% conversion. This is in agreement with the findings of Napper and Parts[20].

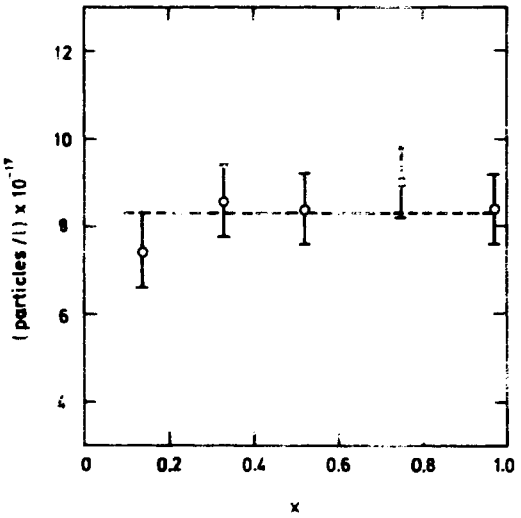

Fig. 16. Number of particles versus conversion. 9.5 g SLS/1 H_2O. 2×10^{-3} moles $K_2S_2O_8$/1 H_2O. 50°C.

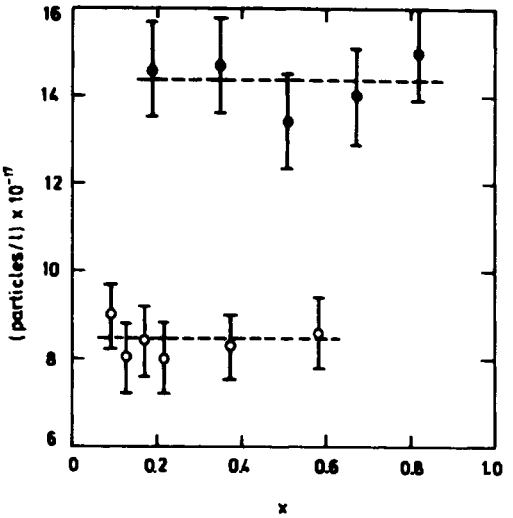

Fig. 17. Number of particles versus conversion. ○ 9.5, ● 24.0 g SLS/1 H_2O. 10^{-3} moles $K_2S_2O_8$/1 H_2O. 50°C.

In the above experiments SLS was used as emulsifier. Latices prepared with SDBS as emulsifier were studied in a similar fashion, and fig. 18 shows that also in this case the number of particles remains constant in the range of conversion investigated. By comparison of the plot shown in fig. 18 with the corresponding conversion versus time curve in fig. 13b it can be concluded that the observed decrease in rate of polymerization cannot be attributed to a decrease in number of particles.

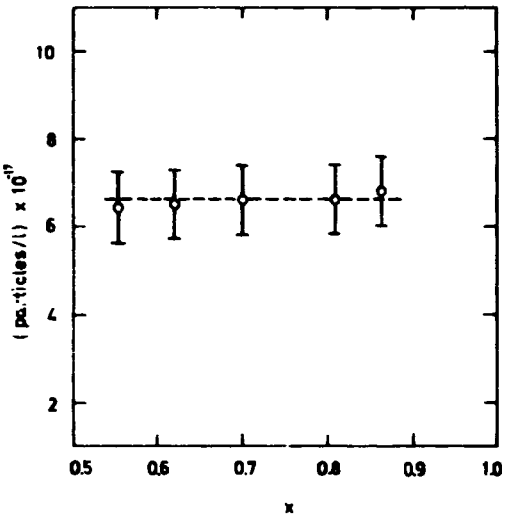

Fig. 18. Number of particles versus conversion. 11.5 g SDBS/l H_2O. 10^{-3} moles $K_2S_2O_8$/l H_2O. 50°C.

3.3.6. Effect of Emulsifier Concentration

The effect of emulsifier concentration and emulsifier type on the shape of the polymerization curve was considered in subsection 3.3.3. This section deals with the effect of emulsifier concentration on the number of polymer particles and rate of polymerization.

The rate of polymerization, R_p, is calculated from the slope of the linear portion of the conversion versus time plots. Fig. 19 shows log-log plots of R_p versus emulsifier concentration at three different rates of initiation. It appears that within the limits of error the effect of emulsifier concentration is independent of the initiation rate. From the slope of the straight lines the 90% confidence limits for the emulsifier dependence exponent are calculated to be 0.12 ± 0.02. Although this power is much smaller than the 0.6 power predicted in the classic theory of emulsion polymerization, it is, nevertheless, generally agreed in the literature that the emulsifier does not affect the rate of polymerization to the same extent in vinyl acetate as in styrene emulsion polymerization.

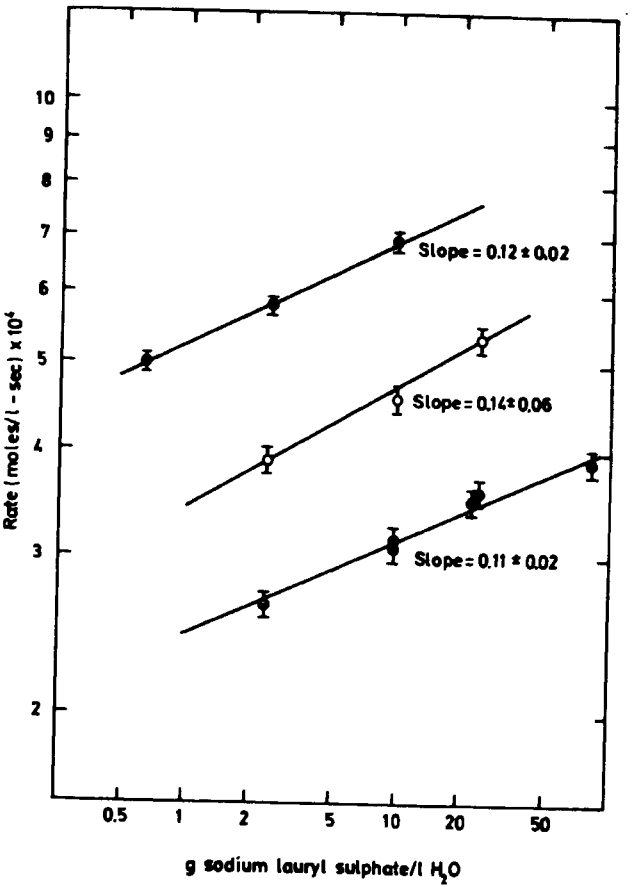

Fig. 19. Effect of emulsifier concentration on polymerisation rate at different rates of initiation. ● 4×10^{-3}, ○ 2×10^{-3}, ⊖ 10^{-3} moles $K_2S_2O_8$/l H_2O. 50°C. The uncertainty on the determination of polymerisation rate is assessed at ± 3%.

The effect of emulsifier concentration on the number of polymer particles was investigated at a persulphate concentration of 10^{-3} moles/l H_2O. From fig. 20 it appears that the number of polymer particles increases with increasing emulsifier concentration, and from the slope of the straight line the emulsifier dependence exponent is calculated to be 0.52 ± 0.17. This value is in good agreement with the data recently reported by Nomura et al.[28].

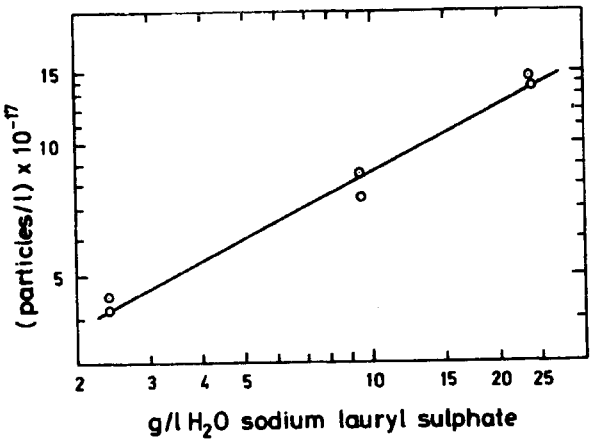

Fig. 20. Effect of emulsifier concentration on number of polymer particles. 10^{-3} moles $K_2S_2O_8$/1 H_2O. 50°C.

When R_p is plotted against the number of particles, it is found that the rate of polymerization is proportional to the power 0.25 ± 0.07 of the number of particles. This result is also obtained from the relationship between emulsifier concentration and number of polymer particles and polymerization rate respectively. The value 0.25 compares favourably with the value 0.2 reported by Patsiga[14]. For the sake of comparison it should be mentioned that in styrene emulsion polymerization the rate of polymerization is first order with respect to number of particles. However, the relatively small effect of the number of particles is not unique for vinyl acetate emulsion polymerization. Thus, Ugelstad[43] has reported that the order of reaction with respect to number of particles is 0.05 to 0.15 in vinyl chloride emulsion polymerization.

Fig. 21 shows a plot of limiting viscosity number $[\eta]$ versus conversion at two different emulsifier concentrations. It appears that there is no significant change in $[\eta]$ as the emulsifier concentration is changed. Since the number of particles varies with emulsifier concentration this means that $[\eta]$ is also independent of the particle number.

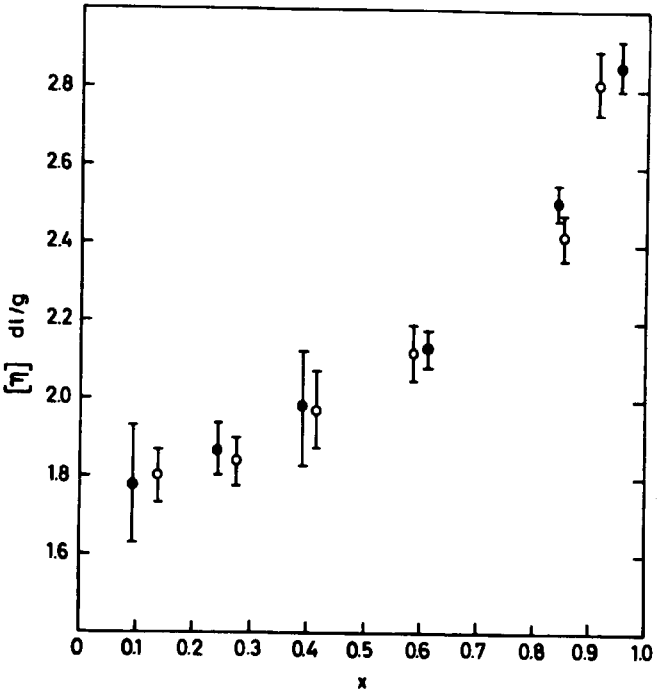

Fig. 21. Limiting viscosity number of poly (vinyl acetate) as a function of conversion at different emulsifier concentrations. ● 9.5 g SLS/1 H_2O, 8.6×10^{17} particles/l. ○ 2.4 g SLS/1 H_2O, 4.25×10^{17} particles/l. 10^{-3} moles $K_2S_2O_8$/1 H_2O. 50°C. The points of measurement are shown with their 80% confidence limits.

3.3.7. Effect of Initiator Concentration

The influence of initiator concentration on the rate of polymerization was investigated at two different emulsifier concentrations. Fig. 22 shows log-log plots of polymerization rate versus initiator concentration. From

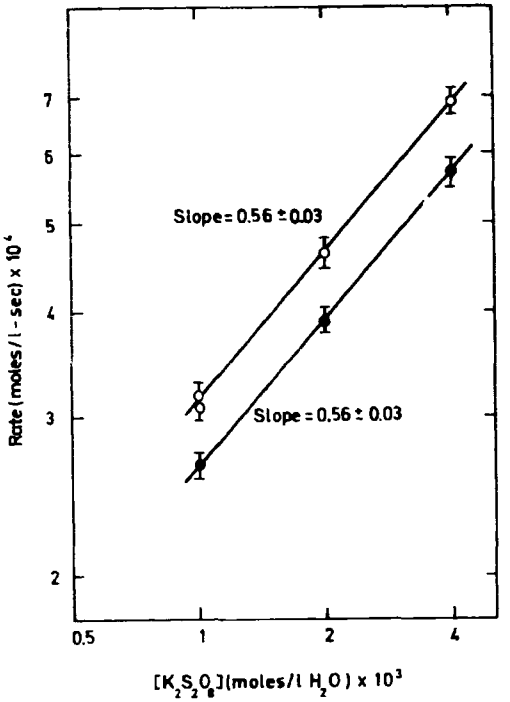

Fig. 22. Effect of initiator concentration on polymerization rate at two different emulsifier concentrations. ● 2.4, ○ 9.5 g SLS/l H_2O. 10^{-3} moles $K_2S_2O_8$/l H_2O. 50°C. The uncertainty on the determination of polymerization rate is assessed at ± 3%.

the slope of the lines the 90% confidence limits for the initiator dependence exponent is calculated to be 0.56 ± 0.02. Thus, the rate of polymerization is approximately proportional to the square root of initiator concentration. This is in agreement with the findings of Dunn and Taylor[26] and Gershberg[25], but contrary to the results reported by Stannett[27] and Patsiga[14], who observed a first-order dependence with respect to initiator concentration. For vinyl chloride Ugelstad[43] has reported the order 0.5 with respec to initiator concentration.

The effect of addition of an extra amount of initiator during the polymerization was also investigated. Fig. 23 shows that the polymerization rate

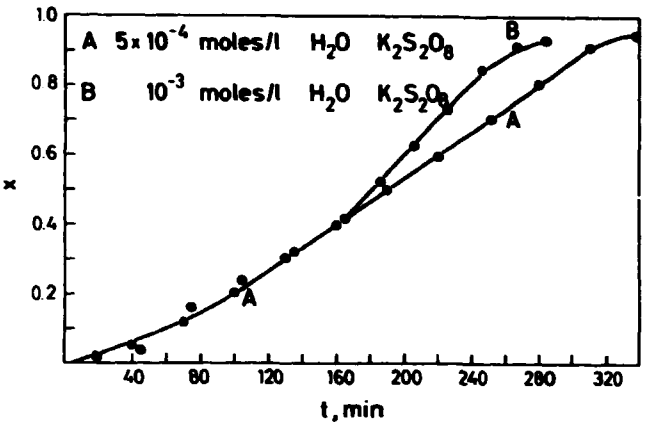

Fig. 23. Effect of addition of an extra amount of initiator during the polymerization. 9.5 g SLS/l H_2O. 50°C.

increases when more initiator is added. From the slope of the curves it is found that the ratio between rates before and after the addition is approximately proportional to the square root of the ratio between the respective initiator concentrations. This effect is also observed in vinyl chloride emulsion polymerization[44], but ordinarily not in styrene polymerization.

In fig. 24 is shown the number of particles as a function of conversion at three different initiator concentrations. Although the points are somewhat scattered, it is reasonable to conclude that the initiator concentration does not affect the number of particles. Also at this point the emulsion polymerization of vinyl acetate resembles that of vinyl chloride[44,45], but is different from styrene where the number of particles depends on the initiator concentration to the 0.4 power. The resemblence between vinyl chloride and vinyl acetate is further pronounced from the fact that in both cases the number of particles becomes constant early in the polymerization[44,45].

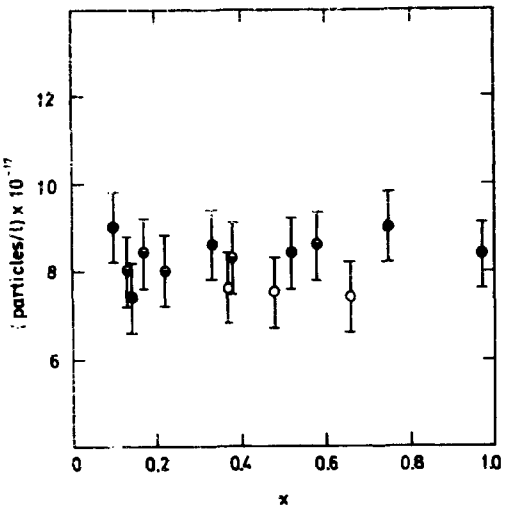

Fig. 24. Number of particles versus conversion at three different initiator concentrations. ● 2×10^{-3}, ⊖ 10^{-3}, ○ 5×10^{-4} moles $K_2S_2O_8$/l H_2O. 9.5 g SLS/l H_2O. 50°C.

In fig. 25 is plotted the limiting viscosity number $[\eta]$ versus conversion at three different initiator concentrations, and it appears that $[\eta]$ is independent of the initiator concentration. The independence of $[\eta]$ of initiator concentration and number of polymer particles suggests that the molecular weight is controlled primarily by transfer to monomer and polymer. This matter will be discussed in further detail in subsection 3.4.3.

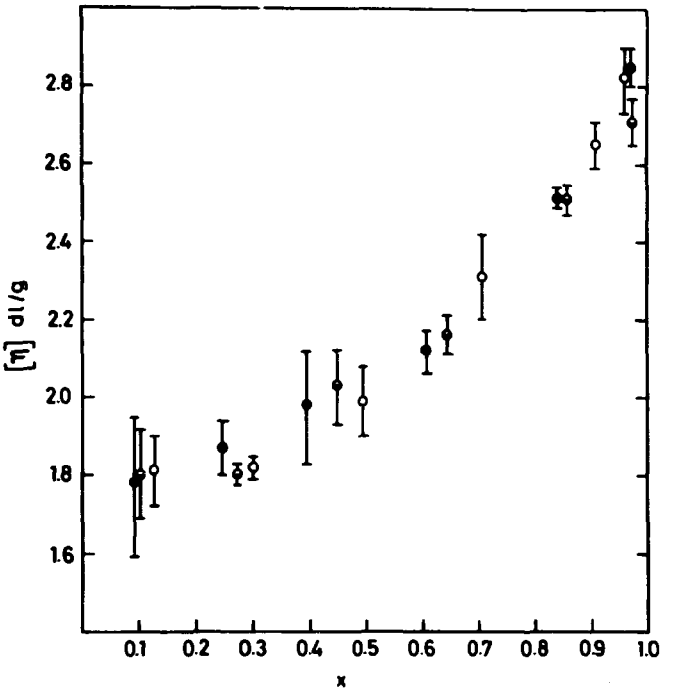

Fig. 25. Limiting viscosity number of poly (vinyl acetate) as a function of conversion at different rates of initiation. ○ 5×10^{-4}, ● 10^{-3}, ⊖ 4×10^{-3} moles $K_2S_2O_8$/l H_2O. 9.5 g SLS. 50°C.

3.3.8. Effect of Electrolytes

Patsiga[14] and Stannett et al.[27] have investigated the effect of adding electrolytes to polymerizing systems. They have found that both phosphate buffer and potassium sulphate increase the rate of polymerization. Phosphate buffer exerted the strongest effect of the two. The rate of polymerization in emulsions containing 0.05 moles/l H_2O phosphate buffer was nearly twice as high as in systems where no buffer was added.

An attempt to reproduce these effects failed. Fig. 26 shows that the rate of polymerization is unaffected by addition of 0.02 moles/l Na_2HPO_4, and the same result was obtained in similar experiments with potassium sulphate.

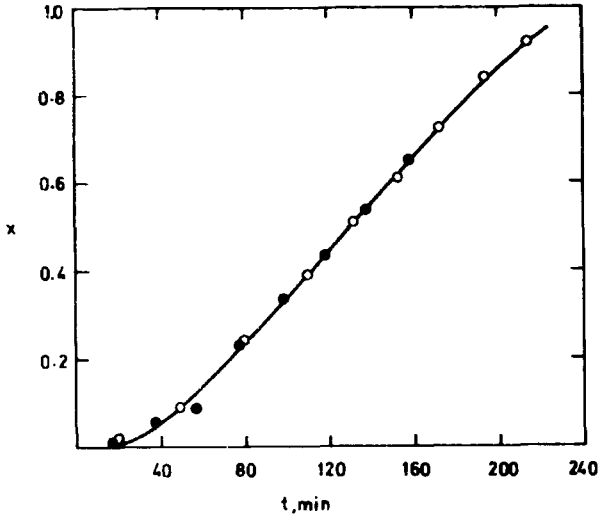

Fig. 26. Conversion versus time plots at different concentrations of Na_2HPO_4. ○ 0.02 moles Na_2HPO_4/1 H_2O. ● No salt added. 10^{-3} moles $K_2S_2O_8$/1 H_2O. 9.5 g SLS/1 H_2O. 50°C.

3.3.9. Effect of Temperature

Only a cursory study of the effect of temperature was performed. The purpose of these experiments was to investigate whether there was a difference between the temperature effect on the rate of polymerization of emulsions containing SLS and SDBS, and also to study the temperature effect on the limiting viscosity number.

Figs. 27 and 28 show conversion histories obtained with SLS and SDBS at 50° and 60°C. From the plots the average energy of activation is calculated to be 23.0 and 24.6 kcal/mole for emulsions containing SLS and SDBS respectively. The difference 1.6 kcal/mole lies within experimental error, and a possible interference of the emulsifier SDBS with the polymerization is therefore not reflected significantly in the overall energy of activation.

The effect of temperature on the limiting viscosity number, $[\eta]$, is reflected in fig. 29, where $[\eta]$ of polymers produced at 50 and 60°C is plotted versus conversion. As usually observed, $[\eta]$ decreases with increasing temperature.

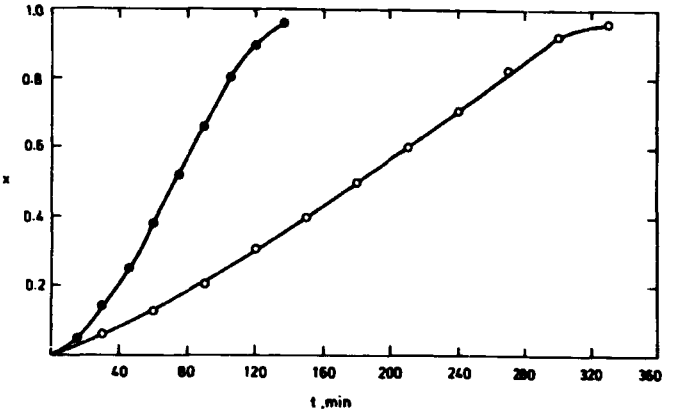

Fig. 27. Conversion versus time plots at two different temperatures. ○ 50°C. ● 60°C. 9.5 g SLS/1 H_2O. 5×10^{-4} moles $K_2S_2O_8$/1 H_2O.

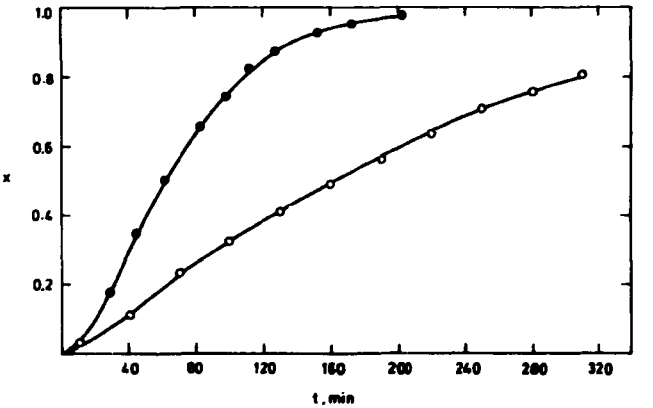

Fig. 28. Conversion versus time plots at two different temperatures. ○ 50°C. ● 60°C. 11.5 g SDBS/1 H_2O. 10^{-3} moles $K_2S_2O_8$/1 H_2O.

Owing to the likelihood of extensive branching of vinyl acetate polymerization at high conversions, transformation of the viscosity data to molecular weight was omitted in the plots shown in fig. 29. However, as shown by Stein[46], samples withdrawn before 20% conversion are nearly unbranched, and for such samples it is possible by means of a Mark-Houwink equation to obtain from viscosity data an approximate value for the molecular weight. As already suggested in subsections 3.3.6 and 3.3.7 molecular weights of polymers produced in vinyl acetate emulsion polymerization may be controlled primarily by transfer to monomer and polymer. For polymers

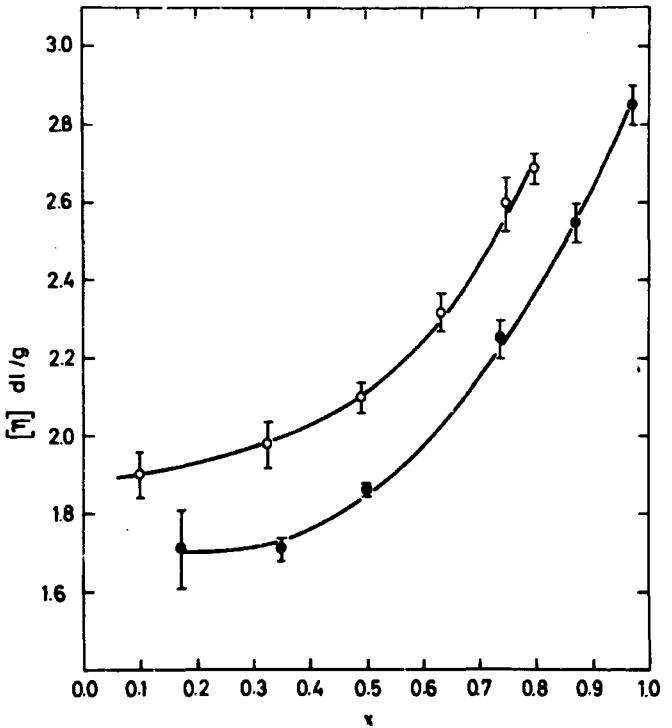

Fig. 29. Limiting viscosity number of poly (vinyl acetate) solutions versus conversion at two different temperatures. ○ 50°C. ● 60°C. 11.5 g SDBS/l H_2O. 10^{-3} moles $K_2S_2O_8$/l H_2O. The points of measurement are shown with their 80% confidence limits.

produced at conversions below 20%, transfer to polymer and terminal double bond polymerization may be neglected in molecular weight considerations, and the principal factor controlling molecular weight is transfer to monomer. In this case it is easily shown that

$$\ln \frac{M_{T1}}{M_{T2}} = \frac{E_{tr} - E_p}{R} \left(\frac{1}{T_1} - \frac{1}{T_2}\right), \qquad (18)$$

where M_{T1} and M_{T2} denote molecular weights of polymers produced at temperatures T_1 and T_2 respectively, E_{tr} and E_p are energies of activation for transfer to monomer and propagation respectively, and R is the gas constant. Substitution of the Mark-Houwink equation

$$[\eta] = KM^a \qquad (19)$$

into eq. (18) gives the following relationship between the limiting viscosity number $[\eta]$ and the temperature

$$\ln \left(\frac{[\eta]_{T1}}{[\eta]_{T2}}\right)^{1/a} = \frac{E_{tr} - E_p}{R} \left(\frac{1}{T_1} - \frac{1}{T_2}\right). \qquad (20)$$

Introducing values of $[\eta]$ measured at 15% conversion and using the value 0.72 for a[47], the difference $E_{tr} - E_p$ is calculated to be 3.4 kcal/mole. This result compares reasonably with the value 2.9 kcal/mole reported by Dixon-Lewis[48], and also with the value 2.7 kcal/mole calculated from data of Bevington[39] and Motoyama[39]. The determination of $[\eta]$ is not very accurate, and the above computations should therefore be regarded with reservation, the more so as they involve a calculation of number average molecular weight by using a Mark-Houwink equation on moleculary heterogeneous polymers.

3.3.10. Effect of Stirring Rate

During the initial stages of an emulsion polymerization agitation is most important to maintain the intimate mixture of water and monomer. An effect of stirring rate on the rate of polymerization could not be excluded in advance, and therefore a few experiments with different stirring rates were conducted. However, as appears from fig. 30, the rate of polymerization is unaffected by a change in agitation rate from 280 – 560 rpm.

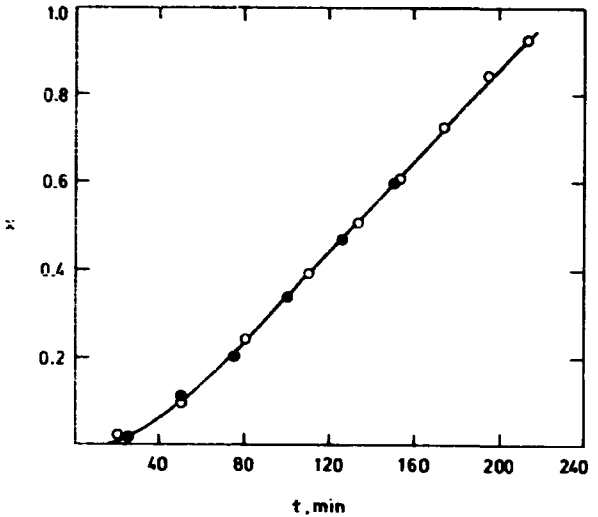

Fig. 30. Conversion versus time plots at different stirring rates. ○ 280 rpm. ● 560 rpm. 9.5 g SLS/l H_2O. 10^{-3} moles $K_2S_2O_8$/l H_2O. 50°C.

Below 150 rpm it is not possible to maintain good mixing in the system, and above 700 rpm the emulsions become unstable, when the conversion exceeds 50 - 60%.

3.3.11. Bulk Polymerization of Vinyl Acetate

In emulsion polymerization a single polymer particle can be regarded as a locus of bulk polymerization with intermittent initiation. A decrease in termination rate, which is observed in bulk polymerization, should therefore also occur in a single polymer particle. For the sake of comparison vinyl acetate was polymerized in bulk at 50°C with α, α'- azobisisobutyronitrile as initiator, and fig. 31 shows a conversion versus time plot obtained from such an experiment. Together with the experimental curve is shown the theoretical curve obtained by integration of the rate expression for bulk polymerization given in eq. 21.

$$-d[M]/dt = k_p[M](k_r f[I]/k_{tp})^{1/2}, \qquad (21)$$

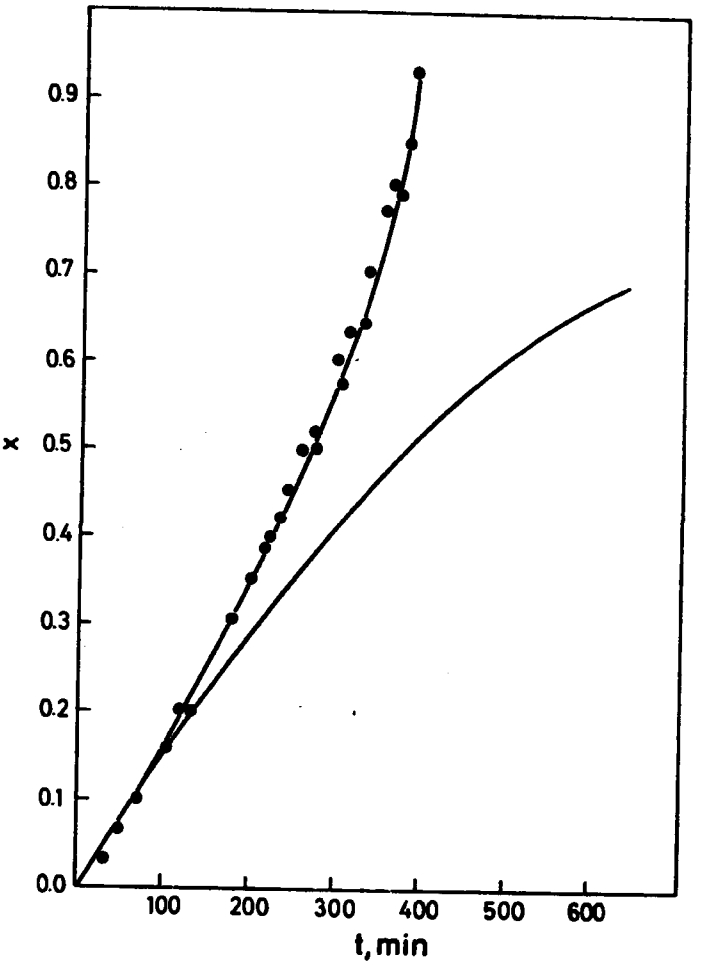

Fig. 31. Bulk polymerisation of vinyl acetate at 50°C. 4×10^{-3} moles AIBN/l. ◆ Experimental. — Theoretical.

where [M] denotes concentration of monomer, and t reaction time. k_p, k_r, and k_{tp} are rate constants for propagation, initiator decomposition, and termination respectively. [I] denotes initiator concentration, and f is an initiator efficiency factor. The theoretical curve is obtained by using the following values for the rate constants

$$k_p = 3500 \text{ l/mole-sec}^{39)}$$

$$k_{tp} = 10^8 \text{ l/mole-sec}^{39)}$$

$$fk_r = 1.7 \times 10^{-6}/\text{sec}^{49)}.$$

The computations are based on the assumption that [I] remains constant during the polymerization. This is reasonable, since it can be calculated that less than 2% of the initiator is consumed during the reaction. The initiator efficiency factor is also assumed to be constant, although it may decrease somewhat during the polymerization.

From fig. 31 it appears that there is an appreciable autoacceleration, beginning at 10% conversion. On the assumption that k_p remains constant during the polymerization, k_{tp} can be obtained as a function of conversion by fitting the theoretical expression given in eq. 21 to the experimental curve in fig. 31. The curve fitting was performed on a digital computer by means of Chebyshev polynomials. Eq. 22 gives the relation between k_{tp} and conversion x thus obtained.

$$k_{tp} = 2 \exp (A + A_1 x + A_2 x^2 + A_3 x^3) \text{ l/mole sec}, \qquad (22)$$

where

$$A = 17.6620$$

$$A_1 = -0.4407$$

$$A_2 = -6.7530$$

$$A_3 = -0.3495.$$

In fig. 32 is shown the corresponding plot of k_{tp} versus conversion, and for the sake of comparison fig. 33 shows a similar curve obtained from bulk polymerization of styrene at 50°C[50]. In both cases k_{tp} decreases rapidly with conversion.

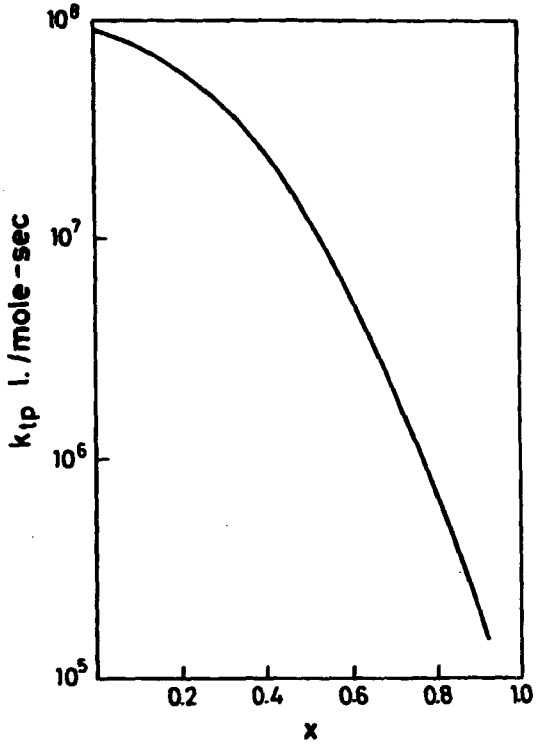

Fig. 32. Termination rate constant versus conversion in bulk polymerization of vinyl acetate at 50°C.

The assumption that k_p remains constant during the polymerization is in agreement with the conclusions of Schulz[51]. Most investigators adhere to the opinion that the propagation rate constant is independent of conversion when the polymerization is conducted at temperatures higher than the glass-transition temperature of the polymer being produced. This is the case in the present investigation since the glass-transition temperature of poly(vinyl acetate) is 28°C[59, 60].

The application of eq. 22 to emulsion polymerization will be discussed in subsection 3.4.2.

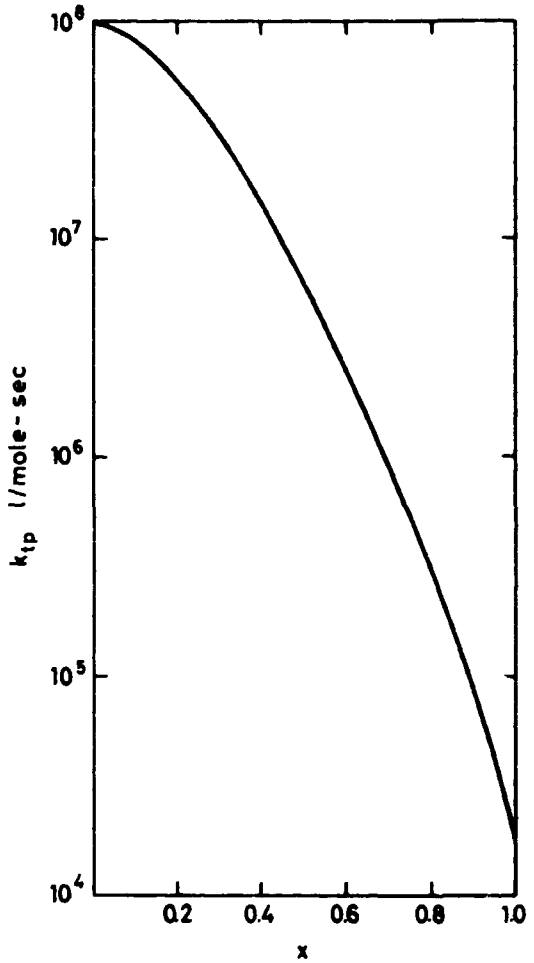

Fig. 33. Termination rate constant versus conversion in bulk polymerization of styrene at 50°C [50].

3.4. Discussion

3.4.1. Introduction

A characteristic feature in vinyl acetate emulsion polymerization is that the rate of polymerization is constant over most of the conversion range. This behaviour was also observed in the present investigation in experiments with SLS as emulsifier. The transition in kinetics, which was observed in experiments with the emulsifier SDBS, is an interesting phenomenon, which, however, should be considered as an exception. As far as it is known this effect has not been observed in experiments with other emulsifiers, neither of the nonionic nor of the anionic type. The effect may be due to reaction of SDBS with free radicals, but since this reaction is not known in detail and it is not known whether it takes place in the aqueous phase, in the polymer phase, or in the boundary layer between the two phases, it is impossible at present to account for this behaviour in a model for vinyl acetate emulsion polymerization.

The results obtained with the emulsifier SLS are supposed to be characteristic of vinyl acetate emulsion polymerization, and the subsequent discussion will be based on these results.

In recapitulation of the data presented in the preceding sections the following points concerning vinyl acetate emulsion polymerization can be established.

I The average concentration of free radicals per particle increases with increasing initiator concentration.

II The rate of polymerization is approximately proportional to the square root of the initiator concentration in the inverval 10^{-3} to 4×10^{-3} moles $K_2S_2O_8$/l H_2O.

III The rate of polymerization is proportional to the 0.25 power of the number of particles.

IV The number of polymer particles remains constant in the interval 10 - 15 to 100% conversion.

V The number of polymer particles is independent of the initiator concentration.

VI The number of polymer particles is approximately proportional to the square root of the emulsifier concentration.

VII The limiting viscosity number is independent of the initiator concentration, emulsifier concentration, and number of polymer particles.

This picture does not resemble that of styrene emulsion polymerization, but as it has been pointed out several times there is a remarkable resemblance to vinyl chloride emulsion polymerization[43,44,45].

If it is assumed that the polymerization takes place solely in the monomer-swollen polymer particles, then the average number of free radicals per particle, $\bar{n}$, can be calculated from eq. 23

$$R_p = k_p[M_p]N\bar{n}/N_A . \tag{23}$$

With $[M_p]$ obtained from a material balance (compare eqs. 35 and 36) and N obtained from particle size analysis it can be calculated that in any of the experiments performed here $\bar{n}$ is less than 0.025, a value which is small compared with unity. In vinyl chloride emulsion polymerization $\bar{n}$ is also small compared with unity[43]. Thus, in spite of the different natures of the two monomers they seem to behave quite similarly when polymerized in emulsion.

Fortunately, Ugelstad[43] has derived a very lucid and reasonable model for vinyl chloride emulsion polymerization, and it is the purpose here to show that with certain extensions this model is also applicable to vinyl acetate emulsion polymerization.

3.4.2. Presentation of the Model

As with the derivation of the recursion formula it is assumed that the rate of formation of particles containing n radicals at any time equals the rate of their disappearance. It is furthermore assumed that the rate of desorption of radicals from the particles is given as

$$R_{des} = k_d n N_n , \tag{24}$$

where N_n denotes the number of particles containing n free radicals, and k_d is a rate constant for desorption.

The total rate of reabsorption of radicals is assumed to be given as

$$R_{abs} = k_a C_w , \tag{25}$$

where C_w is the concentration of free radicals in the water phase, and k_a is a specific rate constant for the event.

Finally, it is assumed that at any time the initiation rate equals the termination rate, and that termination in the water phase is negligible.

Since the average concentration of radicals per particle is small compared with unity, only particles containing 0, 1, and 2 radicals need be considered, and with the above assumptions the following equations serve to define the kinetics:

$$\frac{dN_1}{dt} = k_a C_w \frac{N-(2N_1 + N_2)}{N} + 2k_d N_2 - k_d N_1 = 0 \tag{26}$$

$$\frac{dN_2}{dt} = k_a C_w \frac{N_1}{N} - 2k_d N_2 - 2k_{tp} \frac{N_2}{vN_A^2} = 0 \tag{27}$$

$$2k_i f[I] = 4k_{tp} \frac{N_2}{vN_A^2} . \tag{28}$$

In eq. 28 k_i denotes the decomposition rate constant of potassium persulphate.

An explicit solution of eqs. 26 - 28 can be obtained by using the approximation $N \gg N_1 \gg N_2$, and the number of particles containing one radical is found to be

$$N_1 = (2k_i f[I])^{1/2}\left(\frac{N_A^2 v_p}{2k_{tp}} + \frac{N}{2k_d}\right)^{1/2} . \tag{29}$$

Since the average concentration of free radicals per particle, $\bar{n}$, is given approximately as

$$\bar{n} \approx N_1/N ,$$

the rate of polymerization can be obtained from eq. 29 in conjunction with eq. 23:

$$R_p = \frac{k_p[M_p]}{N_A}(2k_i f[I])^{1/2}\left(\frac{N_A^2 v_p}{2k_{tp}} + \frac{N}{2k_d}\right)^{1/2} . \tag{30}$$

This equation has been derived by Ugelstad, and the assumptions on which it is based are discussed in detail in reference 43. It is seen that the rate constant k_a does not appear in the final rate expression. This is due to the

neglecting of termination in the aqueous phase.

To fit the rate expression given in eq. 30, Ugelstad has defined the desorption rate constant k_d as

$$k_d = K_d D_p (N/V_p)^{2/3} k_{tr}/k_p , \qquad (31)$$

where k_{tr} is the transfer constant to monomer, D_p is the self-diffusion coefficient of monomeric radicals in the polymer particles, and K_d is a numerical constant. Eq. 31 expresses that only monomeric radicals formed by transfer to monomer can escape the particles. In their treatment of emulsion polymerization Smith and Ewart[3] allow any radical the possibility of escaping the particles. Furthermore, in accordance with eq. 31 the rate of desorption is proportional to $v^{-2/3}$, where v denotes the volume of a latex particle. Smith and Ewart[3] propose that k_d is proportional to $v^{-1/3}$ (compare eq. 2).

In this work k_d will be defined in a different manner. Suppose a monomeric radical is formed by transfer to a monomer molecule. This radical can either escape the particle, or it can add a monomer molecule to form a dimeric radical. Less probable reactions, such as transfer to monomer or polymer and termination are neglected. If the radius of the particle is chosen as the mean displacement necessary for a radical to escape the particle, then the average time, τ, that elapses between the formation of the monomeric radical and its desorption from the particle can be obtained from Einstein's diffusion equation[52]

$$\sqrt{2D_p\tau} = r . \qquad (32)$$

The time lapse between successive additions of monomer molecules is given as $1/(k_p[M_p])$, and by comparison of this with eq. 32 the probability of the radical escaping the particle before adding one monomer molecule is given as

$$\Phi = \frac{2D_p}{r^2} / \left(\frac{2D_p}{r^2} + k_p[M_p]\right) . \qquad (33)$$

If desorption of dimeric and larger radicals is neglected owing to a rapid decrease in D_p, then the desorption rate constant is given as the product of Φ and the frequency at which monomeric radicals are being formed:

$$k_d = \Phi k_{tr}[M_p]/N_A . \qquad (34)$$

In vinyl chloride emulsion polymerization the separate monomer phase vanishes at 70-80% conversion. This means that the composition of the monomer-swollen polymer particles and with that the rate constants k_{tp} and k_d remain constant until that conversion is reached. In this case prediction of rates of polymerization by means of eq. 30 is a straightforward matter. In the case with vinyl acetate, however, the composition of the reaction medium is constant only until 20% conversion. This means that it is necessary to know k_{tp}, k_d, and $[M_p]$ as functions of conversion when predicting polymerization rates beyond that conversion.

The relationship between $[M_p]$ and conversion x is easily derived from a material balance, and is given in eqs. 35 and 36.

$$[M_p] = \frac{(1 - x)d_m}{(1 - x + xd_m/d_p)86} \text{ moles/l, } x > x_c , \qquad (35)$$

where d_m and d_p are densities in g/l of monomer and polymer respectively, and the factor 86 equals the molecular weight of vinyl acetate. x_c is the conversion at which the separate monomer phase vanishes ($x_c = 0.2$). At conversions equal to or below x_c, $[M_p]$ is given as

$$[M_p] = \frac{(1 - x_c)d_m}{(1 - x_c + x_c d_m/d_p)86} \text{ moles/l, } x \leq x_c . \qquad (36)$$

The relationship between k_{tp} and x is given in eq. 22. It is thus assumed that the termination rate constant in emulsion polymerization equals that in a bulk system with the same composition as the monomer-swollen polymer particles. There is no reason why this should not be the case.

The variation of k_d with conversion is due partly to a decrease in $[M_p]$ and partly to a decrease in D_p, the self-diffusion coefficient of monomeric radicals in the polymer particles. The variation in D_p with conversion is not known. However, since all other terms in eqs. 30, 33, and 34 can be expressed quantitatively as functions of conversion, it is possible to compute the variation in D_p by fitting eq. 30 to experimental data. Fig. 34 shows the relative decrease in D_p thus obtained, and it appears that D_p must diminish by two orders of magnitude in the interval 0 to 90% conversion

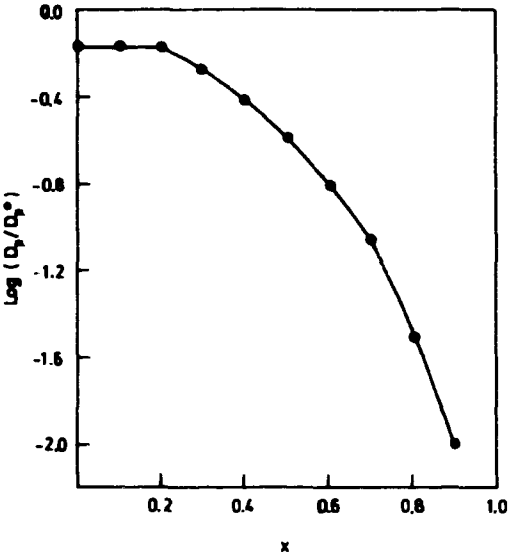

Fig. 34. Plot of log (D_p/D_p^o) versus conversion. Computed from experimental data with the aid of eqs. 30, 33, and 34.

for eq. 30 to fit experimental data. This is not unreasonable. In an investigation of the diffusion of water through swollen polymer membranes Peterlin et al.[53] have found a similar decrease in the self-diffusion coefficient of water in going from a highly swollen to a nearly dry membrane. On the basis of thermodynamic considerations these investigators have deduced a general expression for the self-diffusion coefficient of low-molecular-weight compounds in polymers:

$$D_p = D_p^o \exp(-\beta x_v(1-\alpha)/(1+\alpha x_v)) , \qquad (37)$$

where D_p^o is the self-diffusion coefficient of the diffusing compound in its own medium and

$$\beta = V^*/V_{fm}$$
$$\alpha = V_{fp}/V_{fm}$$
$$x_v = (1-H)/H .$$

V^* is a characteristic volume parameter describing the diffusion of a permeant molecule in the medium. According to Cohen and Turnbull[69], V^* is a critical free volume fraction proportional to the cross section of the diffusing molecule multiplied by the diffusional jump distance. V_{fm} and V_{fp} are free volume fractions of monomer and polymer respectively, and H is the volume fraction of the low molecular weight compound.

For the application of eq. 37 to emulsion polymerization the following relationship between x_v and conversion x is easily derived

$$x_v = \frac{x\, d_m}{(1-x)d_p} . \qquad (38)$$

Substitution of eq. 38 into eq. 37 gives

$$D_p = D_p^o \exp\left(\frac{-\beta x d_m(1-\alpha)}{(1-x)d_p + \alpha x d_m}\right) . \qquad (39)$$

By substitution of eq. 39 into eq. 33 and eq. 33 into eq. 30 the values of α and β can be calculated by fitting eq. 30 to experimental data. This gives the following values

$$\alpha = 0.3$$
$$\beta = 3.2.$$

In these computations eq. 30 was integrated numerically on a digital computer and the following values of the constants were used

k_p = 3500 l/mole-sec[39]
$2k_i f$ = 10^{-6}/sec
k_{tr} = 0.75 l/mole-sec[39]
d_p = 1150 g/l
d_m = 900 g/l
D_p^o = 10^{-8} dm^2/sec.

Kolthoff and Miller[54] have reported the value 10^{-6}/sec for k_i at 50°C. Thus, since f usually lies between 0.5 and 1, the value 10^{-6}/sec for $2k_i f$ is not unreasonable.

It has not been possible in the literature to find a value for the self-diffusion coefficient of vinyl acetate in vinyl acetate. However, the self-diffusion coefficient of many organic compounds lies between 10^{-7} and 10^{-8} dm^2/sec, and the value for D_p^o used here is therefore not unrealistic.

3.4.3. Analysis of the Model

From eq. 30 it appears that the model predicts that the rate of polymerization is proportional to the square root of initiator concentration. This compares reasonably with the experimental value 0.56. The fact that the experimental value is 0.56 and not exactly 0.5 may possibly be due to traces of oxygen added via the nitrogen purge gas. The presence of oxygen will cause part of the termination to take place as a first-order reaction, and this will result in an increase in the initiator dependence exponent. If this is the explanation, a rise in the initiator dependence exponent might be expected when going to low initiator concentrations. This was actually confirmed in a few experiments in which the initiator concentration was below 10^{-3} moles/l H_2O. Thus, when the polymerization rate measured from fig. 9 is compared to the rates measured from fig. 11, the initiator dependence exponent is found to be 0.65.

The exponential dependence of polymerization rate on number of particles is not immediately evident from eq. 30. For this reason the exponent from the relationship between number of particles and polymerization rate was calculated as a function of conversion, and fig. 35 shows the result of this computation. It appears that the exponent decreases from 0.35 to 0.19 in the interval 20 - 80% conversion. The experimental value was found to be 0.25 ± 0.07.

The parameters α and β should be further considered. As shown in Appendix II, α can be estimated to be 0.24 by means of the free-volume theory proposed by Bueche[65]. This value is in good agreement with the above-cited value of 0.3. Unfortunately, the value of β cannot be calculated theoretically, and it is therefore difficult to give an opinion on whether the value given above is reasonable. The only standard of reference is the value 4.5 reported by Peterlin et al.[53] for the diffusion of water through various membranes of different compositions.

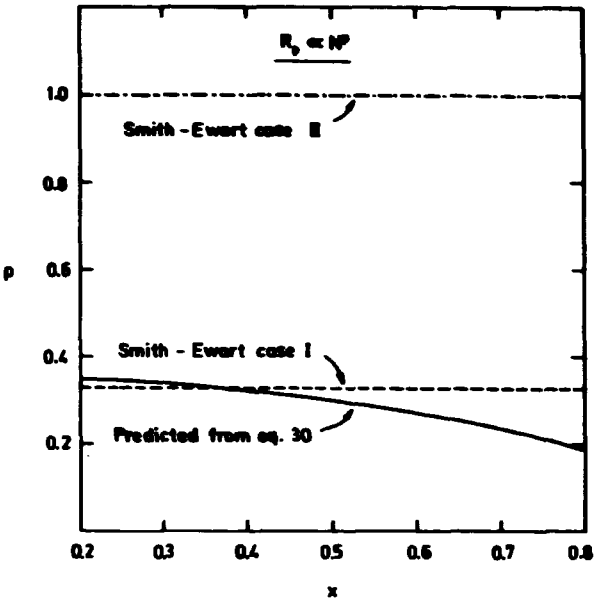

Fig. 35. The exponent p in $R_p \propto N^p$ as a function of conversion. The plots were obtained from eq. 30 and Smith-Ewart cases I and II.

Fig. 36 shows a comparison between experimental and calculated conversion versus time plots at different numbers of particles. The theoretical curves are obtained by integration of eq. 30, using the calculated values of α and β. It appears that the model correctly reflects the effect of number of particles on the rate of polymerization and the shape of the curves (compare subsection 3.3.3). In fig. 37 is shown a similar comparison between experimental and calculated conversion versus time plots at different rates of initiation.

Although the termination rate constant decreases rapidly during the polymerization, the term $N_A^2 v_p / k_{tp}$ only plays a secondary role for the rate of polymerization. This is illustrated in fig. 38, where the contribution of this term to the polymerization rate is calculated in per cent of the total polymerization rate as a function of conversion at different concentrations of polymer particles. Thus on the assumption that the model presented here is a phenomenological description of vinyl acetate emulsion polymeriz-

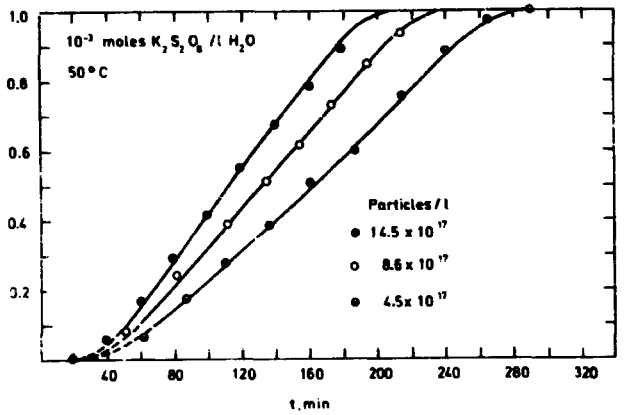

Fig. 36. Comparison between calculated and experimental conversion versus time plots. The solid lines were obtained by numerical integration of eq. 30, using the constants given on page 61.

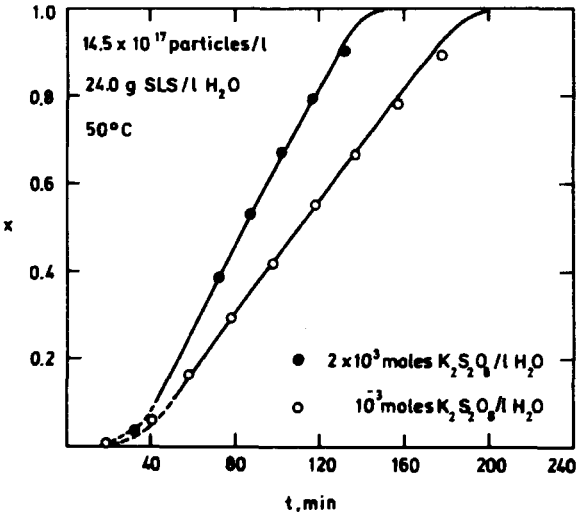

Fig. 37. Comparison between calculated and experimental conversion versus time plots. The solid lines were obtained by numerical integration of eq. 30, using the constants given on page 61.

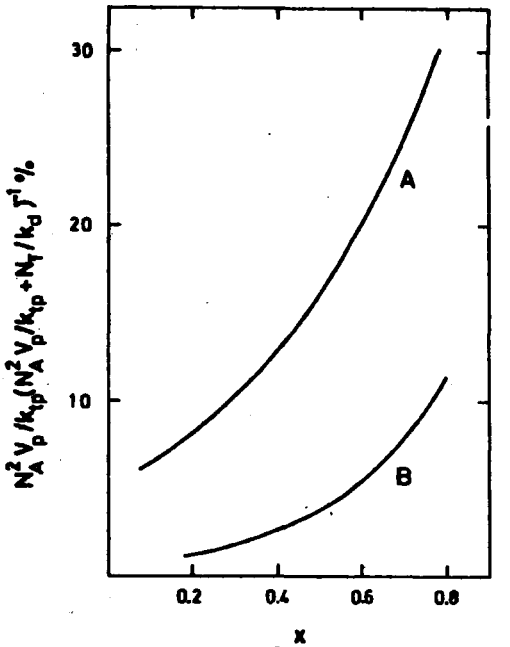

Fig. 38. Contribution of the term $N_A^2 V_p/k_{tp}$ to polymerization rate as a function of conversion.
Curve A: 5 x 10^{16} particles/l.
Curve B: 10^{18} particles/l.

ation, it can be concluded that the constant rate behaviour of the reaction is mainly due to a decrease in the desorption rate constant.

The fact that the limiting viscosity number is independent of initiation rate suggests that the molecular weight is not controlled by bimolecular termination, but rather by transfer to monomer and polymer and terminal double bond polymerization. If that is so, then the rate of termination, which in the stationary state equals the rate of initiation, should be much less than the sum of the rates of transfer to monomer and polymer. Fig. 38a shows calculated plots of the respective rates. The plots were obtained by using the model for calculation of N_f and the value 1.0 l/mole-sec for the rate constant for transfer to polymer at 50°C[39]. It appears that during most of the conversion range the rate of bimolecular termination is two orders of magnitude less than the sum of the rates of transfer to monomer

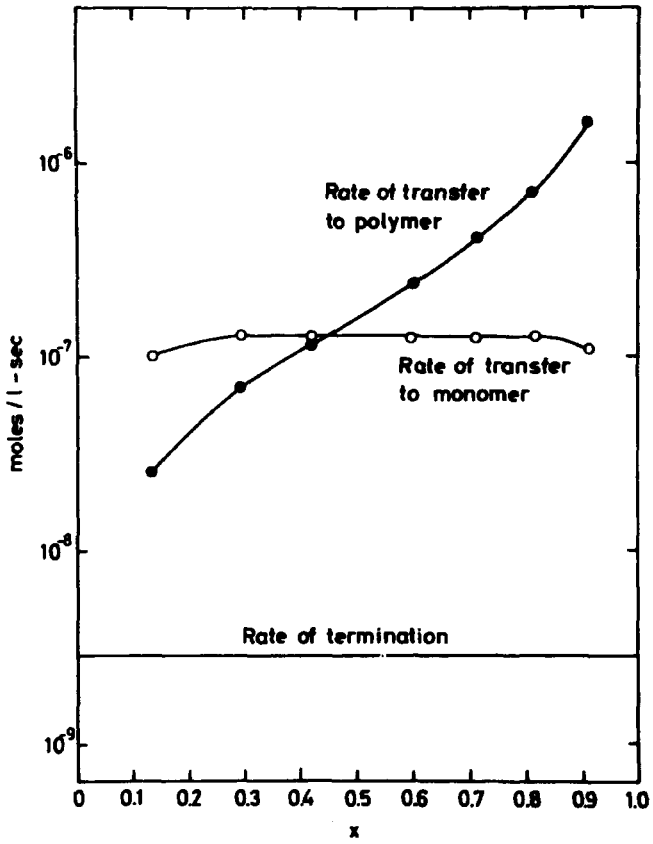

Fig. 38a. Calculated rates of transfer to monomer, transfer to polymer and termination as a function of conversion. The plots correspond to an initiator concentration of 4×10^{-3} moles $K_2S_2O_8$/l H_2O and 8×10^{17} particles/l.

and polymer. The plots shown correspond to the highest rate of initiation used experimentally. At lower rates of initiation the termination rate will be even smaller in proportion to the rates of transfer.

Transfer to polymer and terminal double bond polymerization lead to

polymers with trifunctional branch points and, as shown by Graessley[85], result in an increase of molecular weight with increasing conversion. As shown in several plots in the present work $[\eta]$ increases with increasing conversion. However, although this must naturally be attributed to an increase of molecular weight, the increase in $[\eta]$ is, owing to branching, not quantitatively representative for the actual increase in molecular weight.

3.4.4. Comparison with Literature

As previously mentioned, three different models of vinyl acetate emulsion polymerization have recently been published in the literature. It is interesting to compare these models with the model suggested here.

Assuming a rapid equilibrium of radicals between the aqueous phase and the polymer phase and between the different polymer particles, Harriott[34] has reasoned that the emulsion polymerization of vinyl acetate could be treated with simple homogeneous kinetics, and he has deduced the following rate expression:

$$R_p = k_p[M_p]\,(2k_i[I]X_wX_p/k_{tp})^{1/2}, \qquad (41)$$

where X_w and X_p are volume fractions of water phase and polymer phase respectively. From this expression it appears that the rate of polymerization should be independent of the number of particles. This is not in agreement with the data reported by Patsiga[14] and Nomura[28], nor with the results obtained in the present work. Furthermore, from the data presented here it can be calculated that $k_p/\sqrt{k_{tp}}$ increases by a factor 15 in the conversion range 20 - 80%. Since $[M_p]$ decreases only by a factor 4 in the same interval and all other terms in eq. 41 remain constant, this will imply that the conversion versus time curve in the interval 20 - 80% conversion is concave towards the time axis. This has never been observed experimentally.

On the basis of a very comprehensive study of vinyl acetate emulsion polymerization Stannett, Litt, and Patsiga[27] have derived the rate expression

$$R_p = K_1([I]\,[M_p]N)^{1/2}\,(1 + K_2\frac{[M_p]}{r^2[M_{aq}]})^{-1/2}, \qquad (42)$$

where K_1 and K_2 are combinations of various rate constants, r the average radius of the particles, and $[M_{aq}]$ the concentration of monomer in the aqueous phase. In agreement with the findings of Dunn and Taylor[26], Stannett et al. have found that $[M_{aq}]$ is proportional to $[M_p]^{1/2}$ in the interval 0 - 90%. When $[M_p]^{1/2}$ is substituted for $[M_{aq}]$ in eq. 42, it appears that this expression predicts that the polymerization rate decreases with the 0.25 - 0.5 power of $[M_p]$ over most of the polymerization range. This is not consistent with the data reported in an earlier publication by Stannett et al.[16], where the rate of polymerization was found to be constant until 85% conversion, nor with the data obtained in the present work.

In a study of the role of polymer particles in vinyl acetate emulsion polymerization Nomura et al.[28, 58] have derived the following rate expression:

$$R_p = \frac{k_p[M_p]}{N_A}\left(\frac{k_i f[I]\delta_m k_p}{3D_w k_{tr}\varphi}\right)^{1/2}\left(\frac{3}{4\pi q(1-\Psi_c)}\right)^{1/3} M_o^{1/3} N^{1/6} x_c^{1/3}, \quad (43)$$

where q is the density of the monomer-swollen polymer particles, D_w is the self-diffusion coefficient of monomeric radicals in the aqueous phase, M_o is the initial monomer concentration in g/l H_2O, and δ_m the partition coefficient of monomeric radicals between aqueous and polymer phases. φ and Ψ_c are given as

$$\varphi = \left(1 + \frac{D_w}{\delta_m D_p}\right)^{-1}$$

and

$$\Psi_c = 1 - x_c.$$

Nomura et al.[28] have defined the desorption rate constant as

$$k_d = \left(\frac{3D_w\varphi}{\delta_m r^2}\right)\frac{k_{tr}}{k_p}, \quad (44)$$

and eq. 43 can thus be written as

$$R_p = \frac{k_p[M_p]}{N_A}\left(\frac{k_i f[I]}{k_d}\right)^{1/2}\frac{1}{r}\left(\frac{3}{4\pi q(1-\Psi_c)}\right)^{1/3} M_o^{1/3} N^{1/6} X_c^{1/3}. \quad (45)$$

Since

$$\left(\frac{3}{4\pi q(1-\phi_c)}\right) M_o^{1/3} X_c^{1/3} = \left(\frac{3M_o}{4\pi q}\right)^{1/3} = \left(\frac{3V_p}{4\pi}\right)^{1/3} = rN^{1/3},$$

eq. 45 reduces to

$$R_p = \frac{k_p[M_p]}{N_A}(2k_i f[I])^{1/2}\left(\frac{N}{2k_d}\right)^{1/2}. \quad (46)$$

This expression is equivalent to eq. 30, except that the term $N_A^2 V_p/2k_{tp}$ is missing in eq. 46. There is, however, a further discrepancy between the model suggested by Nomura et al. and that proposed in the present work. This appears by comparing the definition of the desorption rate constant given in eq. 44 with that given in eq. 34. Unfortunately, the derivation of eq. 44 is not completely clear in the paper presented by Nomura et al.[28]. However, by rearrangement, eq. 44 can be written as

$$k_d = a_p \frac{1}{v}\frac{1}{r}\left(\frac{D_p D_w}{\delta_m D_p + D_w}\right)\frac{k_{tr}}{k_p}, \quad (47)$$

where r, a_p, and v denote average particle radius, area, and volume respectively. Thus, since the term $1/v$ equals the concentration of radicals in particles containing one radical and the term $D_p D_w/(\delta_m D_p + D_w)$ may be regarded as a mean diffusion coefficient, it seems that eq. 44 has been derived by application of Fick's diffusion equation. This presupposes that the desorption process is a continuous phenomenon, i.e. a single particle must contain a large number of monomeric radicals, so that the concentration gradient does not change appreciably when a radical escapes the particle. The desorption process is, however, a discrete phenomenon, involving the escape of the only radical present in the particle. In eq. 34 the desorption rate constant is defined in terms of Einstein's diffusion equation, and this may be more reasonable since this equation applies to the random motion of a single radical.

3.5. Conclusion

From the preceding sections the following principal conclusions can be drawn:

I The emulsion polymerization of vinyl acetate can be described in terms of the model for vinyl chloride deduced by Ugelstad[43, 44]. This model is in the main similar to case I in Smith and Ewart's hypothesis, the major difference being the term which accounts for the desorption of radicals.

In contrast to styrene emulsion polymerization, transfer to monomer plays an important role in polymerization of vinyl acetate and vinyl chloride. This is reflected in the magnitude of the respective transfer constants. Thus for vinyl chloride and vinyl acetate the transfer constants equal 6[47, 55] and 0.75 l/mole-sec[39] at 50°C respectively, while it is only 0.01 l/mole-sec[56, 57] for styrene. This means that desorption of radicals from the polymer particles takes place much more frequently in emulsion polymerization of vinyl acetate and vinyl chloride than in styrene, and therefore the average concentration of free radicals per particle is relatively low in the former systems. Further evidence of the importance of transfer reactions in vinyl acetate emulsion polymerization is the fact that the molecular weight is apparently controlled primarily by transfer to monomer and polymer.

II From subsections 3.3.4 to 3.3.7 it appears that the data obtained in the present work compare favourably with the data reported by Nomura et al.[28]. Thus it has been possible to obtain concurrent results in the research of vinyl acetate emulsion polymerization.

4. RADIATION-INDUCED EMULSION POLYMERIZATION OF VINYL ACETATE

4.1. Literature Survey

There are numerous reports in the literature on radiation-induced polymerization of vinyl monomers such as styrene, vinyl acetate, methyl methacrylate, etc. Most of these reports deal with solution and bulk polymerization, and it is generally concluded that the polymerization in such systems proceeds via a mechanism identical to that observed with chemical initiation. Chapiro[70] has given a very lucid and comprehensive review of radiation-induced polymerization.

Only relatively few reports deal with radiation-induced polymerization in emulsion systems. References 1 and 2 and 71-81 comprise most of the investigations reported during the past decade.

In the following will be given a brief review of studies in radiation-induced emulsion polymerization of vinyl acetate. The mechanism of radical formation in emulsion systems will not be discussed here. A brief discussion of this matter will be given in subsection 4.4.2 in relation to the results obtained in the present work.

In conventional emulsion polymerization radicals are produced solely

in the aqueous phase. Radiation-induced polymerization is more complex, since here radicals are produced both in the aqueous phase and in the monomer-swollen polymer particles. The amounts of radicals produced in the two phases depend on the composition of the emulsion and the nature of the monomer. For some monomers, e.g. styrene, the yield of radicals and ions upon irradiation is relatively small compared with the yield in the same amount of water. In calculations on emulsion polymerization kinetics, which are already encumbered with uncertainty, the production of active species in the organic phase is therefore generally neglected. However, in some cases, e.g. with irradiation of vinyl acetate, the yield of radicals capable of initiating polymerization is of the same magnitude as in water, and the production of radicals in the organic phase cannot be neglected.

Owing to the difference in initiation many investigations of radiation-induced emulsion polymerization also comprise a study of chemical initiation with the primary purpose being a comparison between the two systems.

Stannett et al.[75, 80] have investigated the radiation-induced emulsion polymerization of vinyl acetate in a batch system, and they have compared their data with results obtained in a prior investigation of chemically initiated polymerization. This comparison reveals the following deviations between the two systems:

I In radiation-induced polymerization the rate of reaction is proportional to the emulsifier concentration. In the chemically initiated process there is no effect of emulsifier concentration on rate of polymerization.

II In radiation-induced polymerization the rate is proportional to the 0.7 power of the number of particles. In experiments with chemical initiation the number of particles exerts a much smaller effect, in that the rate is proportional to the 0.2 power of the number of particles.

III The rate of polymerization is proportional to the 0.7 - 0.9 power of the dose rate. With chemical initiation the rate is proportional to the first power of the initiator concentration.

IV In radiation-induced experiments the rate of polymerization is proportional to the 0.26 power of the dose rate at a constant number of particles. With chemical initiation the initiator dependence exponent equals 0.8.

Although these results suggest that the kinetic behaviour of radiation-induced emulsion polymerization is very different from that in conventional emulsion polymerization, there is, however, one feature common to the two systems, namely the linearity of the conversion versus time curve in the interval 30 to 85% conversion.

Stannett et al. have also determined the viscosity average molecular weight as a function of dose rate, emulsifier concentration, and temperature. Only the temperature has an influence on molecular weight, which decreases with increasing temperature. The independence of molecular weight of dose rate and emulsifier concentration suggests that the degree of polymerization is primarily controlled by chain transfer to monomer and polymer.

A closer inspection of the data reported by Stannett et al. reveals the very interesting fact that below a certain dose rate the polymerization rate decreases with increasing temperature, i. e. the overall energy of activation is negative. This point has not been commented on by the investigators. A very low, but positive, overall energy of activation is not surprising in radiation-induced polymerization as the activation energy for initiation equals zero. However, a negative energy of activation is difficult to explain. It seems to indicate a rather complex behaviour of the polymerizing system.

O'Neill et al. [72] have recently studied the radiation-induced emulsion polymerization of vinyl acetate in a recycle flow reactor system, the principle of which is shown schematically in fig. 39. It consists of a tubular flow reactor positioned inside a ^{60}Co-source and connected by transfer lines to a stirred vessel outside the ^{60}Co-source. The emulsion is circulated in this system by means of a pump. Parallel to this investigation O'Neill et al. have also studied the radiation-induced polymerization in a batch system.

In a study of the effect of emulsifier concentration these investigators have found that both in the recycle flow reactor system and in the batch system the rate of polymerization is proportional to the 0.25 power of the emulsifier concentration. Furthermore, there is no discontinuity in the dependence of rate on emulsifier concentration at the critical micelle concentration. As previously mentioned this has also been observed in systems with persulphate initiation.

The results obtained from experiments with the recycle system are very interesting in relation to the present work. At a low flow rate, i. e. with a long residence time in the irradiation zone, the polymerization proceeds smoothly to high conversions. However, as the flow rate is increased the polymerization rate decreases and at very high flow rates polymerization does not take place. This effect O'Neill explained as being due to the presence of oxygen in the system. Analysis of the exit stream of the purge gas (nitrogen) showed an oxygen concentration sufficiently high to influence the polymerization in the irradiation zone. Oxygen is a strong inhibitor in vinyl acetate polymerization. If the residence time in the

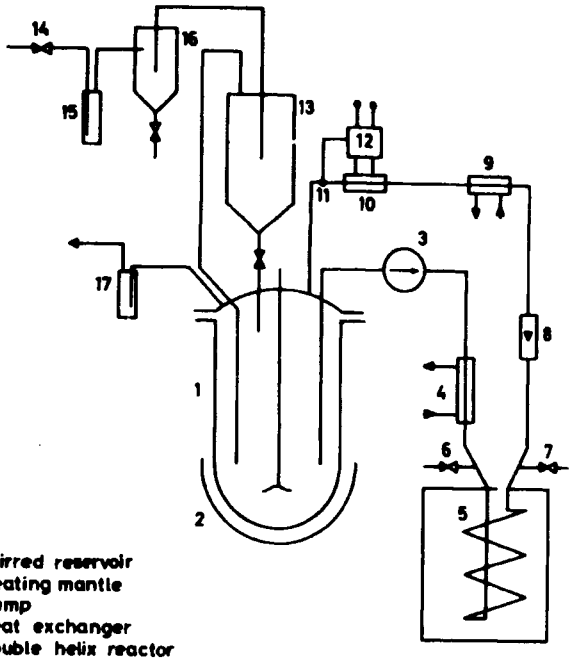

1. Stirred reservoir
2. Heating mantle
3. Pump
4. Heat exchanger
5. Double helix reactor
6,7. Sampling points
8. Rotameter
9. Cooler
10-12. Thermostat
13. Storage tank
14. N_2 inlet
15. Humidifier
16. Seperator
17. N_2 outlet

Fig. 39. Key diagram of the experimental set-up used by O'Neill et al. [72].

tubular flow reactor is long, the oxygen contained in a volume element may be consumed before the element reaches the exit of the reactor, and polymerization takes place in part of the reactor. However, if the residence time is short, there may not be sufficient time for the oxygen to be consumed, and polymerization cannot take place.

This explanation assumes that a volume element of the emulsion receives the same quantity of oxygen in the " at-source" section of the system, whether the flow rate is high or low. Since the source of oxygen is not known with certainty, this cannot be verified. The observed effect of the flow rate is nevertheless interesting, since it reveals one of the pecularities inherent in such a flow system.

From the data reported by O'Neill et al. it appears that the limiting viscosity number of the polymers produced decreases somewhat with increasing dose rate in the interval 30 - 780 krads/h. This result is contradictory to the data reported by Stannett et al. [75, 80]. However, it should be mentioned that the data of Stannett et al. were obtained at dose rates lower than 70 krads/h and it may be that the dependence of $[\eta]$ on dose rate first becomes significant at dose rates higher than 100 krads/h, i.e. at high dose rates transfer reactions do no longer preponderate the molecular weight, but also bimolecular termination plays a role.

The principal conclusion of O'Neill et al. is that the kinetical behaviour of the radiation-induced emulsion polymerization of vinyl acetate is similar to that observed in the conventional system. This is contradictory to the conclusion of Stannett et al.

Ley et al. [73] have studied the emulsion polymerization of several monomers, including vinyl acetate, by intermittent ^{60}Co-irradiation. This investigation is particularly interesting for the present work, in that the recycle flow reactor system studied here is in itself a system with intermittent irradiation.

By means of a sensitive recording dilatometer Ley et al. followed the build-up and decay of polymerization rate during the successive irradiation and dark periods. From such experiments the half-life times of the propagating radicals can be obtained, and if the kinetics of the polymerizing system are known, the termination rate constant can be computed from the half-life time. Most interesting are the values of the first half-life times obtained for styrene and vinyl acetate. For styrene the half-life time equals 80 minutes, while for vinyl acetate the value is 0.8 minutes. Since the termination rate constants for vinyl acetate and styrene are of approximately the same magnitude in systems of equal composition, this is further

evidence of the different behaviour of those monomers in emulsion polymerization.

Although the half-life time for vinyl acetate is relatively short, it does nevertheless indicate that a certain amount of polymerization takes place after the system has been removed from the ^{60}Co-source. This subject will be discussed in detail in subsection 4.4.3.

From the data reported by Stannett et al. [75, 80] and O'Neill et al. [72] it cannot be concluded whether the radiation-induced emulsion polymerization behaves similarly to the chemically initiated polymerization or not. Although these investigators have used the same recipe constituents, their conclusions are contradictory. It should be mentioned that for styrene emulsion polymerization it has been shown that the radiation-induced process can be described in terms of Smith-Ewart's case II [1, 2], and it behaves similarly to the chemically initiated process [47].

4.2. Experimental

4.2.1. Materials and Polymerization Equipment

The materials used in the radiation-induced experiments were treated in exactly the same manner as in the experiments with chemical initiation. Also the composition of the emulsions was the same.

The polymerization was performed in a recycle flow reactor system consisting of a tubular flow reactor positioned inside a ^{60}Co-source and connected by transfer lines to a stirred vessel positioned outside the ^{60}Co-source. In fig. 40 is shown a key diagram of the experimental set-up. The emulsion handling system, which is made of glass, is designed to operate within a pressure range of 10^{-2} - 2×10^{3} torrs. The temperature control circuit is made up of copper tubes insulated with foam rubber.

Fig. 41 shows the design of the in-source reactor assembly. The 15 mm i.d. tubular flow reactor is contained in a polystyrene cannister which constitutes the in-source thermostat. The cannister is supplied with water of constant temperature from the thermostat in the out-source section.

The transfer lines and the water supply pipes pass the top shielding plug of the ^{60}Co-plant through four helical lead-in bushes. When the reactor assembly is to be irradiated, the irradiation chamber is lowered to a position on level with the eight ^{60}Co-strips, and this mechanism makes it necessary for the transfer lines connecting the in-source and out-source sections to be flexible, and they are therefore made of polyethylene.

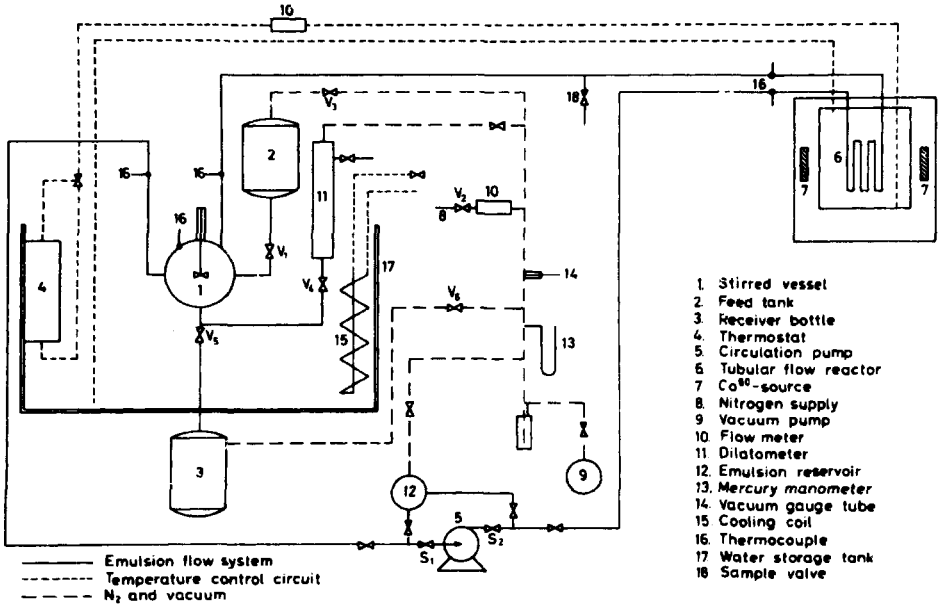

Fig. 40. Key diagram of experimental set-up used in the present investigation.

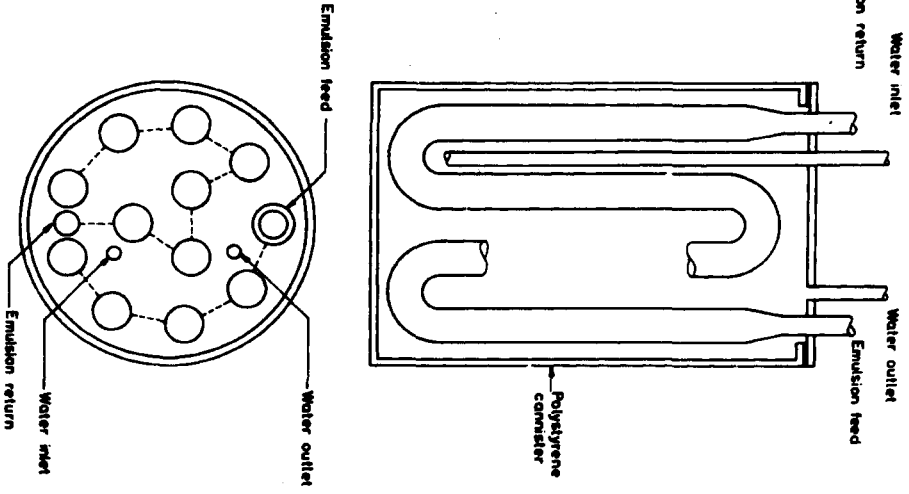

Fig. 41. Design of in-source reactor assembly.

The various reactors used in this study only differ in the length of the tube, and they are designed to have exactly the same geometry with respect to the radiation field to achieve identical dose rates even though the volumes of the reactors are different.

Figs. 42a and b show the design of the stirred vessel. It consists of a 1-litre, round-bottomed vessel provided with:

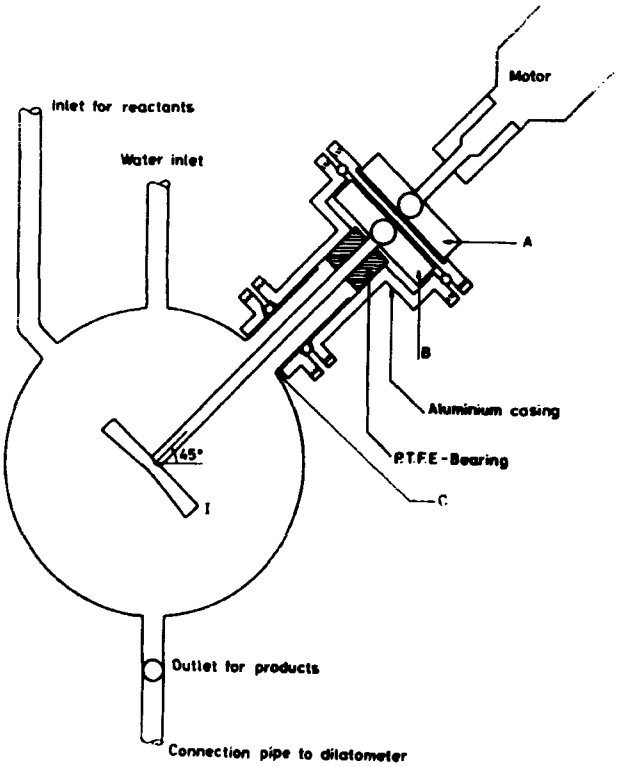

Fig. 42a. Cross-section of the stirred vessel, seen from one side.

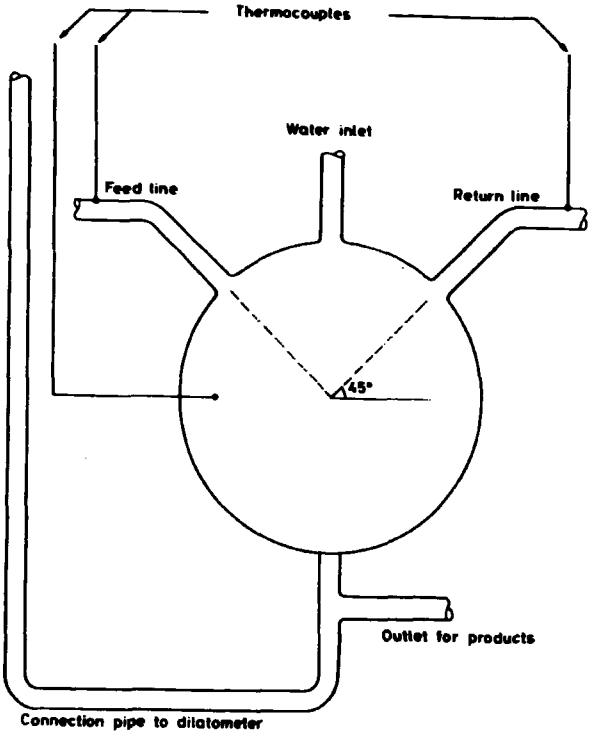

Fig. 42b. Cross-section of the stirred vessel, front view.

1) Stirrer
2) Inlet for reactants
3) Outlet for products
4) Inlet for return stream from flow reactor
5) Outlet for feed to flow reactor
6) Inlet for rinsing water
7) Chromel-alumel thermocouples
8) Connection pipe to dilatometer.

The demand on the system to operate under both vacuum and pressure conditions (see below) made it necessary to construct a special stirrer, the principle of which is shown in fig. 42a. It consists of a variable-speed synchronous motor capable of 150 to 1000 rpm. The mechanical force is transferred to the impeller 1 by means of a magnetic clutch made up of two cruciform magnets A and B of which B is contained in an aluminium casing fitted tightly to the glass tube C. The impeller is revolvable round the shaft, and the stirrer is thus easily dismantled from the vessel.

The total volume of the vessel is 1200 ml including the volume of the aluminium casing. The total volume of the transfer lines (i.d. 10 mm) is 600 ml.

The degree of conversion was measured by means of an automatic dilatometer the principle of which is shown in fig. 43. It consists of two brass tubes between which are fixed two glass tubes. The volume between the glass tubes is partly filled with glycerol, which by means of a mercury bridge is in dynamic contact with the reacting fluid. With an a.c. voltage (50V) between the two brass tubes the whole system constitutes a variable capacitor, the capacitance of which varies with the amount of glycerol between the brass tubes.

The capacitance is measured by a level transducer (Endress and Hauser, model SM 3a) and the signal from this is transmitted to a 10 mV recorder (Varian Associates, model G-10). During the polymerization the amount of glycerol between the brass tubes decreases gradually as the degree of conversion increases, and since the capacitance depends linearly on the amount of glycerol between the tubes, the signal from the transducer will after a suitable calibration be a direct measurement of the immediate degree of conversion. The dilatometer was calibrated against the degree of conversion measured from samples withdrawn during a run.

The use of a dilatometer in this investigation offered three distinct advantages

1) The dilatometric method is obviously exceedingly time-saving compared with the method of collecting samples which should be coagulated, washed, dried, and weighed.

2) In experiments where samples for particle size analysis or molecular weight determinations need to be taken at predetermined degrees of conversion, this can only be done by means of a dilatometer, since only by this method the immediate degree of conversion is determined simultaneously with the accomplishment of the experiment.

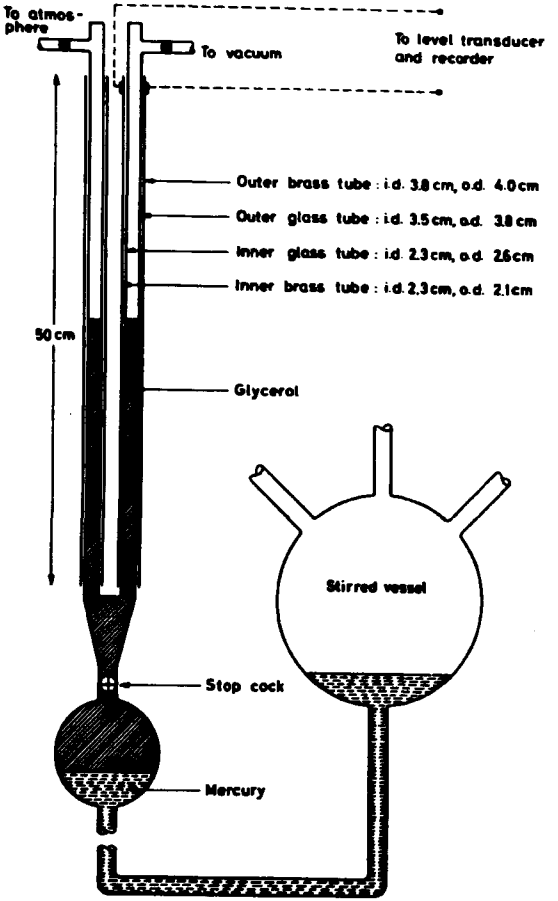

Fig. 43. Design of dilatometer.

3) The duration of a possible induction period can be determined with much greater accuracy by use of a dilatometer than by sampling.

The emulsion was circulated in the system by means of a lobe pump (Stainless Steel Pumps Ltd., model 3/8 ND-Handipump). This pump is characterized by a relatively low shear force. Furthermore pulsation is minimum. This is important, in that intense pulsation would make the fluid in the dilatometer oscillate, and thus a spurious signal would be superimposed on the signal from the transducer, making the measurement inaccurate. Constructed of stainless steel and with P.T.F.E. shaft seals the pump is impervious to vinyl acetate.

The temperature, measured by chromel-alumel thermocouples at five different positions (compare fig. 40) in the emulsion handling system, was registered by a Siemens select switch compensograph (Type M2).

Vacuum service was provided by a one-stage, high-speed rotary pump (Edwards Vacuum Components Ltd., model ES 50). Pressures less than 100 torrs were registered with a vacuum gauge (LKB Autovac Gauge, model 3294 G). Pressures higher than 100 torrs were measured with a conventional mercury manometer. Compressed nitrogen was used for pressure equalizing.

The emulsion was prepared in a three-litre feed tank provided with stirrer and inlet and outlet for nitrogen. The feed tank was connected to the emulsion handling system by means of high-vacuum fittings. Prior to the inlet of the emulsion, the system was sparged for 20 minutes with nitrogen and finally evacuated to 5×10^{-2} torrs. During the evacuation the circulating pump was shut off from the remaining part of the system by means of the valves S_1 and S_2 (fig. 40). This was necessary, since the pump was not completely leak-free under vacuum.

The emulsion was sucked into the system by opening of valve V_1. The feeding lasted 1-2 min, and at the end of this period the pressure was adjusted to 760 torrs by opening of valves V_2 and V_3. By opening of valves S_1 and S_2 the pump was filled with emulsion from the reservoir 12 (fig. 40). With filling in this way it was possible to avoid the presence of a gas phase in the system. This was most important, since the presence of a gas phase would make the dilatometric measurement impossible.

The emulsion was circulated in the system for 15 min, and when the temperature was stabilized, the amount of glycerol in the dilatometer was adjusted to set the indicating meter of the level transducer at zero. Finally the flow rate was adjusted to the desired value, and the in-source reactor assembly was lowered to the irradiation position.

In principle the apparatus and the procedures described here are very similar to those used by Stannett and Stahel[1] and O'Neill[72]. However, two major differences should be mentioned. Firstly, in the present work the polymerization was accomplished in the absence of any gas phase, while the experiments in the previous investigations were conducted in the presence of a nitrogen atmosphere. Secondly, in this investigation the conversion versus time curve was obtained by means of a dilatometer, while the previous investigators used sampling. Probably the dilatometric method gives the most accurate results, since it reproduces every detail of the conversion history.

4.2.2. Dosimetry

Dose rates were measured by Fricke dosimetry[83]. The system applied was a 10^{-3} molar ferrous ammonium sulphate in 0.8 N H_2SO_4. The solution was saturated with air and irradiated for 15.0 ± 0.1 min at 25°C. The optical density of the solution was measured on a Cary 15 spectrophotometer.

4.2.3. Particle Number Analysis

The number of particles was estimated by means of the procedure outlined in subsection 3.2.2.1.

4.2.4. Viscometry

The limiting viscosity number was determined by means of the procedure described in subsection 3.2.3.

4.3. Results

The major part of the radiation-induced experiments were performed early in the study. Most of these experiments were conducted with the emulsifier SDBS. As appeared from the experiments with chemical initiation, which were performed later in the study, this choice may have been unfortunate. However, the major part of the radiation-induced experiments were conducted with the purpose of studying the effect of flow rate and reactor volume on polymerization rate, and it may be supposed that these effects are uninfluenced by the emulsifier type.

Unfortunately, it was impossible to obtain complete conversion in the radiation-induced experiments. At about 80% conversion there was an incipient coagulation of the latex. This may be attributed to the fact that the emulsion was subject to a certain amount of shear in the circulation pump.

4.3.1. Reproducibility of the Conversion versus Time Curve

A few experiments were conducted in order to test the reproducibility of the polymerization curve. Fig. 44 shows conversion versus time plots obtained from two experiments conducted under identical conditions, and it appears that the reproducibility is very good.

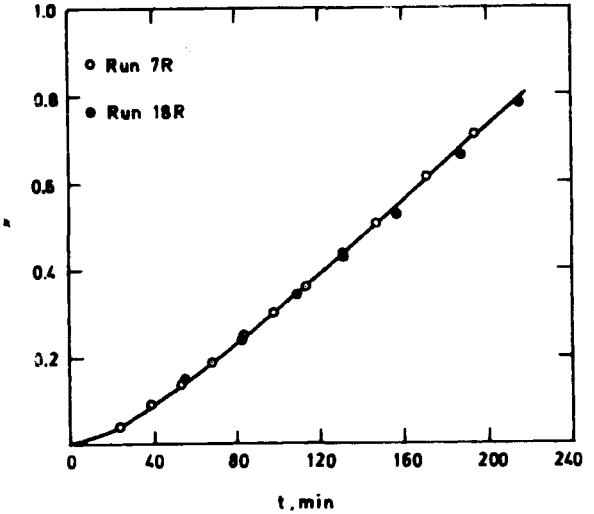

Fig. 44. Conversion versus time plots showing experimental reproducibility. 11.5 g SDBS/l H_2O. 82 krads/h. In-source reactor volume 210 cc. Flow rate 0.021 l/sec. 20°C.

The duration of the induction period in the radiation-induced experiments was considerably shorter than in experiments with chemical initiation. In most cases it amounted to 1-5 min. This may be explained as being due to the much higher rate of radical production in experiments with radiation initiation. Hence, the small traces of oxygen initially present in the emulsion are consumed much faster.

4.3.2. Shape of the Conversion versus Time Curve

Fig. 45 shows polymerization curves from experiments with different emulsifier types. Curve A was obtained with SLS as emulsifier, and it appears that as in the case with chemical initiation the curve becomes linear from approximately 20% conversion. Curves B and C were obtained with

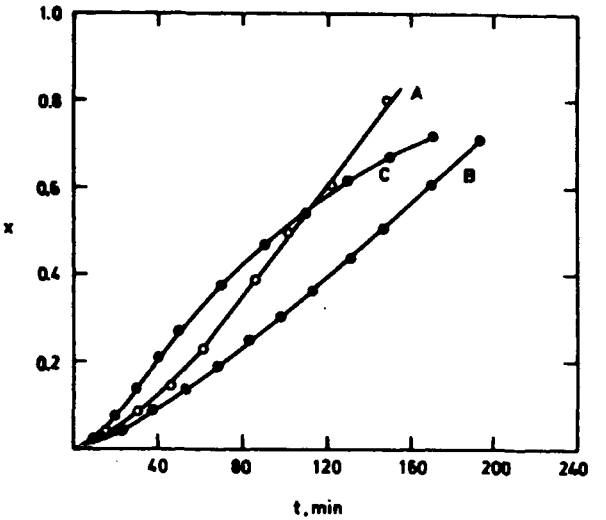

Fig. 45. Conversion versus time plots obtained with different emulsifier types. A 9.5 g SLS/l H_2O. B 11.5 g SDBS/l H_2O. C 80.5 g SDBS/l H_2O. 82 krads/h. In-source reactor volume 210 cc. Flow rate 0.021 l/sec. 20°C.

SDBS as emulsifier, and it is seen that as with chemical initiation there is a transition in the kinetics, when going from a low to a high emulsifier concentration. However, in the radiation-induced experiments it was necessary to add a considerably larger amount of SDBS to obtain the anomalous shape of the polymerization curve, and at a concentration of 11.5 g SDBS/l H_2O, where the anomalous shape was observed with chemical initiation, there was no effect with radiation initiation.

4.3.3. Number of Particles during Polymerization

In most of the radiation-induced experiments the lattices produced were rather unstable and tended to coalesce within a short time after their preparation. This was especially the case in experiments with low flow rate. Therefore, reliable data on particle numbers were obtained only in a limited number of experiments.

Fig. 46 shows a plot of number of particles versus conversion from an experiment with SDBS as emulsifier. Contrary to the results from chemical initiation there is an increase in the number of particles during most of the

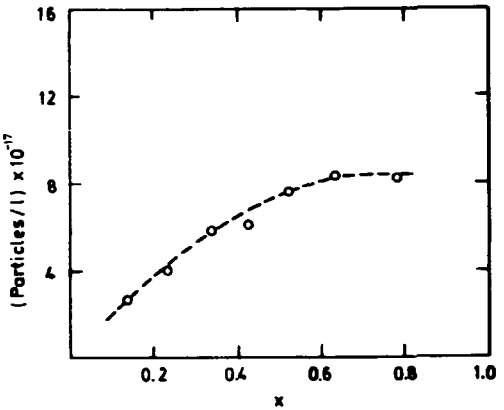

Fig. 46. Number of particles versus conversion. 11.5 g SDBS/l H_2O. 62 krads/h. In-source reactor volume 210 cc. Flow rate 0.021 l/sec. 20°C.

conversion range. A similar result was obtained with SLS as emulsifier. This suggests that the particle nucleation is different in the two systems. This may be due either to the difference in initiation mechanism or to the different design of the polymerization equipment. Thus, it cannot be excluded that the particular flow process will affect the nucleation of particles. However, a possible difference in particle nucleation does not necessarily imply that the polymerization kinetics of the two systems are different.

4.3.4. Effect of Emulsifier Concentration

Fig. 47 shows conversion versus time plots obtained at different concentrations of SLS. As with chemical initiation the rate of polymerization increases with increasing emulsifier concentration. From the linear parts of the curves it is calculated that the rate of polymerization increases by the 0.1 power of the emulsifier concentration. From the particle size analysis it was found that beyond 50% conversion, where the number of particles is approximately constant, the rate of polymerization increases by the 0.3 power of the number of particles. Both of these results agree with the data obtained with chemical initiation.

The effect of the emulsifier SDBS on the polymerization curve was already considered in subsection 4.3.2. A closer inspection of the curves shown in fig. 45 reveals the interesting fact that during the initial stage of

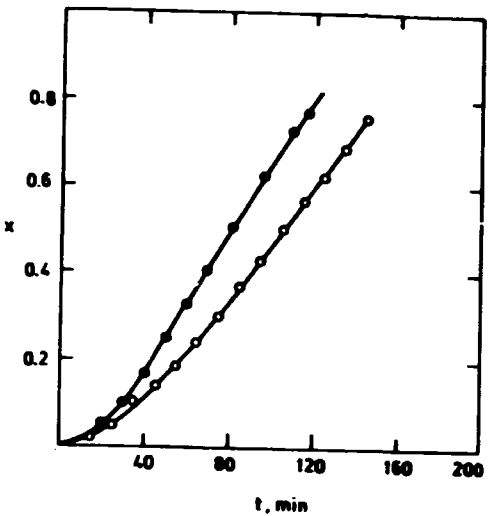

Fig. 47. Conversion versus time plots at different concentrations of SLS. ○ 9.5 g SLS/l H_2O. ● 66.5 g SLS/l H_2O. 62 krads/h. In-source reactor volume 0.210 cc. Flow rate 0.021 l/sec. 20°C.

the polymerization the rate increases with increasing concentration of SDBS, while during the later stages of the reaction the effect is the opposite. Furthermore, comparison of curves A and B in fig. 45 shows that at equimolar concentrations of the two emulsifiers, the rate of polymerization is higher with SLS than with SDBS as emulsifier.

Fig. 48 shows plots of the limiting viscosity number versus conversion obtained from experiments with different concentrations of SDBS. It appears that $[\eta]$ is independent of the concentration of SDBS. The plots shown in fig. 48 correspond to polymerization curves B and C shown in fig. 45. Hence, the limiting viscosity number is unaffected by the transition in kinetics. Furthermore, since the ratio of particle numbers was approximately 3 in these experiments, it can be concluded that $[\eta]$ is independent of the particle number. This was also observed with chemical initiation.

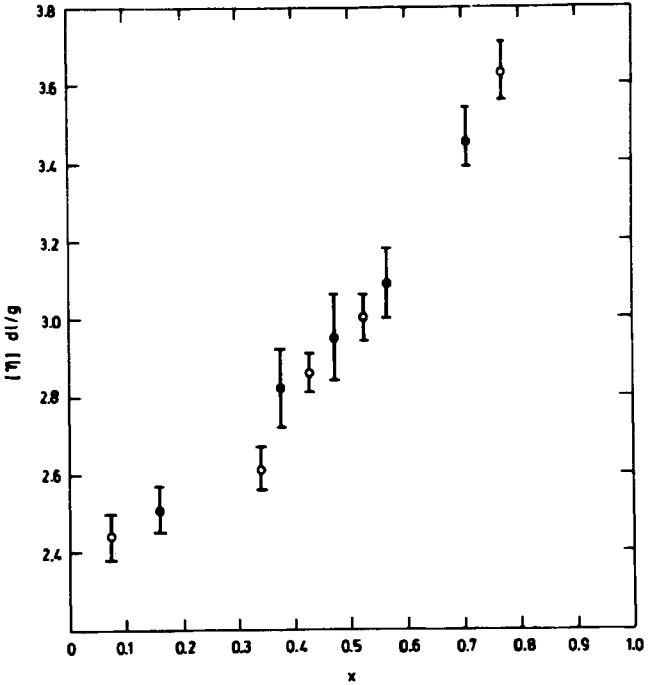

Fig. 48. Limiting viscosity number of poly (vinyl acetate) as a function of conversion at two different concentrations of SDBS. ○ 11.5, ● 80.5 g SDBS/l H_2O. 62 krads/h. In-source reactor volume 210 cc. Flow rate 0.021 l/sec. 20°C. The points of measurement are shown with their 80% confidence limits.

4.3.5. Effect of Flow Rate and Reactor Volume

A characteristic feature in radiation-induced experiments accomplished in a recycle flow reactor system is that each volume element experiences fluctuations in its concentration of free radicals. In its way through the source there is a build-up of free radicals, and when it leaves the source the concentration of radicals decays. This behaviour is similar to that observed in the well-known rotating sector experiments, and it is peculiar to a process intiated by radiation and cannot be obtained with chemical initiation.

The frequency of the fluctuation in radical concentration of a single flow element is determined by the space time in the flow reactor, i.e. the flow rate at constant reactor volume. For reasons which will be outlined in subsection 4.4.3 one should expect the flow rate to affect the rate of polymerization, and therefore a series of experiments with different flow rates were performed.

Fig. 49 shows conversion versus time plots obtained at flow rates 0.021 and 0.0053 l/sec. It appears that the rate of polymerization increases as the flow rate is increased. Table 2 gives data from various experiments performed at two different flow rates. The rates of polymerization given here are the maximum rates calculated from the slope of the respective conversion versus time plots. In any case the rate of polymerization increases by 10-25% as the flow rate is increased from 0.0053 to 0.021 l/sec. Since the polymerization curves are reproducible within this range, the effect must be considered as significant.

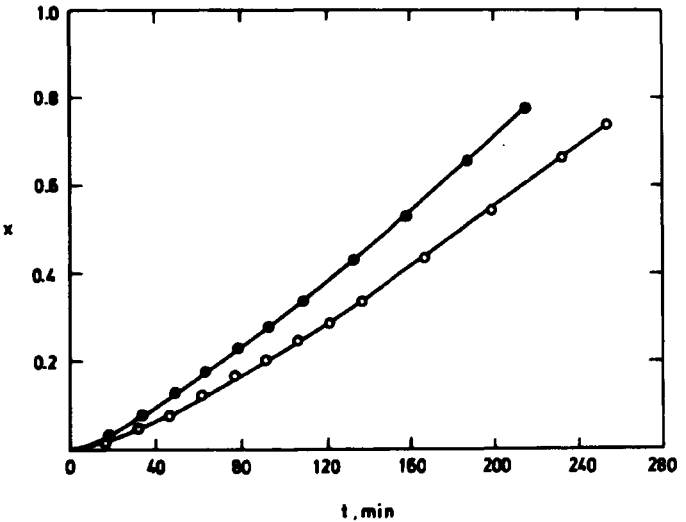

Fig. 49. Conversion versus time plots at two different flow rates. ● 0.021, ○ 0.0053 l/sec. 11.5 g SDBS/l H_2O. 62 krads/h. In-source reactor volume 210 cc. 20°C.

Table 2

Polymerization rates at different flow rates and in-source reactor volumes (V_i)

Emulsifier conc. g/l H_2O	Flow rate l/sec	V_i l	R_p moles/sec	R_p/V_i moles/l-sec
11.5	0.021	0.310	0.00069	0.00222
11.5	0.021	0.210	0.00052	0.00247
11.5	0.0053	0.310	0.00058	0.00187
11.5	0.0053	0.210	0.00042	0.00200
80.5	0.021	0.310	0.00112	0.00361
80.5	0.021	0.210	0.00081	0.00385
80.5	0.0053	0.310	0.00099	0.00319
80.5	0.0053	0.210	0.00069	0.00330

Fig. 50 shows a comparison between conversion versus time plots in one of which the flow rate was decreased from 0.021 to 0.0053 l/sec at 38% conversion, while the other was run at a constant flow rate of 0.021 l/sec. The change in flow rate has apparently no effect on the subsequent course of polymerization. This suggests that the above-mentioned effect of flow rate is caused by an effect during the early stages of the polymerization. In their investigation of the radiation-induced emulsion polymerization of styrene in a recycle flow reactor system Stannett and Stahel[1] have observed that the number of particles increases with increasing flow rate, and they have explained this as being due to interference of the flow rate on the particle nucleation process. If this is the case also in vinyl acetate emulsion polymerization, the rate of polymerization should increase when the flow rate is increased at the beginning of the polymerization, while there should be no effect at conversions beyond 40-50%, since at this point the particle nucleation has ceased. However, at present this statement cannot be verified experimentally, since reliable data on particle number in experiments with low flow rate could not be obtained.

The effect of the in-source reactor volume was also investigated. From table 2 it appears that the rate of polymerization increases with increasing

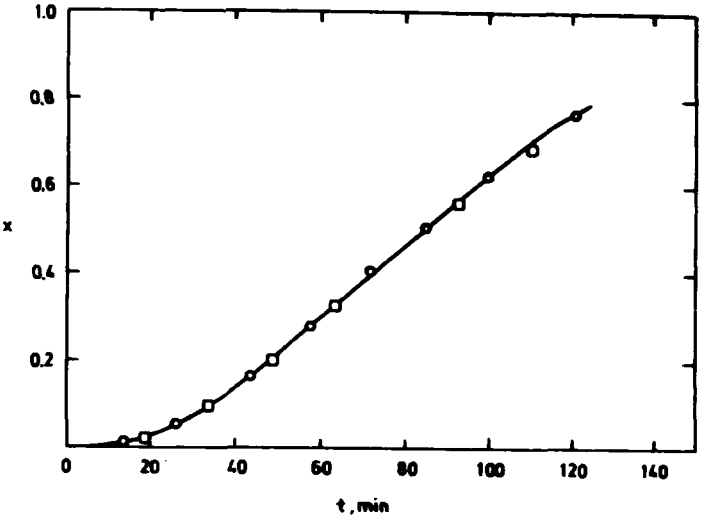

Fig. 50. Conversion versus time plots obtained at 62 krads/h. O constant flow rate 0.021 l/sec throughout the experiment. □ flow rate changed from 0.021 l/sec to 0.0053 l/sec at 38% conversion. 66.5 g SLS/l H_2O. In-source reactor volume 210 cc. 20°C.

reactor volume. However, as shown in the last column of table 2, the rate of polymerization per unit volume of reactor decreases somewhat as the reactor volume is increased. Since dosimetry measurements showed that the dose rates in two reactors differed by less than 1%, it can be excluded that the effect of reactor volume is due to a difference in dose rate.

Fig. 51 shows the limiting viscosity number $[\eta]$ as a function of conversion at different flow rates and reactor volumes, and it appears that within the limits of experimental error neither of these two parameters affects $[\eta]$. In other words the limiting viscosity number is independent of the dose per pass through the source.

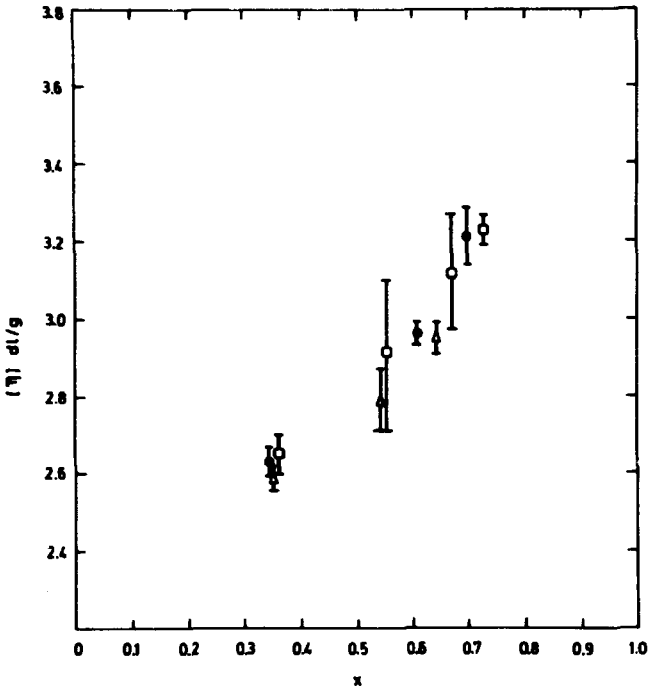

Fig. 51. Limiting viscosity number of poly (vinyl acetate) as a function of conversion at different flow rates and reactor volumes. □ 0.0053 l/sec, 310 cc. ○ 0.0053 l/sec, 210 cc. △ 0.021 l/sec, 310 cc. 62 krads/h. 80 g SDBS/l H_2O. 20°C. The points of measurement are shown with their 80% confidence limits.

4.3.6. Polymerization with Intermittent Irradiation

In radiation-induced polymerization the production of free radicals can be stopped at any time simply by removing the reactor assembly from the irradiation zone, i.e. there is no need to add a short-stopper as with chemical initiation. From experiments with intermittent irradiation it is possible to obtain information about a prospective post-polymerization.

Fig. 52 shows a conversion versus time plot from an experiment in which the irradiation was intermitted for 60 min. during the run. The circulation of the emulsion was continued during the interruption. The plot shows that there is a post-polymerization in that the degree of conversion

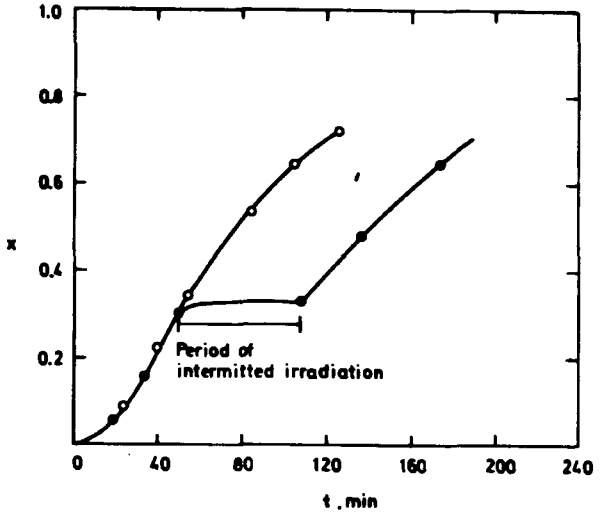

Fig. 52. Conversion versus time plots obtained at 62 krads/h. ● intermission of irradiation for 60 min at 30% conversion. ○ No intermission of irradiation. 80.5 g SDBS/l H_2O. In-source reactor volume 310 cc. 20°C.

increases by about 3% during the intermission.

The plot furthermore shows that polymerization starts immediately when the irradiation is continued. This means that during the intermission no oxygen has entered the system. Otherwise an induction period would have been observed.

In fig. 52 is also shown a plot from a similar run without interruption of the irradiation. Apart from the period of intermitted irradiation the curves are identical within the experimental error. Thus, interruption of the irradiation has no effect on the subsequent course of the polymerization.

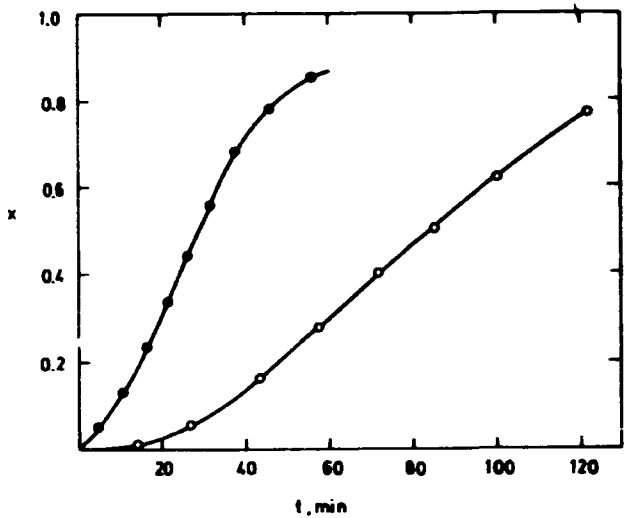

Fig. 53. Conversion versus time plots obtained at two different dose rates. ○ 62 krads/h. ● 301 krads/h. 66.5 g SLS/l H_2O. Flow rate 0.021 l/sec. In-source reactor volume 210 cc 20°C.

4.3.7. Effect of Dose Rate

Fig. 53 shows conversion versus time plots obtained at dose rates of 62 and 301 krads/h. From the slope of the linear parts of the curves it is found that the rate of polymerization increases by the square root of the dose rate, i.e. the dose rate has a similar effect on polymerization rate as the initiator concentration. The square root dependence is contrary to the results reported by Stannett et al.[75, 80], who have found a dose rate dependence exponent of 0.7 - 0.9.

Fig. 54 shows plots of the limiting viscosity number $[\eta]$ versus conversion obtained at dose rates of 62 and 301 krads/h. It appears that $[\eta]$ decreases with increasing dose rate. This is in agreement with the data reported by O'Neill et al.[72] which were discussed in subsection 4.1. The effect of dose rate on $[\eta]$ obviously decreases with increasing conversion. This feature will be further discussed in subsection 4.4.3.

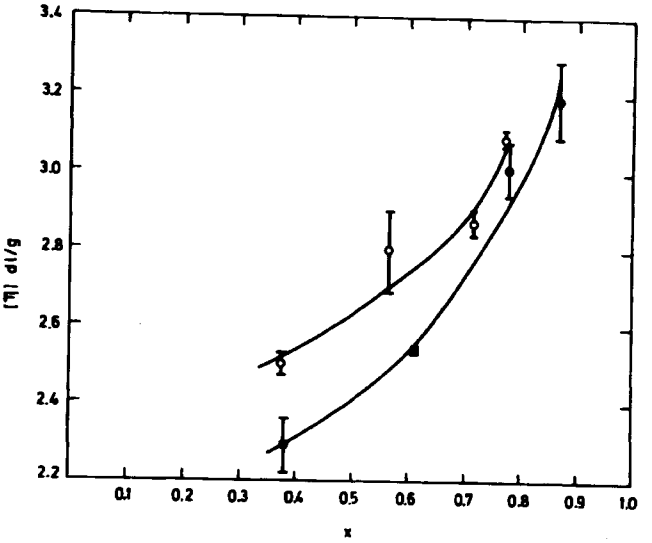

Fig. 54. Limiting viscosity number of poly (vinyl acetate) as a function of conversion at two different dose rates. ○ 62 krads/h. ● 301 krads/h. 66.5 g SLS/l H_2O. Flow rate 0.021 l/sec. In-source reactor volume 210 cc. 20°C. The points of measurement are shown with their 80% confidence limits.

4.4. Discussion

4.4.1. Introduction

From the preceding sections the following points concerning the radiation-induced emulsion polymerization of vinyl acetate can be established:

I The effect of concentration of SLS on the rate of polymerization is similar to that observed with chemical initiation.

II The transition in kinetics observed with chemical initiation at high concentrations of SDBS is also observed with radiation initiation. However, with radiation initiation the transition takes place at a higher concentration of SDBS.

III The rate of polymerization increases with increasing flow rate, but only when the flow rate is increased from the beginning of the polymerization. A change in flow rate beyond 40% conversion does not affect the rate of polymerization.

IV The rate of polymerization increases by the square root of the dose rate.

V The number of particles, N, increases in the interval 0 - 50% conversion. Beyond 50% N is approximately constant.

VI The limiting viscosity number is independent of emulsifier concentration, number of polymer particles, and residence time in the tubular flow reactor, but decreases with increasing dose rate in the interval 62 - 301 krads/h.

Although the data obtained in this part of the investigation are very sparse, they seem to indicate several similarities between radiation-induced and chemically initiated polymerization, and it is therefore tempting to base the quantitative treatment of these data on the same principles as were used to formulate the kinetics of the chemically initiated polymerization.

The quantitative treatment of the data is complicated by the fact that the polymerization was conducted in a dynamic system, where the concentration of free radicals in each volume element depends on the position of the element in the system. It is therefore necessary to modify eqs. 26 and 27, which are valid only for a stationary system, to a set of analogous differential equations. In order to calculate the overall rate of polymerization

it is necessary first to compute the rate in any position of the system and then to integrate over the whole system.

The quantitative treatment is further complicated by the necessity of taking into account that initiation takes place not only in the water phase, but also in the monomer-swollen polymer particles.

4.4.2. Computation of the Initiation Rate

In order to calculate the rate of polymerization theoretically it is necessary first to compute the rate of production of free radicals in the water phase and in the polymer phase. Since the chemistry of the system is not known in detail, these computations must depend on a rough estimate.

First the aqueous phase will be considered. Irradiation of pure water results in formation of hydroxyl radicals, hydrogen atoms, and hydrated electrons. Each of these species may act as effective initiators of the polymerization by reaction with vinyl acetate dissolved in the water. Thus, the hydroxyl radical and the hydrogen atom presumably add very fast to the carbon-carbon double bond of the vinyl acetate molecule to form a radical which can attack a second vinyl acetate molecule. The fate of the hydrated electron is more uncertain. However, the fact that the electron reacts very fast with CO_2 ($CO_2 + e^- \rightarrow CO_2^-$) may lead to the supposition that the electron adds to the $\rangle C = 0$ group in the ester linkage:

$$CH_2 = CH\text{-}O\text{-}\overset{O}{\overset{\|}{C}}\text{-}CH_3 + e^- \rightarrow CH_2 = CH\text{-}O\text{-}\overset{O^-}{\overset{\|}{C}}\text{-}CH_3 .$$

As pointed out by Hart[86] the anion thus formed possibly decomposes into an alcohol anion and an acyl radical which may attack the carbon-carbon double bond in a second vinyl acetate molecule.

With the assumption that each of the primary products of the water radiolysis leads to formation of growing polymer radicals it is possible from the radiation-chemical yield of the different species to compute the overall rate of initiation in the water phase, ρ_w, and at a dose rate of 62 krads/h the value 8×10^{-8} moles/l-sec is found for ρ_w. In this calculation the yield of radicals from vinyl acetate dissolved in the water phase has been neglected.

By kinetic studies of the radiation-induced polymerization of pure vinyl acetate the radiation-chemical yield of vinyl acetate has been found to equal approximately 12 radicals/100 eV[70]. The radiation-chemical yield for poly(vinyl acetate) has not been reported in the literature. However, for

the present calculation, which is already encumbered with uncertainty, it will be assumed that the radiation-chemical yield of poly(vinyl acetate) is equal to that of vinyl acetate monomer, i. e. it is supposed that incorporation of the vinyl acetate molecule into a polymer chain does not affect the radiation-chemical yield. With this assumption the initiation rate, ρ_p, in the monomer-swollen polymer particles can be calculated to be 8×10^{-8} moles/l-sec at a dose rate of 62 krads/h.

4.4.3. Presentation of the Model

As in the derivation of eq. 30 it is assumed that termination takes place exclusively in the polymer particles, and that there is a rapid equilibrium between radicals in the aqueous phase and the polymer particles, i. e. the rate of production of radicals in the aqueous phase by primary initiation plus the rate of transfer of radicals from the polymer particles to the aqueous phase equals the rate at which radicals enter the polymer particles from the water phase. It will furthermore be assumed that the tubular flow reactor can be regarded as an ideal plug flow reactor, i. e. that dispersion of the fluid can be neglected. Similarly, the stirred vessel will be considered as an ideal backmix reactor. Finally it will be assumed that at any given instant the composition of the emulsion is uniform throughout the whole system. This is reasonable since the conversion per pass through the source is in the worst case less than 1%.

For the subsequent discussion it is convenient to divide the system into four sections:

1. Plug flow reactor
2. Return line from plug flow reactor
3. Backmix reactor
4. Feed line to plug flow reactor.

1. Plug flow reactor. When a volume element enters the plug flow reactor, the number of particles containing 1 and 2 radicals increases until the element has reached the exit of the reactor. With the above assumptions the following equations serve to define the kinetics in this part of the system:

$$\frac{dN_1}{dt} = (\rho_w + k_d N_1 + 2k_d N_2)\left(\frac{N - 2N_1 - N_2}{N}\right) + 2k_d N_2 - k_d N_1 + \rho_p\left(\frac{N - 2N_1 - N_2}{N}\right) \tag{48}$$

$$\frac{dN_2}{dt} = (\rho_w + k_d N_1 + 2k_d N_2)\frac{N_1}{N} - 2k_d N_2 - \frac{2k_{tp} N_2}{vN_A^2} + \rho_p \frac{N_1}{N} . \tag{49}$$

2. Return line from plug flow reactor. When a volume element leaves the source, N_1 and N_2 decrease. The values of N_1 and N_2 as functions of time (or position) in this part of the system are obtained from eqs. 48 and 49 by putting ρ_w and ρ_p equal to zero.

3. Backmix reactor. With the "steady-state backmix flow reactor" equation

Input = Output + Disappearance by Reaction

the following equations can be derived for computation of N_1 and N_2 in the stirred vessel:

$$FN_1^I/V_B - FN_1/V_B - k_d N_1 + 2k_d N_2 + (k_d N_1 + 2k_d N_2)\left(\frac{N - 2N_1 - N_2}{N}\right) = 0 \tag{50}$$

$$FN_2^I/V_B - FN_2/V_B - 2k_d N_2 - \frac{2k_{tp} N_2}{vN_A^2} + (k_d N_1 + 2k_d N_2)\frac{N_1}{N} = 0 \tag{51}$$

In eqs. 50 and 51 F denotes the volumetric flow rate and V_B the volume of the backmix reactor. N_1^I and N_2^I denote number of particles containing 1 and 2 radicals respectively in the feed. N_1 and N_2 are the number of particles with 1 and 2 radicals respectively in the backmix reactor.

4. Feed line to plug flow reactor. In this part of the system N_1 and N_2 are obtained from eqs. 48 and 49 with ρ_w and ρ_p equal to zero and with initial values equal to N_1 and N_2 in the backmix reactor.

The subsequent discussion will be limited to elucidating the solution of eqs. 48-51 with data from an experiment in which the number of particles was determined. A detailed examination of the applicability of eqs. 48-51 for prediction of the effect of the various parameters cannot be made at present, since reliable data on number of particles were obtained only in a few cases. Only a qualitative discussion will be given.

Eqs. 48 and 49 were solved on a PDP-8/I digital computer by means of the Runge - Kutta method, using a step length of 10^{-3} sec. Eqs. 50 and 51 were solved by means of an iteration procedure. To simulate a polymerization at 40% conversion the following values of the constants were used:

k_p = 800 l/mole-sec

k_{tp} = 10^7 l/mole-sec

k_{tr} = 0.11 l/mole-sec

D_p = 10^{-9} dm^2/sec.

The value of k_p at 25°C is reported in the literature to lie within the interval 900 - 1100 l/mole-sec[39] and a value of 800 l/mole-sec at 20°C is therefore not unreasonable. The ratio $k_p/k_{tr} = 1.4 \times 10^{-4}$ is in good agreement with reported data[39], and is furthermore reasonably proportioned to the similar value used to simulate the chemically initiated experiments at 50°C ($k_{tr}/k_p = 2.15 \times 10^{-4}$). The deviation corresponds to an energy of activation of 2.8 kcal/mole for $E_{tr} - E_p$. The value of 10^7 l/mole-sec for k_{tp} is obtained by interpolation of the data reported by Melville[84]. The value of D_p was chosen with reference to the corresponding value (4×10^{-9} dm^2/sec at 40% conversion) used to simulate experiments with chemical initiation, taking into account that the radiation-induced experiments were conducted at a temperature 30°C below that at which the experiments with chemical initiation were performed.

Fig. 55 shows a theoretical plot of number of particles containing 1 radical, N_1, versus the "volumetric distance" through the reactor system. It appears that a stationary state is attained in the plug flow reactor. Furthermore, since N_1 is proportional to the rate of polymerization ($N_2 < 10^{-3} N_1$), it can be concluded that a considerable amount of polymerization takes place outside the source.

Table 3 gives the calculated rates of polymerization in each part of the system. The overall rate equals 0.99×10^{-3} moles/sec and this figure compares reasonably well with the experimental value of 0.80×10^{-3} moles/sec. From table 3 it appears that more than 50% of the polymerization takes place outside the source.

Unless the number of particles is affected by the in-source reactor volume, an increase of this volume will not affect the conditions in the exterior system because a stationary state is obtained in the plug flow reactor. If this is the case, then the calculations can explain the exper-

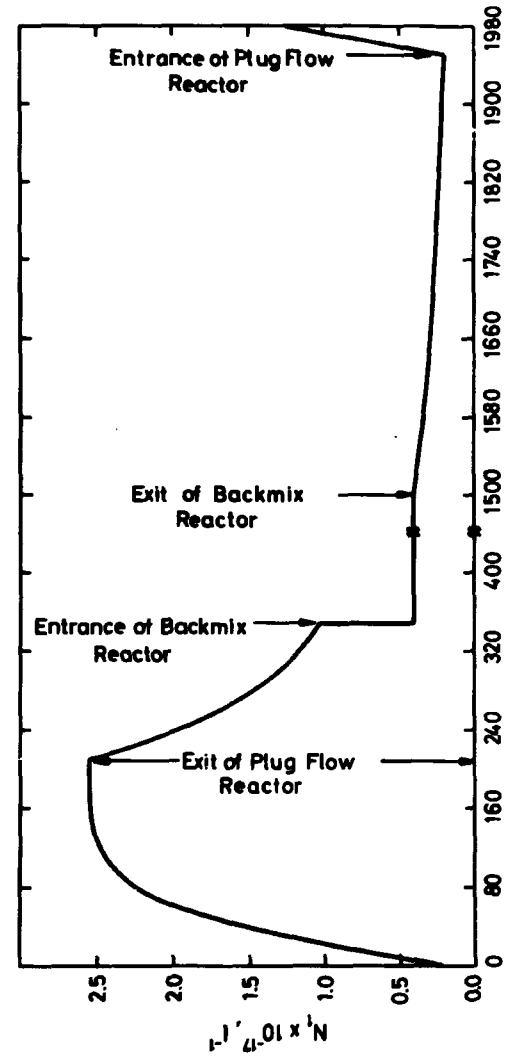

Fig. 55. Theoretical plot of N_1 versus volumetric distance. The plot corresponds to a flow rate of 0.021 l/sec and a reactor volume of 310 cc.

Table 3

Calculated rates of polymerization in each part of the system. Dose rate = 62 krads/h; number of particles/l = 12×10^{17}; flow rate = 0.021 l/sec; in-source reactor volume = 0.210 l; degree of conversion = 0.4

	R_p moles/sec
Plug flow reactor	0.00036
Return line from plug flow reactor	0.00018
Backmix reactor	0.00032
Feed line to plug flow reactor	0.00013
Total	0.00099

imental observation that the rate of polymerization per unit volume of reactor increases with decreasing reactor volume or in other words, doubling of the reactor volume does not result in a doubling of the polymerization rate.

The pre-effect is defined as the difference between the amount of reaction which has occurred in the flow reactor at the time the steady state has been established, and that which would have occurred if the steady state had been established instantaneously. The time that passes until the steady state has been established is independent of flow rate, but the distance the flow element has travelled until the steady state has been reached decreases with decreasing flow rate. Therefore the pre-effect decreases with decreasing flow rate, and this means that the polymerization rate in the plug flow reactor increases with decreasing flow rate.

The after-effect is defined as the amount of reaction which takes place outside the source, and by similar reasoning it can be seen that the after-effect decreases with decreasing flow rate.

As the flow rate approaches zero both the pre-effect and the after-effect approach zero, and since the after-effect is always greater than the pre-effect[87], the net-effect is a decrease in the overall rate of polymerization. Hence, the polymerization rate should decrease with decreasing flow rate.

This statement will be further elucidated by an example. Fig. 56 shows theoretical plots of N_1 versus "volumetric distance" through the reactor system calculated for two different flow rates at 40% conversion and at

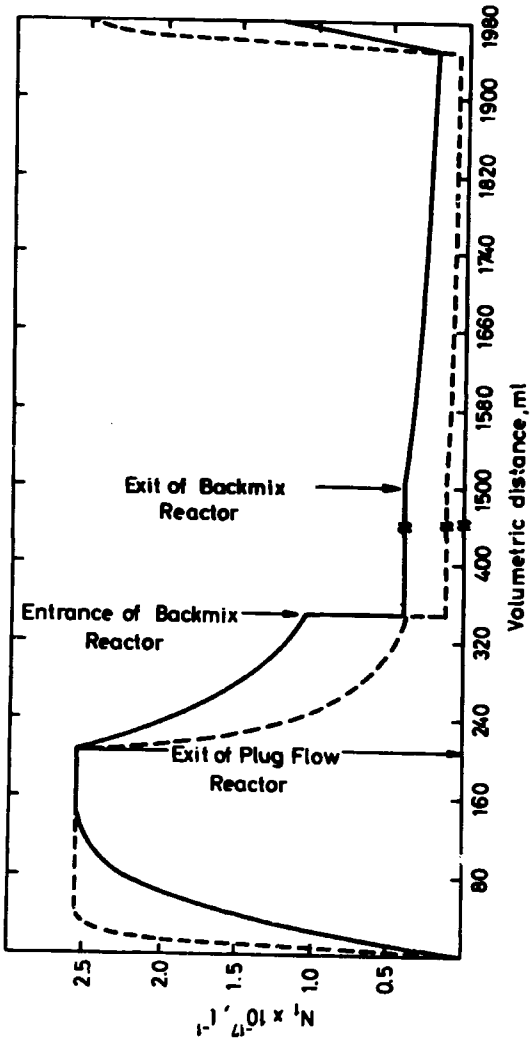

Fig. 56. Theoretical plots of N_1 versus volumetric distance. The solid curve corresponds to a flow rate of 0.021 l/sec. The dotted curve corresponds to a flow rate of 0.0053 l/sec.

constant number of particles, i. e. it has been assumed that the number of particles is unaffected by flow rate at 40% conversion. By integration of the two curves over the whole system it is found that the rate of polymerization decreases by a factor 0.7 as the flow rate is decreased from 0.021 to 0.0053 l/sec.

The effect of flow rate on polymerization rate was already considered in subsection 4.3.5, and a possible interference of flow rate on particle nucleation was invoked. To explain the lack of any effect of flow rate at conversions higher than 40% it was presumed that the flow rate does not affect the particle number at conversions where nucleation has ceased. The above calculation showed, however, that at constant number of particles there should be a detectable effect of flow rate. Therefore, if the particle number is virtually uninfluenced by a change in flow rate at 40% conversion, the theory does not agree with experimental observation.

The experimental observation that $[\eta]$ depends on the dose rate may be explained as a result of the high rate of initiation. In subsection 4.4.2 the rate of initiation was roughly estimated to equal 1.6×10^{-7} moles/l-sec at a dose rate of 62 krads/h. At 40% conversion the sum of rates of transfer to monomer and polymer can be roughly calculated to equal 6×10^{-7} moles/l-sec. At a dose rate of 301 krads/h the corresponding values equal 8×10^{-7} and 14×10^{-7} moles/l-sec. Thus, in contrast to the experiments with chemical initiation, the rate of bimolecular termination is not negligible in comparison with the rates of transfer to monomer and polymer, and therefore the molecular weight will decrease with increasing dose rate. That the effect of dose rate on $[\eta]$ diminishes with increasing conversion may be explained as being due to an increase in transfer to polymer with the extent of conversion (compare fig.38a). Hence, the molecular weight of the polymer that is forming at any given instant will be less influenced by bimolecular termination with increasing conversion. However, there is no conclusive evidence that this is the explanation. Owing to transfer to polymer and terminal double bond polymerization the polymers become greatly ramified at conversions beyond 50%[46, 85], and it is difficult to distinguish between the effects of branching and molecular weight on $[\eta]$.

4.5. Conclusion

The experimental data obtained with radiation initiation seem to indicate several kinetic similarities with the conventional process. However, the data are too meagre to prove conclusively that the kinetics of the two systems are identical.

Application of the model deduced for chemical initiation leads to the result that approximately 50% of the polymerization should take place outside the source. This result is interesting and the more so as both O'Neill[72] and Stannett and co-workers[1, 2] in the treatment of their data have excluded the occurrence of any reaction in the exterior system.

It must be admitted that it has not been possible unequivocally to define the kinetics of the radiation-induced emulsion polymerization of vinyl acetate in the particular flow system, and therefore the original object of the investigation has not been attained.

5. LIST OF SYMBOLS AND ABBREVIATIONS

Latin letter symbols

a	exponent in the Mark-Houwink equation
a_p	average surface area of a polymer particle
a_s	area occupied by one emulsifier molecule
A_2	second virial coefficient
c	concentration of polymeric substance
C_p	concentration of free radicals in the polymer phase
C_w	concentration of free radicals in the water phase
d_i	particle diameter
d_m	density of monomer
d_p	density of polymer
D_p	self-diffusion coefficient of monomeric radicals in monomer-swollen polymer particles
D_p^o	self-diffusion coefficient of monomeric radicals in vinyl acetate
D_w	self-diffusion coefficient of monomeric radicals in the aqueous phase
E_p	energy of activation for propagation
E_{tr}	energy of activation for transfer to monomer
f	initiator efficiency factor
F	volumetric flow rate
G_θ	galvanometer deflection at scattering angle θ
H	volume fraction of low molecular weight compound in polymer
$[I]$	initiator concentration
I_m	Bessel function of the first kind
I_θ	intensity of scattered light at scattering angle θ
k_a	absorption rate constant
k_d	desorption rate constant

k_i decomposition rate constant of potassium persulphate
k_o desorption rate constant in Smith-Ewart's theory
k_p propagation rate constant
k_r decomposition rate constant of AIBN
k_{tp} termination rate constant
k_{tr} rate constant for transfer to monomer
k_{tw} termination rate constant in the aqueous phase
K^* light scattering constant
K_1 combination of rate constants in eq. 42
K_2 combination of rate constants in eq. 42
K constant in the Mark-Houwink equation
K_d numerical constant in eq. 31
m $k_o a_p / k_{tp}$
M_{T1} molecular weight of polymer produced at temperature T1
M_{T2} molecular weight of polymer produced at temperature T2
M_o initial monomer concentration
M_W weight-average molecular weight
$[M]$ monomer concentration in bulk polymerization
$[M_p]$ monomer concentration in monomer-swollen polymer particles
$[M_{aq}]$ monomer concentration in water phase
n number of free radicals in a single particle
$\bar{n}$ average number of free radicals per particle
$\tilde{n}$ refractive index of aqueous dispersions of polymer particles
$\tilde{n}_o$ refractive index of solvent (dispersion medium)
$\tilde{n}_B$ refractive index of benzene
N total number of polymer particles
N_A Avogadro's number
N_i number of particles with diameter d_i
N_n number of particles containing n free radicals
$P(\theta)$ particle scattering factor
q density of monomer-swollen polymer particles
r average radius of a polymer particle
R gas constant
R_{abs} rate of absorption of radicals into particles
R_B Raleigh's ratio for benzene
R_{des} rate of desorption of radicals from particles
R_p rate of polymerization
R_θ Raleigh's ratio at a scattering angle θ
R_θ^o Raleigh's ratio at a scattering angle θ in the absence of interference

S number of emulsifier molecules per unit volume of aqueous phase
t reaction time
T absolute temperature
T_g glass-transition temperature
v average volume of a polymer particle = $\bar{v}_N$
$\bar{v}_N$ number-average particle volume
$\bar{v}_W$ weight-average particle volume
V^* critical free volume fraction
V_{fm} fraction of free volume in monomer
V_{fp} fraction of free volume in polymer
V_p total volume of monomer-swollen polymer particles
x degree of conversion
x_c degree of conversion at which the separate monomer phase disappears
x_v (1-H)/H
X_w volume fraction of water phase
X_p volume fraction of polymer phase
Z_θ dissymmetry at scattering angle θ
$[Z_\theta]$ intrinsic dissymmetry at scattering angle θ

Greek letter symbols

α V_{fp}/V_{fm}
α_g thermal expansion coefficient in the glassy state
α_l thermal expansion coefficient in the liquid state
β V^*/V_{fm}
δ partition coefficient of (all) radicals between aqueous and polymer phases
δ_m partition coefficient of monomeric radicals between aqueous and polymer phases
ϵ $\nu\rho'/k_{tp}N$
ζ $\sqrt{8\epsilon}$
$[\eta]$ limiting viscosity number
λ wavelength (in vacuo) of the light used in light scattering
μ rate of volume increase of polymer particles
ρ initiation rate
ρ' overall rate of entrance of radicals into all N particles
ρ_w initiation rate in the water phase (Y-initiation)
ρ_p initiation rate in the polymer phase (Y-initiation)
ϕ $(1+D_w/\delta_m D_p)^{-1}$
ψ $1-x_c$

Abbreviations

AIBN α,α'-azoisobutyronitrile
SDBS sodium dodecylbenzene sulphonate
SLS sodium lauryl sulphate

6. ACKNOWLEDGMENTS

The present work was performed in partial fulfilment of the requirements for obtaining the licentiate degree (Ph. D.). The work was carried out at the Chemistry Department of the Danish Atomic Energy Commission Research Establishment Risø and at the Instituttet for Kemiindustri under the supervision of professor, Dr. A. Björkman.

The study was performed with assistance from Dr. K. Singer and professor, Dr. J. Kops, and I am grateful for their confidence in my work and guidance and advice during the study.

I am deeply indebted to Professor, Dr. A.E. Hamielec for his encouragement and great interest. His large and wide knowledge of polymer chemistry and physics has been of invaluable importance to me.

To Mr. P. Bo I would like to express my sincere appreciation for many interesting discussions from which I have benefitted during the progress of the work. I am also very grateful to Mr. W.B. Pedersen for his helpful suggestions.

I especially want to express my sincere gratitude to Miss L. Nyhagen* for her invaluable and trustworthy assistance throughout the experimental work. I also wish to thank Professor, Dr. E.W. Langer and Mrs. L. Bjerregaard for their help and advice during the electron microscope investigations. The assistance of Mr. W. Nielsen is also acknowledged.

I am indebted to Mr. J. Nielsen for his help in constructing and assembling the experimental equipment.

Thanks are due to Mrs. H. Vøthz for her careful revision of the language of the manuscript and to Miss I. Pedersen, who skilfully and patiently typed the report.

I am grateful for the kind and efficient assistance of many people from the Chemistry Department and the Accelerator Department.

Finally I wish to thank the Danish Atomic Energy Commission for the granting of the licentiate scholarship and for placing experimental facilities at my disposal.

* Now Mrs. Friis

APPENDIX I

LIGHT SCATTERING COMPUTATIONS

Debye's equation describes the relation between the concentration of polymeric substance, c, and Raleigh's ratio, R_θ, measured at a scattering angle, θ:

$$K^*c/R_\theta = 1/M_W + 2A_2c, \qquad (I1)$$

where

$$K^* = \frac{2\pi^2\bar{n}_o^2 (d\bar{n}/dc)^2}{N_A\lambda^4} \qquad (I2)$$

and

M_W = weight-average molecular weight of the scatterer
A_2 = second virial coefficient
N_A = Avogadro's number
$\bar{n}_o$ = refractive index of the solvent
dn/dc = change in refractive index with concentration
λ = wavelength of the light in vacuo.

Since the polymer particles have dimensions that approach the wavelength of the light (λ = 5460 Å), they will cause interference of the scattered light and for this reason it is necessary to introduce a particle scattering factor, P(θ), into eq. I1. P(θ) is defined as

$$P(\theta) = R_\theta/R_\theta^o,$$

where R_θ^o is the Raleigh ratio in the absence of interference. When interference is taken into account, eq. I1 takes the form

$$K^*c/R_\theta = 1/(M_W P(\theta)) + 2A_2c. \qquad (I3)$$

The particle scattering factor can be obtained from the intrinsic dissymmetry, $[Z_\theta]$, which is the dissymmetry at zero concentration. The dissymmetry Z_θ is defined as the ratio of the intensity of light scattered at an angle θ to the intensity of light scattered at the complementary angle π - θ:

$$Z_\theta = I_\theta / I_{\pi-\theta} = G_\theta / G_{\pi-\theta},$$

where I denotes intensity of scattered light and G galvanometer deflection. $[Z_\theta]$ is obtained by extrapolation of a plot of Z_θ versus c. By means of the tables of Stacey[62], $[Z_\theta]$ is converted into the particle scattering factor $P(\theta)$. For the conversion it is assumed that the particles are spherical.

In the SOFICA instrument the measurements are performed with pure benzene as reference, i. e. the Raleigh ratio is given as

$$R_\theta = \frac{R_B}{I_B} I_\theta \left(\frac{\bar{n}_o}{\bar{n}_B}\right)^2 = \frac{R_B}{G_B} G_\theta \left(\frac{\bar{n}_o}{\bar{n}_B}\right)^2, \qquad (14)$$

where R_B = Raleigh's ratio for benzene = 16.3×10^{-6} cm^{-1} at λ = 5460 Å. I_B is the relative scattered intensity for pure benzene, I_θ is the relative scattered intensity for the solution and G_B and G_θ denote the corresponding galvanometer deflections. The value of G_B is obtained from

$$G_B = 0.943\, G_S,$$

where G_S is the galvanometer deflection measured for a reference glass standard and the factor 0.943 is a constant for the apparatus concerned. In the present investigation the value of G_S is fixed at 10 and therefore G_B equals 9.43.

In the SOFICA instrument the scattering cell is immersed in a vat filled with benzene, and also the scattered light receiver is located in benzene. Therefore, owing to the difference in refractive index between benzene ($\bar{n}_B$) and the scattering solution ($\bar{n}_o$) a refraction correction factor, $(\bar{n}_o/\bar{n}_B)^2$, for the volume viewed by the measuring phototube, has been introduced into eq. 14[63,64].

When the values of R_B and G_B are introduced into eq. 14, and eq. 14 is substituted into eq. 13, the light scattering equation takes the form

$$\frac{K^{**}c}{1.728 \times 10^{-6} G_\theta} = \frac{1}{M_W P(\theta)} + 2A_2 c, \qquad (15)$$

where

$$K^{**} = \frac{2\pi^2 \bar{n}_B^2 (d\bar{n}/dc)^2}{N_A \lambda^4}. \qquad (16)$$

From the slope of the $\bar{n}$ versus c plot shown in fig. 11 the value of $d\bar{n}/dc$ is found to be 0.119 cm^3/g, and with $\lambda = 5.46 \times 10^{-4}$ cm and $\bar{n}_B$ = 1.4977[63] it is found that

$$K^{**} = 1.255 \times 10^{-7} \text{ moles-cm}^2/g^2.$$

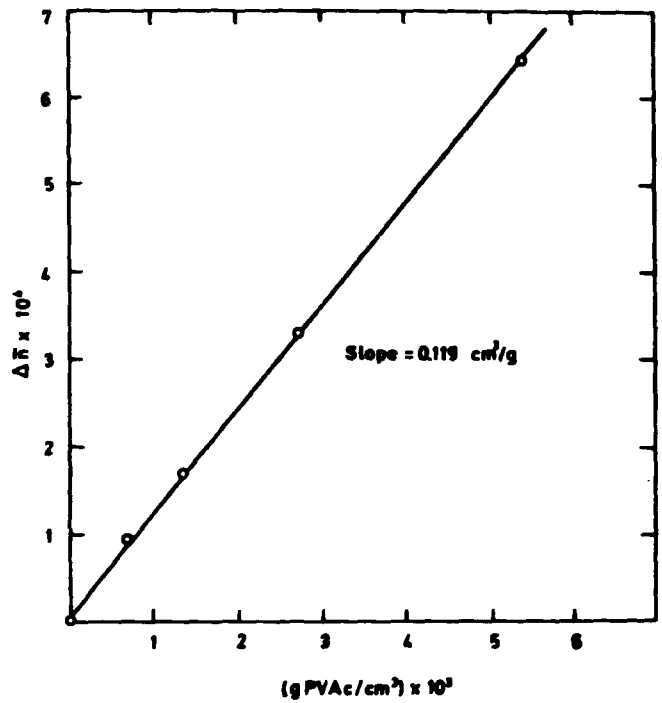

Fig. I 1. Plot of differential refractive index of poly (vinyl acetate) dispersions versus concentration of polymeric substance.

The application of eq. 15 for the determination of the weight-average particle volume will be elucidated by an example. Fig. 12 shows a plot of $K^{**}c/R_{90}$ versus c obtained by measuring G_{90} at four concentrations. The intercept on the x-axis equals 3.49×10^{-9} moles/g and thus

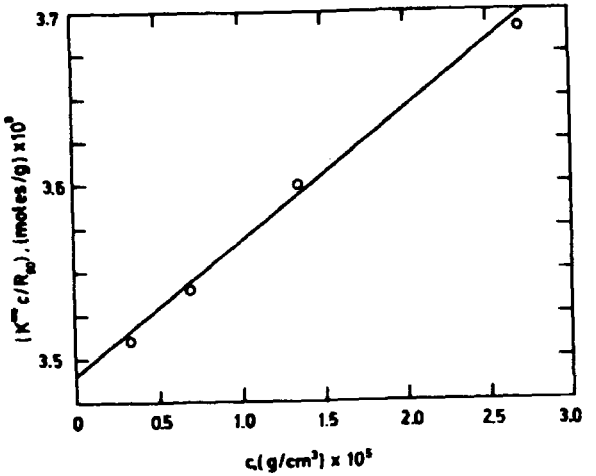

Fig. I 2. Light scattering plot.

$$1/(M_W P(90^\circ)) = 3.49 \times 10^{-9} \text{ moles/g.} \qquad (17)$$

Fig. 13 shows the corresponding plot of $Z_{45} = G_{45}/G_{135}$ versus c, and the value of $[Z_{45}]$ is found to be

$$[Z_{45}] = 2.59.$$

From $[Z_{45}]$ the particle scattering factor is obtained by use of Stacey's tables[52]

$$1/P(90^\circ) = 1.90,$$

and eq. I7 gives

$$M_W = 5.45 \times 10^8 \text{ g/mole.}$$

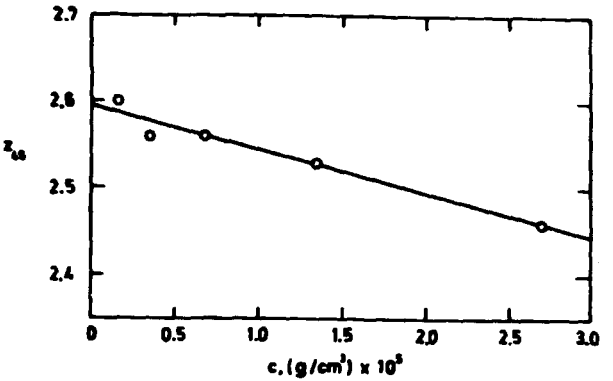

Fig. I 3. Plot of dissymmetry versus concentration of polymeric substance.

The weight-average particle volume is obtained as

$$\bar{v}_W = \frac{M_W}{N_A d_p} = 7.9 \times 10^{-16} \text{ cm}^3,$$

where d_p denotes polymer density.

The same latex was also investigated by electron microscopy and here the value 8.57×10^{-16} cm^3 was obtained for $\bar{v}_W$. Thus, the values obtained by the two techniques differ by less than 10%.

Finally, the weight-average particle number is obtained as

$$N_W = \frac{V_p}{\bar{v}_W} = 3.5 \times 10^{17} \text{ particles/l,}$$

where V_p denotes the volume of polymeric substance per litre of emulsion.

The uncertainty on the particle number determined by light scattering is assessed at $\pm$ 8%.

APPENDIX II

COMPUTATION OF THE PARAMETER α

The fraction of free volume in polymers and low-molecular-weight liquids can be computed from the empirical equation

$$V_f = 0.025 + (\alpha_l - \alpha_g)(T - T_g) \qquad (III)$$

suggested by Bueche[65]. V_f is the fraction of free volume at the temperature T°K. α_l and α_g are coefficients of thermal expansion in the liquid and glassy state respectively, and T_g is the glass transition temperature.

For poly(vinyl acetate) the values of the constants are as follows:

$$\alpha_l = 66 \times 10^{-5}/\text{deg}^{66)}$$
$$\alpha_g = 21 \times 10^{-5}/\text{deg}^{66)}$$
$$T_g = 301\,^{\circ}\text{K}^{59,60)},$$

and the free volume fraction, V_{fp}, at T = 323 °K is calculated to be

$$V_{fp} = 0.035.$$

For vinyl acetate Barkalov et al.[67] have determined the glass transition temperature to be 144 °K. The coefficient of thermal expansion of vinyl acetate below T_g is not known. However, by application of Simha and Boyer's rule[68] that $(\alpha_l - \alpha_g)T_g \approx 0.1$, the value of $(\alpha_l - \alpha_g)$ can be roughly estimated at 7×10^{-4}/deg and the free volume fraction in vinyl acetate, V_{fm}, at 323 °K is calculated to be

$$V_{fm} = 0.150.$$

α can now be calculated from V_{fm} and V_{fp}:

$$\alpha = V_{fp}/V_{fm} = 0.24.$$

The computation of α is of course very rough. However, it is useful just to estimate the order of magnitude of α.

REFERENCES

1) V. T. Stannett and E. P. Stahel, Chemical Engineering Studies in Radiation Polymerization of Vinyl Monomers: Part II Emulsion Polymerization. Department of Chemical Engineering, North Carolina State Univ., Raleigh, North Carolina, U. S. A.

2) S. Omi and E. P. Stahel, A Model Study of Radiation-Induced Emulsion Polymerization in a Recycle Reactor System. Department of Chemical Engineering, North Carolina State Univ., Raleigh, North Carolina, U. S. A.

3) W. V. Smith and R. H. Ewart, J. Chem. Phys. 16, 592 (1948).

4) W. D. Harkins, J. Am. Chem. Soc. 69, 1428 (1947).

5) W. H. Stockmayer, J. Polymer Sci. 24, 314 (1957).

6) J. T. O'Toole, J. Appl. Polymer Sci. 9, 1291 (1965).

7) G. E. Ham, Kinetics and Mechanism of Polymerization. Part II, vol. 1 (Marcel Dekker, New York, 1969) 1-138.

8) E. Trommsdorf, H. Köhle, and P. Lagally, Makromol. Chem. 1, 169 (1948).

9) W. S. Zimmt, J. Appl. Polymer Sci. 1, 323 (1959).

10) H. Gerrens, Z. Electrochem. 67, 741 (1963).

11) N. Friis, A. E. Hamielec, and O. Lang Rasmussen, Emulsion Polymerization of Methyl Methacrylate, to be published.

12) S. S. Medvedev, International Symposium on Makromolecular Chemistry (Pergamon Press, New York, 1959) 174.

13) D. M. French, J. Polymer Sci. 32, 395 (1958).

14) R. A. Patisiga, Ph. D. thesis, State Univ. College of Forestry at Syracuse Univ., Syracuse, New York 1962.

15) E. Vanzo, Ph. D. thesis, State Univ. College of Forestry at Syracuse Univ., Syracuse, New York 1963.

16) V. Stannett, M. Litt, and R. Patsiga, J. Phys. Chem. 64, 801 (1960).

17) J. T. O'Donnell, R. B. Mesrobian, and A. E. Woodward, J. Polymer Sci. 28, 171 (1958).

18) S. Okamura, and T. Motoyama, J. Polymer Sci. 58, 221 (1962).

19) W.J. Priest, J. Phys. Chem. 56, 1077 (1952).

20) D.H. Napper and A.G. Parts, J. Polymer Sci. 61, 113 (1962).

21) D.H. Napper and A.E. Alexander, J. Polymer Sci. 61, 127 (1962).

22) A. Netschey and A.E. Alexander, J. Polymer Sci. A-1 8, 399 (1970).

23) A. Netschey and A.E. Alexander, J. Polymer Sci. A-1 8, 407 (1970).

24) E.V. Gulbekian, J. Polymer Sci. A-1 6, 2265 (1968).

25) D. Gershberg, Paper presented at Joint Meeting of AIchE and IchE (England), London, England, June 14, 1965.

26) A.S. Dunn and P.A. Taylor, Die Makromol. Chem. 83, 207 (1965).

27) M. Litt, R. Patsiga, and V. Stannett, J. Polymer Sci. A-1 8, 3607 (1970).

28) M. Nomura, M. Harada, K. Nakagawara, W. Eguchi, and S. Nagata, J. Chem. Eng. (Japan) 4, 160 (1971).

29) A.S. Dunn and L.C.H. Chong, Br. Polym. J. 2, 49 (1970).

30) J.W. Breitenbach, H. Edelhauser, and R. Hochrainer, Monatshefte für Chemie 99, 625 (1968).

31) J.W. Breitenbach, K. Kuchner, H. Fritze, and H. Tarnowiecki, Br. Polym. J. 2, 13 (1970).

32) B.G. Elgood, E.V. Gulbekian, and D. Kinsler, Polymer Letters 2, 257 (1964).

33) A. Netschey, D.H. Napper, and A.E. Alexander, Polymer Letters 7, 829 (1969).

34) P. Harriot, J. Polymer Sci. A-1 9, 1153 (1971).

35) M. Morton, P.P. Salatiello, and H. Landfield, J. Polymer Sci. 8, 279 (1952).

36) E.C. Leonard, Vinyl and Diene Monomers. Part I (Wiley-Interscience, New York, 1969) 281.

37) F.A. Bovey, I.M. Kolthoff, A.I. Medalia, and E.J. Meehan, Emulsion Polymerization (Interscience Publishers Inc., New York, 1965) 157.

38) M.S. Matheson, E.E. Auer, E.B. Bevilacqua, and E. Hart, J. Am. Chem. Soc. 71, 2610 (1949).

39) G.E. Ham, Kinetics and Mechanism of Polymerization. Part I, vol. 1 (Marcel Dekker, New York, 1969).

40) J.W. Vanderhoff and E.B. Bradford, J. Colloid Sci. 14, 543 (1959).

41) J.W. Vanderhoff and E.B. Bradford, J. Colloid Sci. 17, 668 (1962).

42) J.T. Clarke, R.O. Howard, and W.H. Stockmayer, Makromol. Chem. 44, 427 (1961).

43) J. Ugelstad, P.C. Mork, P. Dahl, and P. Ragnes, J. Polymer Sci. C 27, 49 (1969).

44) J. Ugelstad and P.C. Mork, Br. Polymer J. 2, 31 (1970).

45) E. Peggion, F. Testa, and G. Talamini, Makromol. Chem. 71, 173 (1964).

46) D.J. Stein, Makromol. Chem. 76, 170 (1964).

47) J. Brandrup and E.H. Immergut, Polymer Handbook (Interscience Publishers, New York, 1965) p. IV-16.

48) G. Dixon-Lewis, Proc. Roy. Soc. (London) A 198, 510 (1949).

49) F. Danusso, G. Pejaro, and D. Sianesi, Chim. Ind. (Milan) 41, 1170 (1959).

50) A.E. Hamielec, McMaster Univ., Hamilton, Canada, personal communication.

51) G.V. Schulz, Z. Physik. Chem. NF 8, 290 (1956).

52) A. Scheludko, Colloid Chemistry (Elsevier, Amsterdam, 1966) 47-55.

53) A. Peterlin, H. Yasuda, and C.E. Lamaze, J. Polymer Sci. A-2, 9, 1117 (1971).

54) I.M. Kolthoff and I.K. Miller, J. Am. Chem. Soc. 73, 3055 (1951).

55) G.M. Burnett and W.W. Wright, Proc. Roy. Soc. (London) A 221, 41 (1954).

56) B.M.E. van der Hoff, J. Polymer Sci. 48, 175 (1960).

57) E. Bartholome, H. Gerrens, R. Herbeck, and H. Weitz, Z. Elektrochem. 66, 334 (1956).

58) M. Nomura, M. Harada, W. Eguchi, and S. Nagata, J. Chem. Eng. (Japan) 4, 54 (1971).

59) P. Meares, Trans. Farad. Soc. 53, 31 (1957).

60) L. E. Nielsen, Mechanical Properties of Polymers (Reinhold Publishers, New York, 1962).

61) C. P. Roe, Ind. Eng. Chem. 60, 20 (1968).

62) K. Stacey, Light Scattering in Physical Chemistry (Academic Press, New York, 1956).

63) Y. Tomimatsu, L. Vitello, and K. Fong, J. Colloid Interface Sci. 27, 573 (1968).

64) Instruction Manual for SOFICA Photo-Gonio Diffusometer (Société Française d'Instruments de Contrôle d'Analyses, 1968).

65) F. Bueche, Physical Properties of Polymers (Interscience Publishers, New York, 1962).

66) M. K. Lindemann, Vinyl Ester Polymers, in: Encyclopedia of Polymer Science and Technology 15, 534 (1971).

67) I. M. Barkalov, V. I. Goldanski, N. S. Enikolypian, S. F. Terekhova, and G. M. Trofimova, J. Polymer Sci. C 4, 909 (1964).

68) R. Simha and R. F. Boyer, J. Chem. Phys. 37, 1003 (1962).

69) M. H. Cohen and D. Turnbull, J. Chem. Phys. 31, 1164 (1959).

70) A. Chapiro, Radiation Chemistry of Polymeric Systems (Interscience Publishers, New York, 1962).

71) T. O'Neill and J. Hoigné, J. Polymer Sci. A-1 10, 581 (1972).

72) T. O'Neill, J. Pinkava, and J. Hoigné, Proceedings of the 3rd Tihany Symposium on Radiation Chemistry, Tihany, Hungary, 1971, 1, 713 (1972).

73) G. Ley, C. Schneider, and D. O. Hummel, J. Polymer Sci. C 27, 119 (1969).

74) G. Ley, D. O. Himmel, and C. Schneider, Radiation-Induced Polymerization of some Vinyl Monomers in Emulsion Systems, Advances in Chemistry Series No. 66, 184 (1967).

75) V. Stannett, J. A. Gervasi, J. J. Kearney, and K. Araki, J. Appl. Polymer Sci. 13, 1175 (1969).

76) P. E. M. Allen, G. M. Burnett, G. M. Downer, and J. M. Melville, Makromol. Chem. 58, 169 (1962).

77) P. E. M. Allen, G. M. Burnett, G. M. Downer, and J. M. Melville, Makromol. Chem. 38, 72 (1960).

78) J. W. Vanderhoff, E. B. Bradford, H. L. Tarkowski, and B. W. Wilkinson, J. Polymer Sci. 50, 265 (1961).

79) G. J. K. Acres and F. L. Dalton, J. Polymer Sci. A 1, 3009 (1963).

80) V. T. Stannett, J. A. Gervasi, J. J. Dearney, and K. Araki, Radiation-Induced Emulsion Polymerization, (Research Triangle Institute, Camille Dreyfus Laboratory, Research Triangle Park, North Carolina).

81) N. B. Havewala, Ph. D. thesis, North Carolina State Univ. at Raleigh, North Carolina (1969).

82) A. Henglein, W. Schnabel, and J. Wendenburg, Einführung in die Strahlenchemie (Verlag Chemie GmbH, Weinheim/Bergstr., Germany, 1969).

83) H. Fricke and E. J. Hart, Chemical Dosimetry, Chap. 12 in: H. Attix and W. G. Roesch (editors), Radiation Dosimetry (Academic Press, New York, 1966).

84) H. W. Melville, Z. Elektrochem. 60, 276 (1956).

85) W. W. Graessley and H. M. Mittelhauser, J. Polymer Sci. A-2 5, 431 (1967).

86) E. J. Hart and M. Anbar, The Hydrated Electron (Wiley-Interscience, New York, 1970) 137.

87) C. H. Bamford, W. G. Barb, A. D. Jenkins, and P. F. Onyon, The Kinetics of Vinyl Polymerization by Radical Mechanisms (Butherworths Publications Ltd., London, 1958).